



Spitzer Space Telescope

Multiband Imaging Photometer for Spitzer (MIPS) Data Handbook

Version 3.2.1

Release Date: 6 Feb 2006

Issued by the Spitzer Science Center
California Institute of Technology
Mail Code 314-6
1200 E. California Blvd
Pasadena, California 91125 USA
<http://ssc.spitzer.caltech.edu/>
help@spitzer.caltech.edu



Issue dates and version history

Version 3.2.1 (Feb 2006): Fixing a typo in the header keywords and in the discussion of color corrections.

Version 3.2 (January 2006): Fixing various typos, updating a variety of information for S13, including new calibration factors, new magnitude zero points, new aperture corrections, and a new section on SED pointing history. We also changed from Windows-based MS Word to Macintosh-based MS Word, and not everything translated without problems. Please let us know (help@spitzer.caltech.edu) if you find any strange symbols or formatting.

Version 3.1 (June 2005): Fixing three small but important typos, the most significant one about the Ge default online mosaic pixel sizes. Other two have to do with table breaks on page 28-30 and how to download non-prime Ge data using Leopard.

Version 3.0 (May 2005): Updated information about S11, S12 pipelines. Folded in information developed for March 2005 Data Analysis Workshop, including many new figures. Overall updating and refreshing of information.

Version 2.3 (March 2005): Updated Ge bit values (Table 3.4). Basic information on MIPS-SED added (Chapter 8).

Version 2.2 (February 2005): tweaks to several items for clarity: Tables 3.1, 3.2, 9.1, and 9.2, and sections 4.2.1, 4.2.2, and 5.2.

Version 2.1 (December 2004): tweaks to table of conversion values (**Error! Reference source not found.**), and addition of information on color corrections (Section 3.7.4).

Version 2.0 (November 2004): Significant changes include the following: BCD bmask definitions for MIPS-24 updated, new section on conversion factors, expanded section on color corrections, new and expanded information on aperture corrections, updated pipeline descriptions, new figure on 24 micron first frame effect, new figure on 70 micron first DCE effects, updated Ge examples.

Version 1.1 (June 2004): Updated information on filenaming schemes and references to real-life science done with MIPS data as discussed in the ApJS Spitzer Special Issue (due out September 2004). Various typos fixed and language clarifications.

Version 1.0 (May 2004): This is a new document.

Acknowledgements

This document includes contributions from the MIPS Instrument Support Team (at the SSC), the MIPS Instrument Team (at the University of Arizona), and the Observer Support Team (at the SSC).

Table of Contents

1	Quick-Start Guide.....	6
1.1	Understanding MIPS Data – the “Must Knows”	6
1.2	Quick vocabulary	7
1.3	MIPS-24 (Photometry or Scan)	7
1.4	MIPS-70 and 160 (Photometry or Scan)	7
1.5	MIPS-SED	8
1.6	MIPS-TP	8
1.7	Analysis resources new in 2005-6	8
2	Introduction	9
2.1	Purpose and scope of this document	9
2.2	Basic definitions.....	10
2.3	On-orbit realities of MIPS arrays.....	12
3	Getting started	16
3.1	Using the Archive	16
3.2	Filenames and most important files	16
3.2.1	BCDs	16
3.2.2	Post-BCD products.....	17
3.3	What do all of these files mean?.....	22
3.3.1	Retrieving the AOR file(s).....	22
3.3.2	Visualizing your observation, or how the files relate to the AOR	23
3.3.3	Files you think you should have, but don't (or extra files you have but think you shouldn't)	24
3.4	What do all of these header keywords mean?	25
3.5	Major caveats for the current version of the pipeline	27
3.6	Pipeline history	27
3.7	Basic toolset for working with MIPS data	27
3.7.1	Units and fluxes.....	28
3.7.2	Conversion Factors.....	28
3.7.3	Magnitude Zero Points	29
3.7.4	Color Corrections	29
3.7.5	PSF characterization.....	31
3.7.6	Aperture Corrections	32
4	BCD Pipeline Description.....	38
4.1	Introduction.....	38
4.2	The MIPS-24 pipeline	38
4.2.1	Summary of pipeline	38
4.2.2	S13 pipeline.....	40
4.3	The MIPS-Ge pipeline.....	43
4.3.1	Summary of pipeline	43
4.3.2	S13 updates	44
4.3.3	Things that aren't in the current pipeline.....	45
5	Post-BCD Pipeline Description.....	46
5.1	Introduction.....	46

5.2	MIPS and Pointing Refinement.....	46
5.3	MIPS and Mosaicking/Outlier Detection.....	47
5.4	MIPS and APEX.....	48
5.5	MIPS and Bandmerging.....	48
6	Data Details (“Gotchas” and Examples) – MIPS 24	49
6.1	Pick-off mirror contamination and systematic pointing: practical information	50
6.2	More information on spot positions: for the truly dedicated	53
6.3	Jailbars	55
6.4	Latents.....	56
6.4.1	Short-lived bright latents.....	56
6.4.2	Dark latents.....	57
6.4.3	Long-lived bright latents	60
6.5	First and second DCE effects	61
6.6	Post-anneal slow response drift.....	62
6.7	Bright sources and droop correction.....	63
6.8	Ghosts and glints	63
6.9	Zero-level offset	64
6.10	Distortions	65
6.11	Large- and small-scale gradients	65
6.12	Asteroids!	66
6.13	Example: Self-calibration	66
6.14	Example: NGC 300.....	68
6.15	Additional examples	69
7	Data Details (“Gotchas” and Examples) – MIPS Ge	70
7.1	Introduction	70
7.2	High-level summary	70
7.3	Point vs. extended sources, or why there are 2 BCDs	71
7.4	The GeRT.....	72
7.5	Recommended steps for looking at your data.....	72
7.6	Note on point source photometry	73
7.7	Error images	75
7.8	Variations of the slow response.....	77
7.9	Stim latents.....	77
7.10	First DCE effects, or corrupted stim-minus-background measurements 78	
7.11	Electronic non-linearities	80
7.12	Flux non-linearities.....	81
7.13	160 μm short-wavelength light leak	81
7.14	Offline Enhancements to MIPS 70 Fine Scale or 70/160 large-field	83
7.15	Example: 70 micron faint point source survey.....	86
7.16	Example: 160 micron faint point source survey.....	89
7.17	Example: 70 micron bright extended source.....	91
7.18	Example: 160 micron bright extended source.....	93
7.19	New examples using the GeRT	95
7.19.1	Trails of bright latents	95

7.19.2	Filtering the background behind a bright star	96
7.20	Additional Examples	97
8	MIPS-SED mode	98
8.1	How to make simple coadditions of MIPS-SED BCDs	98
8.1.1	Chop/dither pattern	98
8.1.2	Make simple coadditions	99
8.2	SED pointing history	100
8.2.1	Pre-MC19	101
8.2.2	MC19	102
8.2.3	MC21	104
8.2.4	MC23	106
8.2.5	Summary	108
9	Calibration of MIPS data	109
9.1	Uncertainties and Repeatability	109
9.2	Calibration observations	110
9.3	Absolute Calibration	111
9.3.1	Methodology	111
9.3.2	Uncertainties	111
9.4	Flat fields	113
9.5	Ge calibration overview	113
10	Appendix: FITS header keywords.....	115
10.1	Common header keywords	115
10.2	Header for 24 microns	122
10.3	Header for 70 microns	124
10.4	Header for 70 microns-SED mode	126
10.5	Header for 160 microns	128
10.6	Header for Post-BCD products	129
11	Appendix: Suggested namelists	132
12	Appendix: Analysis code	132

1 Quick-Start Guide

1.1 Understanding MIPS Data – the “Must Knows”

This handbook will evolve over time – if you do not find the information you need, please contact help@spitzer.caltech.edu. Vocabulary (including some used below) is summarized in Section 1.2 and 2.2.

Please be aware – there are some things you *must* understand prior to working with MIPS long-wavelength data. The physical nature of the detectors makes fully automated data processing for all types of observations very difficult. The Spitzer Observers Manual (SOM) includes a detailed discussion concerning the importance of observation planning with MIPS in order to mitigate detector characteristics. However, even with the best planning, some detector artifacts will be present in the SSC processed data.

The MIPS 70 and 160 micron channels have Ge:Ga detectors. This material is known to have multiple time constant behaviors when detecting infrared photons, including the MIPS internal calibration stimulators. Please see the SOM for further discussion (specific sections listed in Section 2.1 below). The SSC automated pipelines are very effective in reducing the instrument signatures to a minimum. But, some of the corrections are observation-dependent and, as such, are very difficult to automate.

Note: The 70 and 160 micron mosaics provided by the SSC are intended for *quick look analysis only*. In general, we do not recommend these be used for detailed science analysis for Ge data. The 24 micron mosaics can, in most cases, be used for detailed analysis. Care must be taken for 24 micron data, as well. The best automated product produced by the pipelines is the Basic Calibrated Data (BCD) frames. **It is important to understand artifacts that can impact your data, and how you might be able to further the processing of the SSC pipelines to improve your data.** Most often you will want to apply some additional corrections to these data that depend on the characteristics of the observation. This Handbook is intended to provide a starting point for such additional reductions.

Ge:Ga detectors have response behavior that is different for point source versus extended emission. The pipeline in general cannot deal with these effects. If your science goals are for point sources only, then the final reductions are facilitated through the use of the median filtered BCDs provided by the SSC. In many cases, little other manipulation is required prior to making the final mosaics. Let your science goals be your guide.

Some key caveats when working with MIPS archive data:

The 70 and 160 micron mosaics provided by the SSC are intended for *quick look analysis only*.

Current estimated uncertainty on point sources extracted from S13 pipeline products is 10% for 24 microns, 20% for 70 microns, and 20% for 160. For more

discussion, please see Section 9. Extended source measurements have been consistent with these measurements.

Do not measure absolute sky brightness (like Zodiacal light) using MIPS Scan and Photometry AOT products. The MIPS Total Power (TP) Mode (soon to be commissioned) is intended to provide the best results for such measurements.

Early observations suggest that faint MIPS 70 micron sources (<100 mJy) have flux non-linearities that are a <20% effect. The level of flux non-linearities for 160 microns has not yet been quantified. Analysis is ongoing, and we will update this document as information becomes available. This is not found to be an issue at 24 microns.

The MIPS 70 micron detector array bias voltage was optimized before MIPS campaign 5, which started on 14 March 2004. Data taken after that time have better detector performance, and typically require less post-BCD processing.

Color corrections will be largest for very red sources.

1.2 Quick vocabulary

Here are the most essential words to know (for more, see Section 2.2):

- AOR = Astronomical Observation Request, the basic unit of Spitzer data.
- BCD = Basic Calibrated Data, the output of the basic pipelines at the SSC. *As of this writing, these typically are the data to start with for MIPS long-wavelength channels!*
- Post-BCD = the output of the extended pipelines here at the SSC. Includes, e.g. mosaics. As of this writing, most of the software (MOPEX) used to generate these pipeline products is available at the SSC website (<http://ssc.spitzer.caltech.edu/>).

With MIPS data, you get a *lot* of files (how many is a function of the mode and length of observation), and in some cases, you will need to apply some hands-on processing to your data.

1.3 MIPS-24 (Photometry or Scan)

MIPS-24 data are the best-behaved of all MIPS data. In most cases, you can start with the Post-BCD products.

The artifacts that you are most likely to encounter are latents (both bright and dark). Bright ones decay quickly and are in the in-scan direction. Dark ones last for hours and can appear anywhere. See Section 6.4.

1.4 MIPS-70 and 160 (Photometry or Scan)

You should start with the BCDs. Unless you are interested in extended emission, ignore the Post-BCDs for now, except for a quick (non-science) look at your data. (See examples in Chapter 7 below.)

The 70 micron data require the most hands-on processing of all MIPS data; the 160 micron data can be difficult, but are generally better behaved than the 70 micron data. See discussion and flowcharts in Section 7.3.

1.5 MIPS-SED

This mode has been commissioned for uplink (e.g., Spot visualizations and spacecraft commanding are fine), and as of this writing, it is about to be commissioned for downlink. There is now a short chapter on MIPS-SED; more extensive discussion will be added to future versions of this document.

1.6 MIPS-TP

As of this writing, this mode has not yet been commissioned for uplink (e.g., Spot) or downlink (e.g., pipeline processing). It will get sections in future versions of this document.

1.7 Analysis resources new in 2005-6

We are generating additional analysis resources all the time! The latest additions to the SSC website that are relevant to MIPS data analysis include the following:

- Data Analysis Cookbooks – step-by-step instructions using SSC software on real data.
- MIPS Interest Group mailing list – provided to enhance community discussion about data analysis issues relevant to MIPS.
- The Germanium Reduction Tools (GeRT) – a collection of tools relevant to MIPS Ge data reduction. (Available as “contributed software.”)
- Presentations from the Data Analysis Workshops, including examples.

2 Introduction

2.1 Purpose and scope of this document

This manual is intended for investigators wishing to understand and work with MIPS data. We are assuming that you, the reader, have a basic understanding of Spitzer in general and MIPS in particular; an excellent document to read for this purpose is the Spitzer Observer's Manual (SOM). The SOM, as well as many other helpful documents and resources, can be obtained from the main Spitzer Science Center (SSC) web pages at <http://ssc.spitzer.caltech.edu/>.

Since you are reading this manual, it would seem that you do not need to know about observation planning, per se. ***However, an understanding of the MIPS data acquisition sequences is crucial to understanding what to do, now that you have data.*** At minimum, please at least scan the MIPS chapter of the SOM, specifically the following sections:

- Section on detector behavior (8.1.3.3 in SOM v. 6.x), covering Ge and Si behaviors, annealing, stimulators, and calibration.
- Section on operating modes (8.2.1 in SOM v. 6.x), covering where the telescope and scan mirror conspire to point MIPS during dithering sequences, where the stimulator flashes are placed in the observing sequence, and the number of frames you should expect to get, e.g., for a single photometry small field observation.
- Sections on data products (8.3.2 in SOM v. 6.x) and data processing (8.3.3 in SOM v. 6.x), providing an overview to some of the items discussed in this data handbook.

Interested investigators might also consider reviewing these sections:

- Section on sources of noise and confusion (8.2.2.1 in SOM v. 6.x), which includes cirrus and confusion limits.
- Sections on sensitivity (8.2.2.4 in SOM v. 6.x) and on sensitivity vs. exposure time (8.2.2.5 in SOM v. 6.x). Additional plots are available on the SSC/MIPS website. Also see section on accuracy, stability, and repeatability (8.2.2.8 in SOM v. 6.x).
- Sections on image quality and distortion (8.2.2.10 in SOM v. 6.x), scan alignment (8.2.2.11 in SOM v. 6.x), and ghost images (8.2.2.12 in SOM v. 6.x).
- Section on data calibration (8.3.1 in SOM v. 6.x).

The initial release of this document covered Photometry/Super Resolution and Scan Map modes. A chapter with basic information on MIPS SED was included in Spring 2005. MIPS TP was available starting with GO-2 and will be covered in a future release.

2.2 Basic definitions

For brevity, MIPS 24-micron data are also referred to as “silicon” data since the detectors are Si-based (Si:As); analogously, MIPS 70 and 160-micron data are also referred to as “germanium” since the detectors are Ge-based (Ge:Ga).

An **Astronomical Observing Template (AOT)** is the list of parameters for a distinct Spitzer observing mode. There are 4 possible MIPS AOTs: MIPS Photometry/Super Resolution, MIPS Scan Mapping, MIPS Spectral Energy Distribution (SED), and MIPS Total Power (TP).

The fundamental unit of Spitzer observing is the **Astronomical Observation Request (AOR)**, which is an AOT with all of the relevant parameters fully specified.

An AOR is composed of several **Data Collection Events (DCEs)**, or single-frame exposures; see Figure 2.1. **Basic Calibrated Data (BCD)** products are data derived from DCEs pushed through the pipelines. BCDs are designed to be the most reliable product achievable by automated processing. **Post-BCD** (also sometimes known as **Browse Quality Data, BQD**) products are derived from a full AOR, e.g., a combination of several BCDs. Post-BCD products include (but are not limited to) mosaics, which are produced for *both* MIPS photometry and scan observations. Automated post-BCD products do *not* combine data from more than one AOR; observers must do this task themselves (see below). MIPS BCDs and post-BCD products are 2-dimensional FITS images with a full set of header keywords, calibrated in MegaJanskys per steradian (MJy/sr). *To convert from MJy/sr to microJy/arcsecond², multiply by 23.5045.*

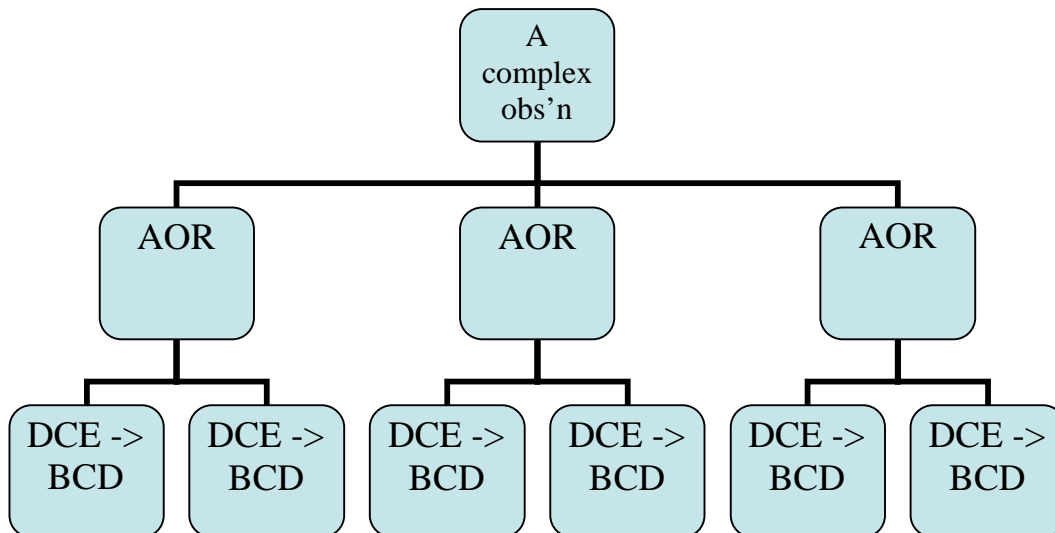


Figure 2.1: Metaphorical representation of a complex observation which is composed of several AORs. Each AOR consists of 100s to 1000s of DCEs (essentially raw data) that become BCDs once they go through the basic pipeline.

Ultimately, you can (or will be able to) do science on the MIPS post-BCD products, but you may wish (indeed, at this point, you *should* wish with 70 and 160 micron data) to **refine some things via your own interactive post-BCD processing**. The post-BCD tools used as part of the SSC pipelines are available on the SSC website for your use – they are in a package called **MOPEX** – but there are also many other tools available in the astronomical community for many common tasks. These post-BCD tools can also be used to combine data from more than one AOR.

The SSC MIPS pipelines handle the MIPS 24 micron data completely separately from the MIPS 70 and 160 micron data. For this reason, frequently in this manual, the MIPS-24 data are discussed separately from the MIPS-Ge (70+160) data. MIPS has built-in calibration light sources, called **stimulators** (or **stims**), that flash during the observing sequence (see SOM). Stim usage is crucial for maintaining the Ge calibration.

In Spring 2005, the SSC released a package called the “Ge Reduction Tool (GeRT)” as “contributed software.” These routines include pieces of the SSC Ge pipeline. The GeRT allows users to perform specific additional analysis tasks on their own data. Most people will find the archived BCD products (filtered or unfiltered) are suitable for their needs, but with the GeRT, you can either “clean up” the BCDs, or reprocess the raw data. The initial release worked only on Solaris platforms; versions for multiple platforms are expected in early 2006.

Raw MIPS data from all bands are available for those observers wishing to attempt processing of their data from the beginning (using the GeRT or other routines). Because the entire pipelines are not publicly available, observers truly wishing to reprocess *all* of their own data (24, 70, and 160 microns) from scratch will need to write their own code. Writing your own code is strongly **not** recommended for Ge data in particular because of the variety of difficult-to-calibrate germanium detector behaviors. Note that raw MIPS-24 data are in “Sample-up-the-Ramp” mode (SUR; see SOM), so they report DN/0.5 sec= “slope” or count rate for units of MIPS-24 uncalibrated images.

What to do if something is wrong ... Data delivered to observers (or placed in the Archive) have passed our Data Quality Analysis (DQA) process. Observers who believe that there is something wrong with their data that the DQA team did not catch (including anomalously high CR hit rates) should explain what they think is wrong with their data in an email message to the Spitzer Helpdesk at help@spitzer.caltech.edu. A response will be sent within 2 business days, if not sooner. If there is something wrong with the observation, the observation may be declared ‘failed’ and repeated. More information about failed observations can be found in the Spitzer Observing Rule #13 (see SSC website). Note that any request for a repeated observation must be filed within two months of your data being made available to you, and the SSC Director reserves the right, in cases where the request for a repeated observation is approved, to place the failed/degraded observations into the public Archive immediately. The request

for a repeated observation will not be granted when the PI has committed an error in specifying the AOR.

Copious **additional documentation** (including a list of acronyms and an ever-growing suite of step-by-step data analysis cookbooks) is available on the **SSC website**, <http://ssc.spitzer.caltech.edu/>.

2.3 *On-orbit realities of MIPS arrays*

There are several ways in which MIPS behaves differently than was expected, pre-launch.

The 24 μm array works exactly as anticipated, except that it is a factor of ~ 2 **more** sensitive than expected. There are only 22 bad pixels in this array; the bad pixel mask (pmask) appears in Figure 2.2 (and on the SSC website) and the bad pixels are listed individually in Table 2.1 (the numbering starts with 1,1 in the lower left corner). There is some contamination on the pick-off mirror (POM) that feeds MIPS, and the scan mirror position does not repeat position exactly from campaign to campaign. In both cases, the 24 micron array is the most affected; see Section 6.1.

The 70 μm array suffers from thermally-activated high resistance in a cable connection that is external to the instrument, but feeds it. This has resulted in a fixed-pattern noise on one side of the array (side B, on the right) that renders that side inoperable. The signal-to-noise ratio and sensitivity are much better on the other side (side A, on the left). Also, one readout on side A (located in the lower right corner of that side, next to side B) is inoperative. The “good side” of the array (side A) is not as sensitive as was anticipated. Observers should plan at least 3 or 4 times redundancy to ensure good data. Mitigation strategies for improving data from side A have been implemented in the pipeline and are summarized below in Section 7; side B is no longer returning useful data. Bad pixel masks (pmasks) showing these effects are shown in Figure 2.3 and are available in fits format on the SSC website. For data taken in IOC/SV or the first 4 MIPS campaigns, the bias setting of the 70 μm array was set at a level that attempted to increase the sensitivity of both sides of the array, but a consequence was that the stimulator flashes left latents in the data. Data taken in MIPS-5 or later have a different bias setting and therefore weaker stim latents. See Section 7.9 below for more information.

One block of 5 contiguous pixels in the 160 μm array exhibits anomalous behavior attributable to a thermally-activated short in cabling external to MIPS but well inside the CTA. In data oriented as observers receive it, this block is located in the bottom row; it is the third group of 5 pixels in from the left. The array is not as sensitive as was anticipated. Observers should plan at least 3 or 4 times redundancy to ensure good data. Bad pixel masks (pmasks) are shown in Figure 2.4 and are available in FITS format on the SSC website.

During the early part of the mission, 160 μm signals from K stars were detected to be about a factor of five stronger than expected. Review of the instrument

design revealed a weakness in the stray light control that results in a short-wavelength (1-1.6 μm) light leak in this band. See discussion below in Chapter 7.

Table 2.1: Bad pixels in 24 micron array.

Pixel # (x)	Pixel # (y)
1	127
1	128
2	127
2	128
3	127
3	128
4	128
42	128
52	86
52	87
53	85
53	86
53	87
53	88
54	86
54	87
100	101
101	100
101	101
101	102
102	101
112	25

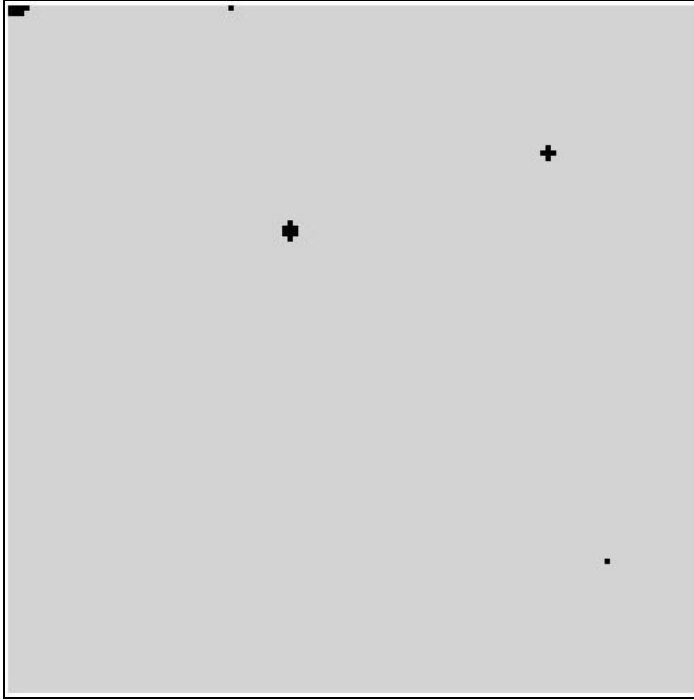


Figure 2.2: Bad pixel mask for 24 microns; black is bad pixels.

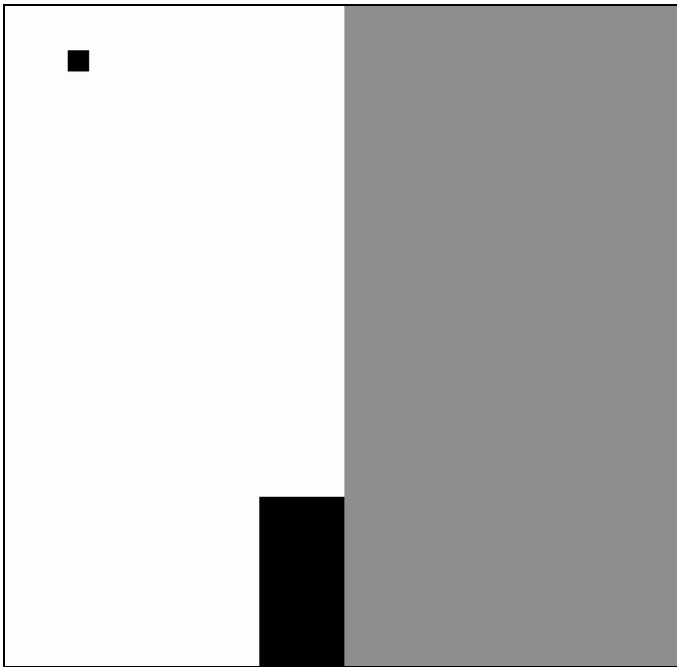


Figure 2.3: Bad pixel mask (pmask) for MIPS-70 data. Black is bit 14, bad pixels; grey is bit 8, bad half of the array.



Figure 2.4: Bad pixel mask (pmask) for MIPS-160 data. The center stripe has no detectors (see SOM for details), and the “bite” in the lower right is the inoperative readout.

3 Getting started

3.1 Using the Archive

The Archive interface is a program called Leopard. This, plus Spot, make up the Spitzer Pride (as in, a group of cats, since Spot's icon is a cheetah). This software can be obtained from the SSC website, and is installed as one package. Please see the Leopard Manual for a comprehensive review of how to retrieve your data, also obtainable from the SSC website. There are also step-by-step data retrieval examples available as part of the suite of SSC data analysis cookbooks.

The Archive interface is fairly straightforward. However, we'd like to highlight a few items.

If you have multiple AORs in the Archive Query Results window and have selected various wavelengths for retrieval for various AORs, the data product types you choose will be delivered (if they exist) for ALL the wavelengths for all of the AORs. You cannot choose to download just the BCD products for one AOR and the BCD and Post-BCD products for another AOR within the SAME download session. You can download them serially within one Leopard session, selecting the first AOR and its products, request the download and while that is occurring, select the other AOR and its data products. Be sure to unselect the wavelengths for the first set.

MIPS produces a LOT of data, and exactly how much is a strong function of the observation mode and (in the case of scan), the scan leg length and speed. Be sure you have enough disk space. The SSC encourages Spitzer Archive users to select the 'Download Directly' option for data delivery. Our FTP staging disk area is only so large and delivery of your requested data may be delayed if the FTP area is too full to contain your request.

Even if you wish to reprocess your BCDs to remove instrumental artifacts, there is no particular need to download the raw data. Starting from the BCDs is just fine for most purposes.

Leopard is smart enough to pick up where it left off if a network hiccup interrupts your data transfer.

3.2 Filenames and most important files

3.2.1 BCDs

All MIPS raw data or BCDs have the same basic filename pattern: SPITZER_M+chnlnum_aorkey_expid_dcenum_version_type.suffix
The "M" stands for MIPS. "CHNLNUM" is the header keyword for "channel number," and channel 1 = 24 μm , channel 2 = 70 μm , and channel 3 = 160 μm . The AORKEY (also a header keyword) is a unique 10-digit number assigned to each AOR in our operations database. The EXPID (=exposure id, or number, also a header keyword) and DCENUM (=DCE number, also a header keyword) refers

to where in the observing sequence this particular frame was obtained. The “version” refers to the number of times that this particular data set has been reprocessed through a validated pipeline. As our understanding of the instrument matures and the pipelines evolve, we anticipate reprocessing everything in the Archive, at which point this number will increment. (Note that the reprocessing does not occur instantaneously; since MIPS generates a lot of data, it takes time to reprocess it. We encourage users to join our general interest mailing list or the MIPS interest group mailing list – see the SSC website – to be notified of such events.) Finally, “type” and “suffix” can be any of a variety of abbreviations, referring to the kind of file and its contents, like “bcd” and “fits,” respectively.

The most important MIPS-24 BCD file type for most users is the `*bcd.fits`, which is the final, best BCD product.

For 70 and 160 microns, there are two important BCD files: `*_bcd.fits`, and `*_fbcd.fits`. We currently recommend the application of a median high-pass-filter for scan maps of regions containing faint point sources (`*_fbcd.fits`), and the standard data reduction (`*_bcd.fits`) for bright and/or extended sources. (See additional discussion below.)

A complete list of the types for MIPS-24 are listed in Table 3.1, the types for MIPS-70 are listed in Table 3.3, and for MIPS-160 in Table 3.5. Additional information on these files, as well as any updates to this information between document releases, is posted on the SSC MIPS website.

Bit mask definitions for the arrays appear in Table 3.2 for MIPS-24 and Table 3.4 for MIPS-Ge. The bad pixel masks (p masks) for all the arrays appeared in Section 2.3.

3.2.2 Post-BCD products

All MIPS post-BCD files have a basic filename pattern that is similar to the BCD files: `SPITZER_M+channel_aorkey_dcenum_version_Enum_type.suffix`. The letter “E” in this example stands for “ensemble” product, but it can also be an “A” for “ancillary” product. In the case of an ensemble product, “dcenum” refers to the first dce that was used in the ensemble creation, “version” refers to the version of that first dce, and “Enum” is the ensemble number.

The most important post-BCD file types for most users are the mosaicked files; these provide at the very least a quick look at your data. Most Ge users in particular will want to regenerate the mosaics along with the rest of the post-BCD products with parameters customized for a particular application; see Section 7 below for some examples.

A complete list of the file types for MIPS-24 are listed in Table 3.1, the file types for MIPS-70 are listed in Table 3.3, and for MIPS-160 in Table 3.5. Additional information on these files, as well as any updates to this information between document releases, is posted on the SSC MIPS website.

Table 3.1: Complete list of file types for MIPS-24.

Abbreviation	Type	Contents of file
*raw.fits	Raw	Raw pixel data with final product header and pointing; 1 st plane is slope, 2 nd plane is the first difference image.
*bcd.fits, *bcd.log	BCD	BCD image (and log file from its creation); saturated values in the slope image have been replaced by the first difference values above a threshold.
*bunc.fits	BCD	Error image associated with the BCD image.
*brmsk.fits	BCD	Outlier mask image associated with BCD.
*bbmsk.fits	BCD	Bit mask associated with BCD, where different bits signify important characteristics of the data; bit definition in Table 3.2.
*slope.fits	Raw	Calibrated BCD slope image.
*slunc.fits	Raw	Error image associated with the slope image.
*slpmk.fits	Raw	Bit mask associated with slope image, where different bits signify important characteristics of the data; bit definition in Table 3.2.
*diff.fits	Raw	Calibrated first difference image.
*dfunc.fits	Raw	Error image associated with the first difference image.
*dfmsk.fits	Raw	Bit mask associated with first difference image, where different bits signify important characteristics of the data; bit definition in Table 3.2.
*msaic.fits, *msunc.fits, *mscov.fits	Post-BCD	Output fits images and log for mosaic routine; in order: image, uncertainties, and coverage map.
*bmed.fits	Post-BCD	Median of all stacked BCDs in AOR (new in S12)
*bmedu.fits	Post-BCD	Uncertainty in median BCD stack (new in S12)
*irsa.tbl	Post-BCD	List of 2MASS sources that occur in this field.
*prefn.tbl	Post-BCD	Table for pointing-refinement-corrected keywords and uncertainties.

Table 3.2: BCD bit bmask definitions for 24 microns.

Bit	Condition
0	Incomplete or questionable row-droop correction (rowdroop)
1	No row-droop correction applied (rowdroop)
2	Hard saturated (satmask)
3	Read-2 correction could not be applied (rowfluxcorr)
4	Saturation corrected and slope value replaced by difference value (desatslope and satmask) (NB: replacement only matters for those pixels that are soft-saturated, e.g., those for which the first difference exceeds a threshold (see section 4.2.1).
5	Latent-image flag
6	Droop removed using questionable value (droopop) (NB: if the pixel is saturated or actually missing from the downlink [bits 13 and 14 respectively], the droop correction will be unreliable.)
7	
8	Flat field could not be applied (flatap)
9	Radhit detection (radhitmedfilt)
10	
11	Pixel masked in pmask - bad hardware state (satmask)
12	Non-linearity correction could not be computed (slopecorr)
13	Soft saturated (satmask)
14	Data missing in downlink (cvti2r4)
15	reserved: sign bit

Table 3.3: Complete list of file types for MIPS-70.

Abbreviation	Type	Contents of file
*raw.fits	Raw	Raw pixel data with pointing in header.
*bcd.fits	BCD	Calibrated BCD image.
*fbcd.fits	BCD	Filtered calibrated BCD image; the median filter is optimized for point sources on a uniform background . Use at your own risk for other applications.
*bunc.fits	BCD	Error image associated with BCD image.
*fbunc.fits	BCD	Error image associated with fBCD image.
*brmsk.fits	BCD	Outlier mask image associated with BCD.
*bmask.fits	BCD	Bit mask associated with the BCD image, where different bits signify important characteristics of the data; bit definition in Table 3.4.
*msaic.fits, *msunc.fits, *mscov.fits	Post-BCD	Output FITS images for mosaic routine; in order: image, uncertainties, coverage map.
*mfilt.fits, *mfunc.fits, *mfcov.fits	Post-BCD	Output filtered FITS images for mosaic routine; in order: image, uncertainties, coverage map.

Table 3.4: Bit mask definitions for Ge data.

Bit	Condition
PMASK	
2	Noisy Pixel
3	Bad electronic nonlinearity
8	Bad half of 70 micron array
14	Bad pixel (e.g., bad readout)
15	reserved: sign bit
BMASK	
0	Stimflash DCE
3	Saturated sample(s) found in raw data
4	
5	Data near stimflash warning
6	Stim extrapolation warning
7	
8	Raw DCE has missing sample(s)
9	Radhit(s) found in raw data
10	Uncertainty Status
11	Bad pixel as defined by the PMASK
12	Slope calibration failed
13	
14	Missing layer, NaN, and/or bad data)
15	Reserved: sign bit
CMASK	
13	No valid calibration
15	Reserved: sign bit

Table 3.5: Complete list of file types for MIPS-160.

Abbreviation	Type	Contents of file
*raw.fits	Raw	Raw pixel data with pointing in header.
*bcd.fits	BCD	Calibrated BCD image.
*fbcd.fits	BCD	Filtered calibrated BCD image; the median filter is optimized for point sources on a uniform background . Use at your own risk for other applications.
*bunc.fits	BCD	Error image associated with BCD image.
*fbunc.fits	BCD	Error image associated with fBCD image.
*brmsk.fits	BCD	Outlier mask image associated with BCD.
*bmask.fits	BCD	Bit mask associated with the BCD image, where different bits signify important characteristics of the data; bit definition in Table 3.4.
*msaic.fits, *msunc.fits, *mscov.fits	Post-BCD	Output FITS images for mosaic routine; in order: image, uncertainties, coverage map.
*mfilt.fits, *mfunc.fits, *mfcov.fits	Post-BCD	Output filtered FITS images for mosaic routine; in order: image, uncertainties, coverage map.

3.3 What do all of these files mean?

Now that you have retrieved your data, you may be impressed (or distressed!) at the sheer number of files you have downloaded. The most important files are listed above in the text, but that is only the tip of the iceberg; a complete listing is given with simple descriptions above and on the SSC website. HOWEVER, if you are a **true beginner** to MIPS, then in order to really figure out what all of these files mean, the first step is to obtain the AOR(s) used for these observations. AORs are essentially the list of commands that are sent to the spacecraft to execute observations, so you can see why it will be beneficial for understanding your abundance of files. At this time, the Archive does not return the corresponding AORs with your data, so you will need to go retrieve it yourself.

3.3.1 Retrieving the AOR file(s)

You are either retrieving your own data, or public data out of the Spitzer Archive; in either case, you can use Spot to download the actual AOR file that was used for the observation. Spot is the software observers use to prepare observations, and is obtainable from the SSC website, along with a User's Guide. Once you have downloaded and installed the software on your computer, ensure your computer is hooked to the internet, go to the File menu, and select "View Program." Enter the program id ("pid") for your program. When you retrieved files from the Archive, the download page should have told you the pids for each of your observations. If you do not know the pid for your program, you can do

one of several things: (1) grab one of your BCD or post-BCD FITS files and find the value of the header keyword “PROGID,” or (2) go to http://ssc.spitzer.caltech.edu/roc/spitzer_programs.txt for a comprehensive list of all Spitzer programs, and locate the pid for yours, or (3) use the ROC search tool to locate your observation by coordinate, and determine the pid from the output of the search tool. Enter the pid in the Spot dialog box. Within a few seconds, Spot talks to our servers at the SSC and downloads the entire program to your computer. From the File menu, choose “Save AORs and targets” and save the AOR file to local disk for later reference. If you are interested in just a few AORs from a large program (and there are many of those), you may want to delete the irrelevant AORs from the program first. Before you ask, no, at this time, there is no way to delete multiple AORs at once; this is planned for a future version of Spot.

If you have retrieved data from multiple programs, you will unfortunately have to repeat this process for each one. Unfortunately, each time you “View Program,” you have to delete all your AORs before you can download a new program. In practice, you can load a program, delete the AORs you don’t care about, and save the good ones to a file, then delete all the AORs. Repeat as necessary. Once complete, load from file each of the individual AORs – you do not need to delete all of your AORs, just keep loading in AORs from individual files. Then save this master list to a file for future reference.

Some observations in our database are from the early part of the mission. During these early phases, AORs were not always used for Spitzer observations; instead of AORs, these are called Instrument Engineering Requests (IERs). The current version of Spot does not handle IERs, and will not display anything if you try to view programs containing them. Contact the Helpdesk if you encounter this problem, and we will forward the observing parameters to you via email.

Once you have a set of AORs loaded into Spot, note the column entitled “Label.” Each AOR’s label was defined by the observer requesting the observations. It is one of the identifying characteristics of that specific AOR, and appears in the FITS headers of the resulting data as AORLABEL. The AOR label, though unique to the program, is not enough to uniquely identify the AOR in our database. Each AOR has a 10-digit number assigned to it called the AORKEY, which is, in fact, the unique identifier in the Archive. The AORKEY is part of the filename of each of the files you obtain from the Archive. Spot also has a column for “TARGET” – this was also defined by the observer requesting the observations, and also appears in the resulting FITS header, under the keyword “OBJECT.”

3.3.2 Visualizing your observation, or how the files relate to the AOR

From within Spot, you can also visualize your observation on the sky. Select (click on) an AOR. Go to the “Images” menu and select an image catalog to query. Many MIPS observations cover a large area, so if you are new at this, choose ISSA to obtain an IRAS All-Sky Survey image (though certainly you can

choose any other wavelength or even use your own image). Once Spot has downloaded and displayed the image, select from the “Overlays” menu the option “current AOR on current image.” Enter a date for the visualization; it can be useful (but is not essential) to use the specific date and time of your observation. If you do not already know this, you can (1) find one of your observation’s BCD (or post-BCD) FITS files, and use the value of the DATE_OBS keyword, or (2) go to <http://ssc.spitzer.caltech.edu/approvdprog/sched/>, locate your observation in the observation logs, note the date and time, and enter it into Spot.

After several seconds, Spot will overlay the observation. *For each frame displayed, you have at least one BCD in your data packet as downloaded from the Archive. This is why you have so many files!*

(A brief side note: Spot can do many nifty things, including overlaying multiple images, like your Spitzer data on top of IRAS or MSX, with a variety of transparencies. See the Spot manual for more information.)

As mentioned above, complete list of the types for MIPS-24 appears in Table 3.1, the types for MIPS-70 are listed in Table 3.3, and for MIPS-160 in Table 3.5. Additional information on these files, as well as any updates to this information presented here, is posted on the SSC MIPS website.

3.3.3 Files you think you should have, but don’t (or extra files you have but think you shouldn’t)

Because all three of the arrays are “on” whenever MIPS is on, even if an observation requests just 24 micron data, data are obtained in the other arrays. This makes intuitive sense in the case of scan maps, where valid data are clearly simultaneously obtained in all three arrays. However, what may surprise you is that even for 24 μm photometry mode observations, there are data obtained at both 70 and 160 μm . Note that these other two arrays image slightly different parts of the sky compared to the 24 μm array; they create in the end unfilled maps because the telescope and scan mirror motions are optimized for the 24 μm array. In this specific case, the stimulator frequency is not set properly to obtain useful 70 and 160 μm data. Here, the 24 μm data are the “prime” data set, and the Ge data are the “non-prime” data. For 70 or 160 micron photometry sequences, the 24 micron data are perfectly fine to use, but they still create an unfilled map. The implications of this data taking strategy are summarized in Table 3.6 below. The FITS header keyword PRIMEARR tells you whether data in a given file were obtained with the prime array; PRIMEARR=1 for prime data, 2 for data that are not prime, and 3 for data that are not valid at all (e.g., Ge data during 24 μm photometry). **Mosaics are only produced for PRIMEARR=1 Ge data, and BCDs are not even produced for PRIMEARR=3 data.** Moreover, in certain scan mirror positions, it is possible to obtain PRIMEARR=3 data for 24 micron data; in this case, the 24 micron array is in the dark. Note also that non-prime 24 micron data may not be correctly flat-fielded given the pick-off mirror contamination; see Section 6.1.

The Archive will serve you non-prime data – it provides BCDs for PRIMEARR=1 or 2, but not 3. It only provides mosaics for PRIMEARR=1, however. If you seem to have much more photometry mode data than you expect, this may be the reason. If you recreate your mosaic and seem to have non-contiguous sky coverage, this may also be the reason – you have combined PRIMEARR=1 and 2 data. If you look at your photometry mosaic and find that the data appear to have missed the target, you are probably looking at your PRIMEARR=2 data rather than your PRIMEARR=1 data; your target will be centered in the PRIMEARR=1 data.

Because MIPS BCDs are high quality, most people should not need the raw data, but it is currently provided (for PRIMEARR=1, 2, or 3) through the Archive interface.

NB: IT USED TO BE, if you wish to obtain non-prime Ge raw data, you had to download the BCDs. Even though the S12 and prior pipelines do not produce BCDs from these non-prime data, the archive had thought of these data as not quite plain raw data, so it served them as part of the BCD download, rather than the raw download. DATA PROCESSED UNDER S13 do not have this ‘feature.’

Table 3.6: Prime and non-prime data

Mode	“Prime” array	Notes on the non-prime data
Scan	All three arrays	No non-prime data
24 μm photometry	24 μm	Ge data has stims without proper background, covers unfilled portion of sky. PRIMEARR=1 for 24; PRIMEARR=3 for Ge.
70 μm photometry	70 μm	24 and 160 μm data covers unfilled portion of sky, but should produce useful serendipitous data. Mosaics may be produced but may look strange due to the amount of “dead space.” PRIMEARR=1 for 70; PRIMEARR=2 for 24 and 160.
160 μm photometry	160 μm	24 and 70 μm data covers unfilled portion of sky, but should produce useful serendipitous data. Mosaics may be produced but may look strange due to the amount of “dead space.” PRIMEARR=1 for 160; PRIMEARR=2 for 24 and 70.

3.4 What do all of these header keywords mean?

As with other NASA observatory data, there are many, many header keywords in BCD data, many of which pertain to instrument telemetry rather than astronomy, per se. This section highlights the most important header keywords for BCD MIPS data. Comprehensive lists of both BCD and post-BCD header keywords are in the Appendix (an alphabetical list is on the SSC website). Most

of the usual FITS header keywords you expect appear in both the BCD and post-BCD products (CRVAL1 and 2, CRPIX1 and 2, BUNIT, etc.). Here, we highlight some Spitzer-specific keywords of interest.

AORLABEL is the name of the AOR as defined by the observer requesting the observations. This name is unique for each AOR within the program, but it is not unique to the entire mission (which is why we have the AORKEY as well, see next paragraph below). **OBJECT** is the observer-defined target name, and may or may not relate directly to the AORLABEL. (See section 3.3.1 above for how to determine the AOR label and target for any given AOR.) **PROGID** is the program identifier for the program that contains the AOR that was used to obtain the data in question; see section 3.3.1 above for why this can be useful.

Each AOR has a 10-digit number called the **AORKEY**, which is, in fact, unique to each observation for the entire Spitzer project. This value is mostly designed to be only computer-readable, but may be of use for, e.g., corresponding with the SSC regarding a specific AOR. The AORKEY is a header keyword, and is also part of the filename for each BCD. Other elements of the filename (**CHNLNUM**, **EXPID**, **DCENUM**) are also header keywords.

AOT_TYPE tells you if the data were taken in scan or photometry mode (or in any of the other MIPS modes). This is particularly useful for double-checking the pixel scale of your 70 μm observations (fine or default). **FOVNAME** is the name of the field of view used for the observations; see Table 4.4 in the SOM for a comprehensive list.

PRIMEARR tells you if the current data is ‘prime’ or not; see section 3.3.3 for more on these issues.

CREATOR includes the SSC software version, e.g., S13 (see Sections 4.2 and 4.3).

DATE_OBS is the time at the start of the AOR, good to within at least 1 second. There are many other times in the header, but if the specific time of the start of your AOR matters, this is the one to use.

ANNTIME is time since the last Ge anneal. **MEDFLTN** is the width of the median filter used to produce the *fbcd files; see Section 7.

Distortion in Spitzer images is represented through header keywords consistent with the latest FITS standard. The most recent versions of your favorite image display programs are able to handle this, but some older programs may not. There is a memo about distortion header keywords in Spitzer images linked in to the archives and analysis pages here: <http://ssc.spitzer.caltech.edu/archanaly/>. For more on distortion, see below or the SOM.

The coordinates and pointing as represented in the **RA_HMS** and **DEC_DMS** and related keywords are the actual pointing (in sexagesimal), reconstructed on the ground from telescope and scan mirror telemetry. If you prefer decimal degrees, look at **CRVAL1** and **CRVAL2**. There are also header keywords for predicted and/or requested positions, but these values reflect when the observation was scheduled, not necessarily when (or where) it was actually executed.

Somewhat confusingly, some of the keywords that appear in the BCD are redefined in the post-BCD stage. In the BCD, **PA** is the position angle of axis 2, in degrees E of N, so positive values are counter-clockwise. **PXSCAL1** and **PXSCAL2** are the scale for axes 1 and 2, respectively, in arcsec/px, at position CRPIX1, CRPIX2. In the Post-BCD, however, **CROTA2** is the orientation of axis 2, in degrees W of N, so positive values are clockwise. **CDELTA1** and **CDELTA2** are the scales for axes 1 and 2, in degrees per pixel.

Note that the predicted pointing header keywords may not necessarily be correct. The spacecraft really is pointing in the correct location, but the header keywords are not necessarily correct.

3.5 Major caveats for the current version of the pipeline

Although the BCD products for all MIPS bands will (not may!) undergo improvements in the coming months/years, the MIPS-24 BCD products are reasonably stable. The MIPS-Ge BCD products may still undergo significant changes; see the discussions below.

The Ge post-BCD mosaics are typically for “quick-look” purposes only. Observers are strongly encouraged to make their own mosaics based on the BCDs/filtered BCDs or their own post-pipeline manipulated BCDs; see Section 7

The mosaic coverage map header keyword BUNIT should be dimensionless, but is instead MJy/sr.

For additional details on the pipelines, including whether or not you need to wait for a reprocessing, see Section 4.

3.6 Pipeline history

A history of the major changes in (and caveats for) each version of the pipeline can be found on the SSC website:
<http://ssc.spitzer.caltech.edu/archanaly/plhistory/> .

3.7 Basic toolset for working with MIPS data

MIPS data are produced as standard FITS files, appropriate for use in IRAF, IDL, or your own favorite image analysis software.

HOWEVER, Spitzer images are in units of *surface brightness*, MJy/sr, which may be unfamiliar to observers coming from other wavelength regimes. The main implication is that photometry as performed using the same routines used for, e.g., optical data **will not return the correct values**. Section 3.7.1 covers these items.

Color corrections may be important for some observers; see Section 3.7.4. Observers doing aperture photometry will want to make aperture corrections, and, on a related front, observers doing PSF fitting may be interested in the PSF shape itself; Section 3.7.5 discusses the PSF.

3.7.1 Units and fluxes

MIPS images are in MJy/sr. (To convert from MJy/sr to microJy/arcsecond², multiply by 23.5045.) When summing up the flux incident on a set of pixels for, e.g., aperture photometry, you need to multiply by the number of steradian per pixel. See Table 3.7 for *average* actual pixel sizes; see the BCD header values of PXSCAL1 and PXSCAL2 in your own data for values specific to your program because the pixel scale changes slightly as a function of mirror position. Note that these values may be refined as our knowledge of the instrument matures. One square arcsecond is 2.3504×10^{-11} steradian.

Note that *post-BCD products are resampled images* such that the pixels have different sizes from the pixels in the original BCDs. Please check the post-BCD header keywords CDELTA1 and CDELTA2 for the pixel sizes (in degrees) in any given mosaic. Example default mosaic pixel sizes for MIPS products are given in Table 3.7; to double-check that your data have these values, see the values of CDELTA* in the header of your data. Note also that the orientation of the mosaic is often different than the BCD (see header keyword PA in the BCD and CROTA2 in the mosaic). The SSC tool APEX reads the header keywords properly and reports flux density units of microJy for point sources, not MJy/sr.

Table 3.7: Sizes of MIPS pixels for MIPS BCD and post-BCD products.

MIPS mode/array	Average BCD PXSCAL1 (arcsec)	Average BCD PXSCAL2 (arcsec)	Default post-BCD product pixel sizes (arcsec)
24 micron	2.49	2.60	2.45x2.45
70 fine scale	5.12	5.28	4.0x4.0
70 default scale	9.88	10.07	4.0x4.0
160 micron	16.0	18.0	8.0x8.0
SED			9.80

3.7.2 Conversion Factors

The best conversion factors between instrumental units and MJy/sr to use for any given data set are included within the headers of the data themselves; grep on BUNIT and FLUXCONV. As of this writing, the best conversion factors are listed in Table 3.9. The MIPS-24 instrumental units are DN/s, but note that the instrumental MIPS-Ge units are dimensionless after the stimflash response calibration. Uncertainties in the conversion values are often limited by our astrophysical understanding of stars in the far infrared, and thus the uncertainties are likely to decrease with time.

This conversion factor at 24 microns was derived from 3 sec exposures. The difference in the conversion factor for scan mode and 10 and 30 sec exposure is under study but should not be more than 2-8% different.

Table 3.8: S13 conversion from instrumental units to MJy/sr.

Array	Conversion factor	Uncertainty
24	0.0447	4%
70	702.	7%
70 fine scale	2808.	15%
SED	20572.7	10%
160	44.7	12%

Table 3.9: S10 conversion from instrumental units to MJy/sr.

Array	Conversion factor	Uncertainty
24	0.04391	10%
70	634.	20%
160	42.	20%

3.7.3 Magnitude Zero Points

Dr. C. Engelbracht has computed MIPS magnitude zero points using the Kurucz (1993) Vega model, which has then been scaled to the Rieke et al. (2006, in prep.) 10.6 μ m zero point of 35.03 ± 0.4 Jy. He has further assumed that Vega is 0 magnitudes in all MIPS bands, and has computed fluxes at 23.68, 71.42, and 155.9 μ m. The resultant zero points are in Table 3.10.

Table 3.10: Magnitude zero points

Wavelength (microns)	Zero point (Jy)	Uncertainty (Jy)
23.68	7.14	0.0815
71.42	0.775	0.00885
155.9	0.159	0.00182

3.7.4 Color Corrections

The conversion of signal to equivalent monochromatic flux density at the weighted average wavelength for the observation depends on the slope of the spectrum of the source across the MIPS bands. For the purposes of comparing sources with differing spectral behavior, the observed fluxes should be color-corrected. Such correction is also required to obtain accurate flux densities. In Table 3.11, we tabulate the color corrections for a representative range of blackbody source temperatures, and Table 3.12 contains color corrections for power laws. Color corrections can also be calculated using the online Performance Estimation Tool (PET) on the SSC website. Source flux densities produced by pipeline processing of MIPS data at the SSC do not include color

corrections – **the observer is responsible for determining whether color corrections are necessary and for applying them.**

Table 3.11: Nominal color corrections vs. blackbody source temperature.

Lambda (μm)	Source Temperature (K)											
	10^4	5000	1000	500	300	200	150	100	70	50	30	20
23.68	1.000	0.999	0.992	0.983	0.970	0.957	0.948	0.947	0.986	1.119	2.031	7.005
71.42	1.000	0.999	0.995	0.989	0.980	0.970	0.959	0.938	0.914	0.893	0.901	1.052
155.9	1.000	1.000	0.999	0.997	0.996	0.993	0.991	0.986	0.979	0.971	0.954	0.944

Table 3.12: Nominal color corrections for power laws

Lambda (μm)	Power law indices (alpha) where $F_\nu \propto \nu^\alpha$						
	-3	-2	-1	0	1	2	3
23.68	0.967	0.960	0.961	0.967	0.981	1.001	1.027
71.42	0.933	0.918	0.918	0.932	0.959	1.001	1.057
155.9	0.965	0.959	0.959	0.965	0.979	1.000	1.029

The flux of a source is typically determined relative to calibrator stars ($F_\nu \propto \nu^\alpha$) using the ratio of the stellar and source signals. The nominal flux derived in this manner must be corrected in order to derive the true monochromatic flux density at the weighted average wavelength for the band by dividing by the appropriate factor in Table 3.11. The result will be the ‘best estimate’ of the true monochromatic flux density of the unknown source at the weighted average wavelength. The photometric bandwidths of the MIPS filters were selected to make these corrections modest, except for sources whose blackbody spectral energy distributions peak at wavelengths longer than the photometric band. In these cases, large corrections are unavoidable; **observers measuring cold objects should take note.**

Note that MIPS and IRAC calculate color corrections slightly differently; the origin of this difference is that our response functions are in slightly different units. As such, to reproduce the color corrections displayed here and in the online PET, you will need to do the following. Take the response functions from the website (units of electrons per unit energy) and divide by lambda (to get electrons per photon). MIPS defines λ_0 as follows:

$$\lambda_0 = \frac{\int \lambda R_\lambda d\lambda}{\int R_\lambda d\lambda} \quad (3.1)$$

where R_λ is the response function. MIPS color corrections are referenced to a 10,000 K blackbody:

$$K = \frac{\int \frac{F_\lambda}{F_{\lambda_0}} \lambda R_\lambda d\lambda}{\int \left(\frac{\lambda_0}{\lambda}\right)^5 \frac{e^{\frac{hc}{\lambda_0 k T_0}} - 1}{e^{\frac{hc}{\lambda k T_0}} - 1} \lambda R_\lambda d\lambda} \quad (3.2)$$

where :

$T_0=10,000$ K,

$\lambda_0=23.675$ microns at MIPS-24,

$\lambda_0=71.440$ microns at MIPS-70,

$\lambda_0=155.899$ microns at MIPS-160, and

$hc/k = 14388$ microns x K

For an input blackbody at T_{eff} , the numerator of equation 3.2 becomes:

$$\int \left(\frac{\lambda_0}{\lambda}\right)^5 \frac{e^{\frac{hc}{\lambda_0 k T_{\text{eff}}}} - 1}{e^{\frac{hc}{\lambda k T_{\text{eff}}}} - 1} \lambda R_\lambda d\lambda \quad (3.3)$$

and for power laws, the numerator becomes (alpha=2 for the Rayleigh-Jeans limit):

$$\int \left(\frac{\lambda_0}{\lambda}\right)^{\alpha+2} \lambda R_\lambda d\lambda \quad (3.4)$$

3.7.5 PSF characterization

Characterizing MIPS PSFs can be difficult because MIPS has five different observing modes, large arrays (distortion!), multiple mirror positions in each mode (distortion!), and large bandpasses (color terms!).

Currently, PSFs produced from the pre-launch version of the program STINYTIM are posted on the SSC website, and these should be appropriate for, e.g., observation planning. (NB: The pre-launch STINYTIM software is also available online if you want to generate your own PSFs; see the contributed software archive.) Because the optics are very smooth at these long wavelengths, the STINYTIM simulation actually matches our observed PSF quite well. One way in which there is a significant difference is the short-wavelength light leak at 160 microns; for more information on this, see Section 7.13 below. **Note that the STINYTIM simulation PSFs are oversampled, and the pixel sizes do not match what you actually get with default Spitzer data.**

In general, if you need to do a detailed PSF subtraction, we recommend that you **create one from your own data** (using objects of similar color to your target) to ensure that you have PSF standards of the same color and brightness and observed with exactly the same AOR parameters. The lack of repeatability in

scan mirror position from campaign to campaign makes it necessary to do the PSF observation in the same campaign as the science observation. The SSC will *not* be maintaining a library of PSFs with characteristics spanning the full range of observer needs for PSF subtraction.

There are various ways to create PRFs to carry out point source extraction with APEX, and very detailed documentation can be found on the SSC website. For a single frame source extraction with APEX, e.g. extraction from a MOSAIC, the PRF is slightly different from that one used in single BCDs. There are PRFs posted on the MIPS portion of the SSC website that have been created from BCDs, from mosaics, and from STINYTIM. The empirical PRFs were created using PRF_ESTIMATE (from the MOPEX package), which is a script that combines those stars selected by the user, from a post-BCD mosaic, into a "mosaic PRF". Usually these stars have a high signal-to-noise and no neighbors, i.e. they are the best and cleanest for the job.

How different is the empirical PRF compared with the one derived using STINYTIM? They are not that different, but they are not identical. The main difference is at the depth of the first Airy ring, which is deeper in the STINYTIM PRF. This illustrated by figures that can be found on the SSC portion of the MIPS website.

Please note: There is not a "magic PRF" that will work for every data set.

3.7.6 Aperture Corrections

For aperture corrections, you should also consider constructing your own PSF from your own data, because **aperture corrections may vary for different source colors**. In Figure 3.1, there is a source of 0.5 Jy from the Extragalactic First-Look Survey (XFLS) main field (at 17:23:44.1 +59:05:18, J2000); there are three radii (1.35, 2, 3 times the FWHM, 5.9 arcsec) in white; the black circle is a 100 arcsec radius. Figure 3.2 shows the "curve of growth" to indicate the fraction of the total flux enclosed by smaller apertures.

The Instrument Support Team (IST) at the SSC and the Instrument Team (IT) at the University of Arizona as part of a large project to better understand and to improve the MIPS photometric calibration, have determined different aperture corrections for the current MIPS Photometric modes (24 μm , 70 μm , 70 μm fine scale and 160 μm) plus Spectral Energy Distribution (SED). The tables below are a first attempt to summarize these efforts, and although we don't expect dramatic changes, they should not be taken as the last word on the subject.

These example corrections should be good to ~5%, but we **emphasize again the importance of deriving this yourself for your own targets and data**. Even if you don't have enough point sources in your own data to generate your very own PSF, we strongly suggest deriving your own aperture corrections using the copious public data, or STINYTIM, or the observed PSFs provided on the web.

Table 3.13: Aperture corrections for 24 microns.

Aperture radius (arcsec)	Aperture correction with background annuli of...		
	None	6-13 arcsec	20-32 arcsec
1.5	9.628	9.490	9.630
3	3.097	3.052	3.098
6	1.697	1.698	1.699
6.6	1.647	1.652	1.648
13	1.164	1.175	1.167

Table 3.14: Aperture corrections for 70 microns, default scale.

Aperture description	Aperture radius in arcsec (px)	Aperture correction with background annuli of...			
		None	Large	First Airy ring	First Airy minimum
			39-65 arcsec 3.96-6.60 px	18-39 arcsec 1.83-3.96 px	13-23 arcsec 1.32-2.34 px
Blue PSF (T=3000 K)					
0.5 x HWHM	4 (0.41 px)	11.950	11.967	12.554	12.690
1 x HWHM	8 (0.81 px)	3.410	3.416	3.627	3.676
2 x HWHM	16 (1.62 px)	1.735	1.741	1.968	2.025
Center of first Airy maximum	18 (1.83 px)	1.652	1.659	1.927	1.997
Outside first Airy ring	35 (3.55 px)	1.172	1.185	1.902	2.191
Red PSF (T=15 K)					
0.5 x HWHM	4 (0.41 px)	15.355	15.405	16.166	16.699
1 x HWHM	8 (0.81 px)	4.170	4.186	4.433	4.608
2 x HWHM	16 (1.62 px)	1.871	1.884	2.087	2.244
Center of first Airy maximum	18 (1.83 px)	1.750	1.764	1.994	2.178
Outside first Airy ring	35 (3.55 px)	1.279	1.308	1.937	2.814
Red power law PSF (nu^{-2})					
0.5 x HWHM	4 (0.41 px)	12.869	12.889	13.547	13.688
1 x HWHM	8 (0.81 px)	3.615	3.622	3.850	3.900
2 x HWHM	16 (1.62 px)	1.771	1.778	2.005	2.058
Center of first Airy maximum	18 (1.83 px)	1.680	1.687	1.953	2.017
Outside first Airy ring	35 (3.55 px)	1.197	1.211	1.928	2.188

Table 3.15: Aperture corrections for 70 microns, fine scale.

Aperture description	Aperture radius in arcsec	Aperture correction with background annuli of...			
		None	Large	First Airy ring	First Airy minimum
			39-65 arcsec	18-39 arcsec	13-23 arcsec
Blue PSF					
0.5 x HWHM	4	9.655	9.665	10.031	10.057
1 x HWHM	8	3.066	3.070	3.219	3.230
2 x HWHM	16	1.700	1.705	1.900	1.915
Center of first Airy maximum	18	1.652	1.6549	1.898	1.918
Outside first Airy ring	35	1.169	1.181	1.787	1.855
Red PSF					
0.5 x HWHM	4	10.552	10.563	10.997	10.952
1 x HWHM	8	3.283	3.287	3.456	3.439
2 x HWHM	16	1.725	1.730	1.929	1.907
Center of first Airy maximum	18	1.670	1.676	1.918	1.891
Outside first Airy ring	35	1.195	1.206	1.838	1.746

Table 3.16: Aperture corrections for 160 microns.

Aperture description	Aperture radius in arcsec	Aperture correction with background annuli of...			
		None	Large	First Airy ring	First Airy minimum
			75-125 arcsec 4.7-7.8 px	32-56 arcsec 2-3.5 px	40-75 arcsec 2.5-4.7 px
Blue PSF (T=1000 K)					
0.5 x HWHM	10	9.381	9.389	10.003	9.960
1 x HWHM	20	2.962	2.966	3.215	3.197
1.5 x HWHM	30	1.874	1.877	2.110	2.093
2 x HWHM	40	1.575	1.579	1.891	1.866
Center first Airy min	50	1.437	1.442	1.886	1.848
Red PSF (T=10 K)					
0.5 x HWHM	10	10.083	10.094	10.663	10.718
1 x HWHM	20	3.124	3.128	3.350	3.372
1.5 x HWHM	30	1.931	1.935	2.130	2.150
2 x HWHM	40	1.601	1.605	1.857	1.884
Center first Airy min	50	1.470	1.476	1.833	1.875

Table 3.17: SED aperture corrections

Wavelength (microns)	Smoothing factor	
	1.0 px	1.7 px
3-pixel extraction aperture		
50	1.711	1.841
60	1.841	2.033
70	1.973	2.209
80	2.138	2.394
90	2.341	2.604
100	2.586	2.847
5-pixel extraction aperture		
50	1.535	1.662
60	1.687	1.831
70	1.856	1.997
80	2.016	2.156
90	2.163	2.306
100	2.310	2.456

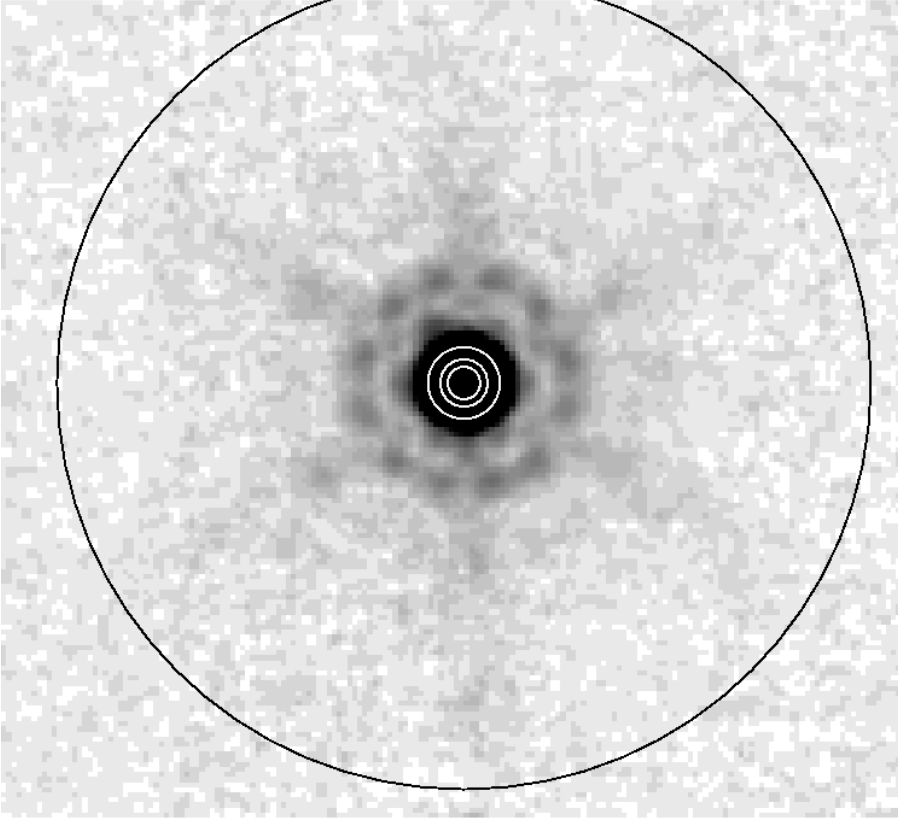


Figure 3.1: Example source from 24 micron Extragalactic First-Look Survey (XFLS) for example aperture corrections.

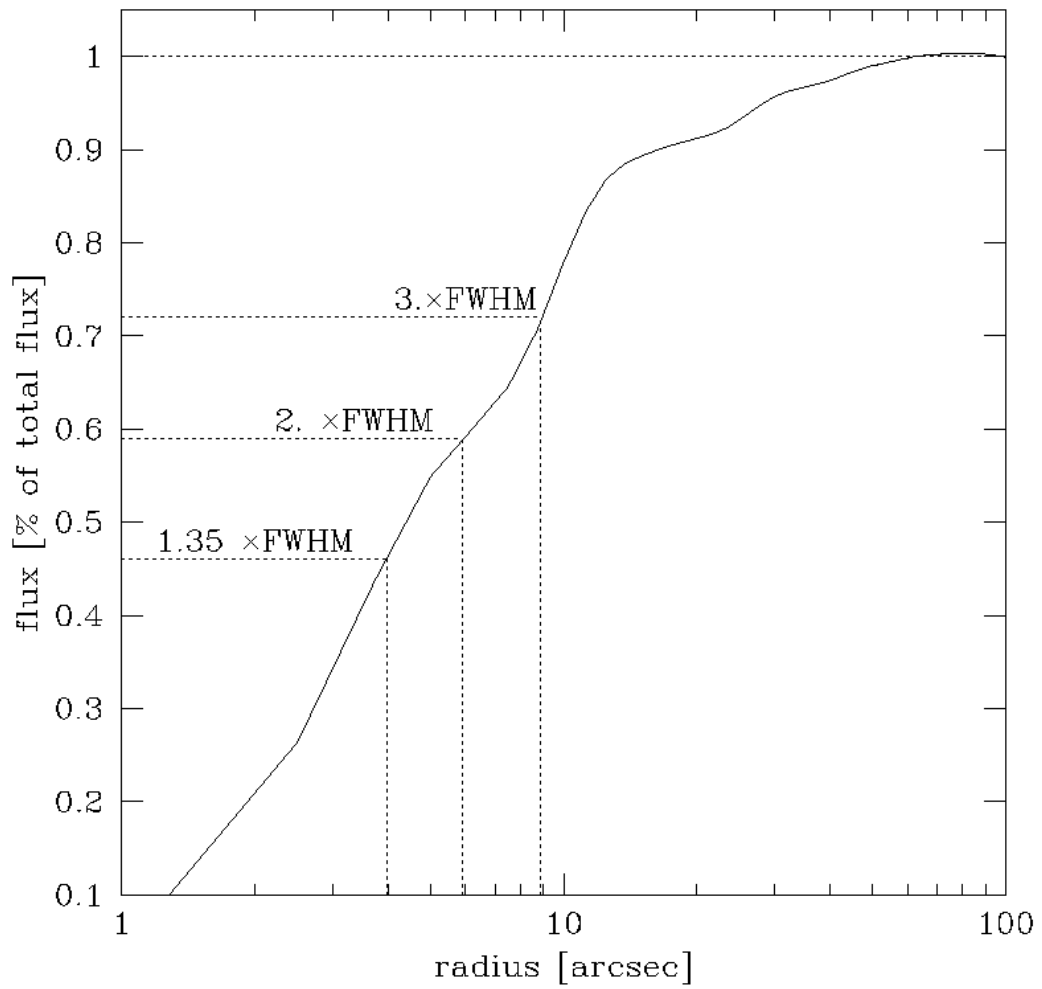


Figure 3.2: Example aperture corrections for 24 micron data (see text). The FWHM is 5.9 arcsec.

4 BCD Pipeline Description

4.1 Introduction

This chapter, combined with the next one, covers how your data get reduced at the SSC, or what we did to your data between when it left the spacecraft and when you get it. As of this writing, the BCD products are for the most part what you should start with when working with MIPS data. The post-BCD data products are a good way to get an overview of your data, but to do science (at least at 70 and 160 microns), you should revert to the BCDs.

As of this writing, the most comprehensive, best description of our BCD pipelines is in a Publications of the Astronomical Society of the Pacific (PASP) article by Karl Gordon et al. (2005, PASP, 117, 503). A copy of this article is also available from the SSC/MIPS website (<http://ssc.spitzer.caltech.edu/mips/>).

Although the Gordon et al. article specifically covers the Data Analysis Tool (DAT) developed by the MIPS instrument team for processing of its own data, the SSC works very closely with the MIPS team and treats the DAT as a testbed for changes to the actual online SSC pipelines. Changes can be made to the DAT on a much more rapid timescale than to our SSC pipelines. As of the Archive opening in May 2004, the DAT and the SSC pipeline produce essentially identical results at the BCD level. The post-BCD processing is so customized to the science and the observation (primarily for Ge data) that the automated pipeline does not reproduce the hand-processed DAT products; see discussions below.

As we increase our understanding of the on-orbit nuances of working with MIPS, our pipelines will undergo additional evolution, and all of the data in the Archive will be reprocessed with the improved pipelines. (Note that the reprocessing does not occur instantaneously; since MIPS generates a lot of data, it takes time to reprocess it. We encourage users to join our general interest mailing list or the MIPS interest group mailing list – see the SSC website – to be notified of such events.) We anticipate that future releases of this Data Handbook will merge with the information from the Gordon et al. article to create a much longer chapter. However, as of this writing, the PASP article is still the best, most complete description of the MIPS pipelines. Additionally, on the SSC web pages, there is an online pipeline change log that records the major changes for each of the SSC pipeline versions.

4.2 The MIPS-24 pipeline

4.2.1 Summary of pipeline

The MIPS-24 pipeline is summarized in the SOM and discussed in more detail in the Gordon et al. paper, as well as Masci et al. (2005), all of which are available on the SSC website. A summary of the most significant steps follows here.

The Si:As array is read out at a constant rate, but this data rate is too high to allow all of the data to be sent to the ground.

Multiple reads of the array are processed on board into a single image consisting of the net integration between resets; the data are fitted onboard by linear regression for each pixel and only the slopes (DN/sample time) for each image are sent to the ground. Another component of the raw data sent to the ground is the “difference image,” which represents the difference of the first 2 reads. On board the spacecraft, the difference image (a 0.5 MIPS-second exposure) is set to zero everywhere except for those pixels whose count rate is large enough to lead to an A-to-D (analog to digital) saturation in the data ramp over the total image integration. This is performed on-board using a nominal (and conservative) difference threshold value of 600 DN/sample time (where one sample time = 0.5 MIPS second = 0.524288 real seconds) over a 30 MIPS second integration, or equivalently, ~50.3 MJy/sr. Later in pipeline processing, a larger difference image saturation threshold is used, 1000 DN/sample time (for a 30 MIPS second integration) or ~83.7 MJy/sr. Above this level, the slope pixels are replaced with difference pixels. In the end, this yields more reliable fluxes for bright sources.¹ Of course, some sources may saturate the ramp even in the first read, leading to what’s called “hard saturation” and then causing the difference value to be zero. The latter cannot be corrected, and the sources will appear to have “holes” where sources saturate (usually in the centers of the PSFs) after processing.

After conversion to floating point and DN/sec, the first step is the “read-2 correction.” An offset in the second read of the 24-micron array causes the SUR (sample-up-the-ramp; see SOM) slope to be too large. This effect, referred to in shorthand as “the read-2 effect,” results in a gradient across the array that depends on the array position and background level. The correction is applied in the regular MIPS pipeline as an analytic function subtracted from SUR slope values.

The Si array suffers from the “droop effect” whereby the output for a pixel is proportional to the photon signal that fell on that pixel plus a signal proportional to the average signal falling over the entire array. (See SOM, both the MIPS and IRS chapters for more discussion of “droop.”) Because saturated pixels will cause the droop to be underestimated, pixels are first “desaturated” using the nonlinearity model and the difference image before the droop correction is calculated. Droop correction is then applied, followed by dark subtraction, nonlinearity correction, flat field division (using mirror position-dependent flat fields), and conversion to units of MJy/sr. Finally, suspected saturated pixels are replaced by those from the first difference image to create reliable slope data

¹ More specifically, the pipeline re-scales this nominal threshold according to the image integration time since a shorter integration can tolerate a larger count rate before the ramp starts to saturate, and hence bias the slope value. The following scaling is used:
 $\text{Difference_Sat_Threshold} = 1907.34 \times (30/\text{EXPTIME}) \times 0.04391 \text{ [MJy/sr]}$,
 where the factor of 1907.34 is (1000/0.524288) DN/real seconds, i.e., the nominal threshold for a 30 MIPS second integration, EXPTIME is the image integration time in MIPS seconds, and the factor of 0.04391 is the conversion factor from DN/real seconds to MJy/sr.

where possible, resulting in a larger dynamic range. Latent images and radhits (cosmic rays) are flagged but not removed at the BCD level. The post-bcd mosaic software is effective in removing radhits from the mosaics (see section 5.3)

4.2.2 S13 pipeline

Starting in mid-November 2005, the current version of the pipelines, in SSC parlance, is the “S13” version. Any campaign taken after that date will be automatically processed with S13. With this pipeline release, earlier campaigns will be reprocessed with S13 as soon as possible after the release, probably starting in early 2006. (MIPS generates a lot of data, and it takes time to reprocess it.) The next version of the pipelines, S14, is due in Spring 2006, and may or may not similarly result in a reprocessing of the archive. A history of significant pipeline changes is available on the SSC website.

To the BCD level, our pipelines are presently essentially identical (within 0.15-0.3%) to those described in the Gordon et al. PASP paper (as described above). The post-BCD pipeline (e.g. mosaic construction) is also essentially identical.

Figure 4.1 and Figure 4.2 show example MIPS-24 raw and BCD products; Figure 4.3 and Figure 4.4 show example MIPS-24 final mosaics for photometry and scan maps, respectively.

The biggest change in S13 is a new calibration factor (a change of 2%). New header keywords have been added to indicate predicted backgrounds (ZODY_EST, ISM_EST, CIB_EST) and whether or not the campaign is a warm MIPS campaign (WARMFLAG). Finally, NaNs are now set properly in the P-mask pixels and hard saturated pixels from the difference image.

S12 included some large changes to the operational MIPS-24 pipeline, including improved flat fielding as a result of the implementation of interpolated scan-mirror dependent flats (see Section 6.1) and our first attempt at non-prime scan-mirror dependent flats. There was an improved pointing refinement algorithm for scan mode using 2MASS-to-24 micron source matches and with inclusion of new pointing keywords in BCD FITS headers. There was a new post-BCD product that is an un-normalized median stack of all BCDs per science AOR (with corresponding uncertainty) to enable better latent image tracking.

Should you wait for your data to be reprocessed under S13? Note that the MIPS-24 pipeline has been reasonably stable since S10. Although S13 changed the calibration factor by 2%, you may easily implement such a change yourself without waiting for a reprocessing; see Table 3.8. Although S12 was a big change to the pipeline operationally, there were few changes impacting the science results. **Most science results for MIPS-24 will only change slightly, so there is no particular need to wait for reprocessing**, especially since reprocessing MIPS data can take many months.

The anticipated S14 updates to the 24 micron pipeline include the following: (a) DCE0 correction; (b) better refined pointing and pick-off mirror spot positions.

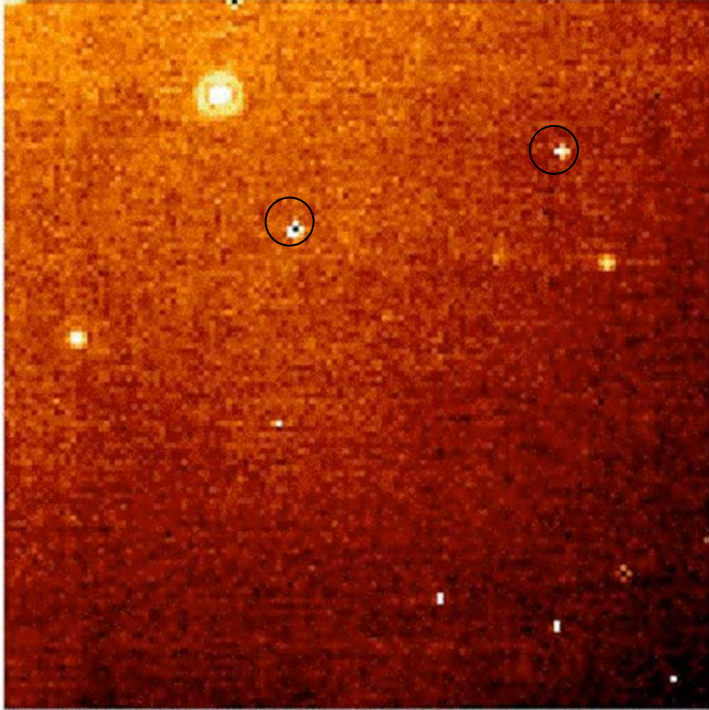


Figure 4.1: Automated MIPS-24 pipeline products : raw data (DCE). Bad pixels are circled (see Table 2.1); note cosmic rays, which are flagged – but not removed – by the pipeline. Compare the background here, which varies by 30% before flat fielding, to the much flatter background in the next figure.

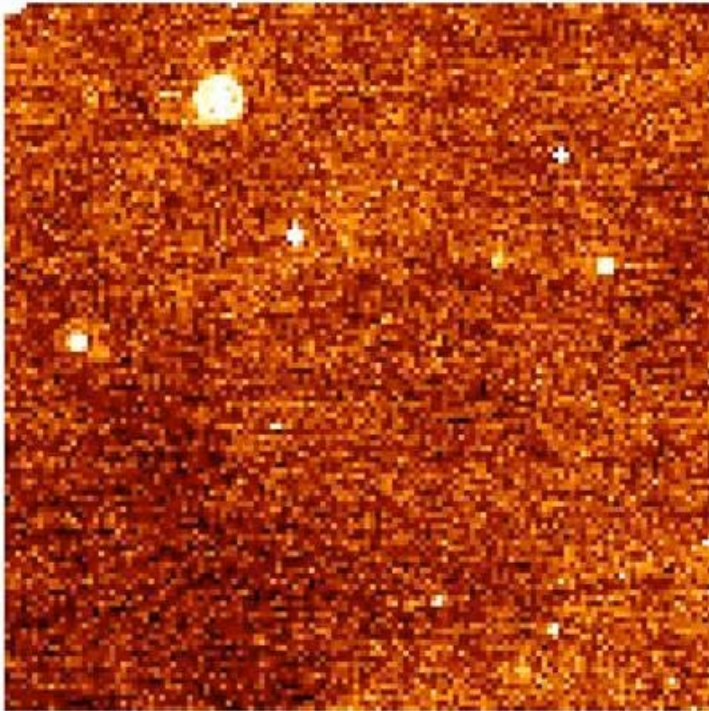


Figure 4.2: Automated MIPS-24 pipeline products: single BCD. This is on a different scale than the previous figure; note cirrus structure that has appeared (compared to raw image) in the background.

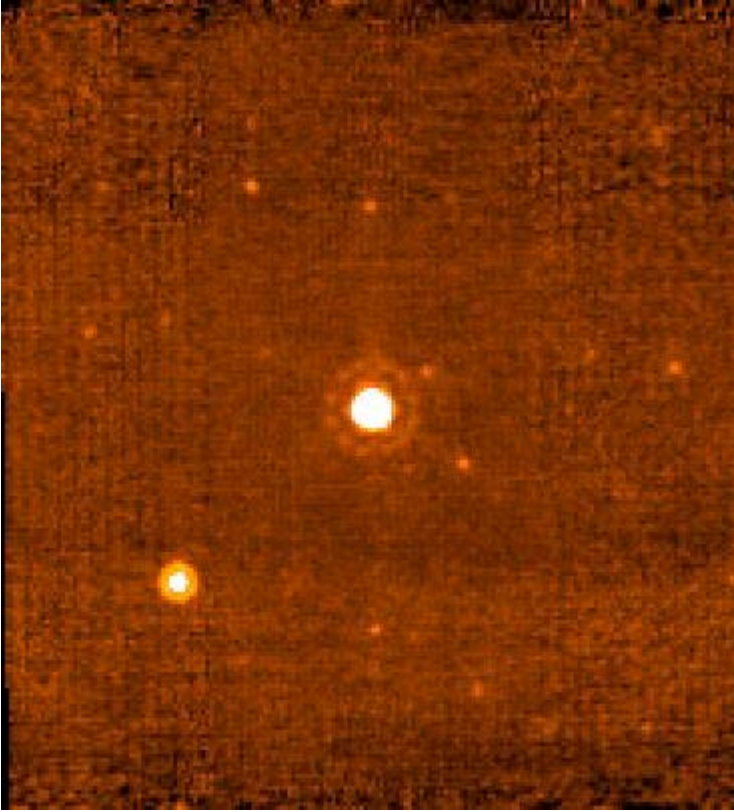


Figure 4.3: Automatically-produced mosaic combining multiple BCDs from a photometry observation.

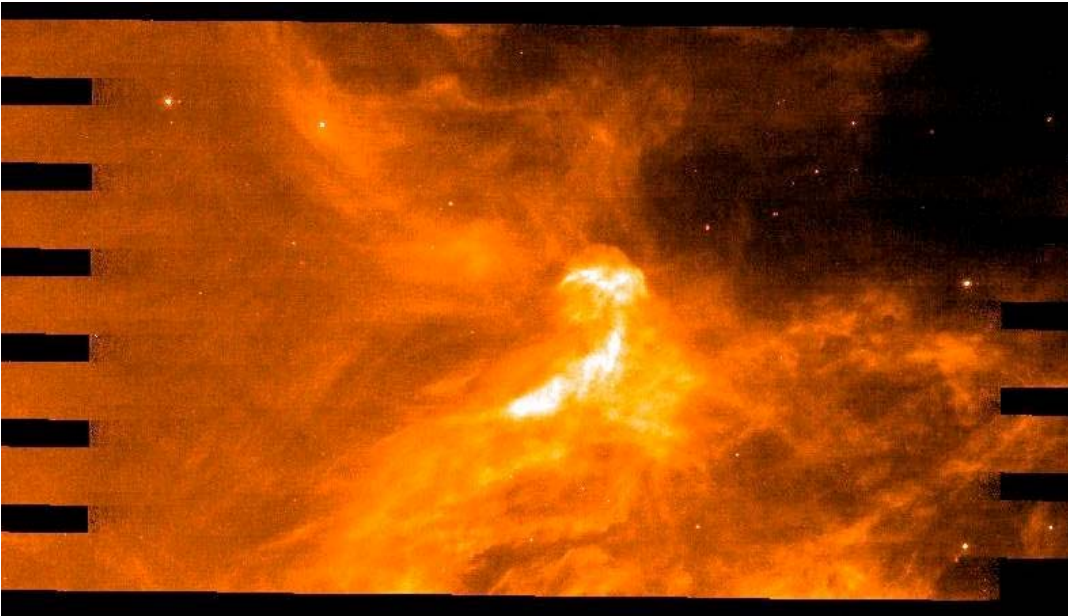


Figure 4.4: Automatically-produced mosaic combining multiple BCDs from a scan map observation.

4.3 The MIPS-Ge pipeline

4.3.1 Summary of pipeline

To the BCD level, our pipelines yield quantitatively similar results to those described in Gordon et al. (2005, PASP, 117, 503). For best results, the post-BCD pipeline (e.g. mosaic construction) needs to be customized by each user for the specific observation and the science goals; see below.

The details of the MIPS-Ge data reduction are described in the Gordon et al. (2005) paper. The two main pipeline processing steps that produce the Basic Calibrated Data (BCD) product are (1) the calculation of the slopes of the data ramps and (2) the calibration of the slope images.

Slope Calculation: The RAW data cubes for each DCE are reduced to an uncalibrated slope image by calculating the slopes of the data ramps for each pixel. The ability to measure the slopes is affected by the high rate of cosmic ray hits on the detectors. A Bayesian technique (Hesselroth et al., 2000, Proc. SPIE Int. Soc. Opt. Eng., 4131, 26; article available on the SSC website) is used to identify statistically significant changes in the slope of the ramp associated with cosmic ray events. Slopes are calculated on the ramp segments between cosmic ray events and are averaged to yield the final slope for each pixel.

Slope Calibration: After the calculation of the slopes, the uncalibrated slope image is calibrated to produce the BCD (see Sec. 6 of Gordon et al. 2005). The key aspect of the calibration of the MIPS-Ge arrays is the frequent use of stimulator flashes to track the responsivity variations of the Ge detectors as a function of time. To accurately measure the amplitude of the stimflash requires a background DCE to be observed at the same position on the sky (and immediately before) the stimflash DCE. The stimflash-background signal is interpolated as a function of time to derive the stimflash response function. The stimflash response function is divided from the slope images to remove the time dependent responsivity variation from the data. The dark correction is then subtracted from the data, and the data are divided by a normalized illumination correction, which removes combined effect of the pixel-to-pixel gain variations and stimflash illumination pattern. The data are flux-calibrated by applying a flux conversion factor derived from observations of calibrator sources to put the BCDs in units of MJy/sr (surface brightness).

The goal of BCD pipeline processing is to produce the best possible data products that can be derived from automated processing. Currently, the SSC produces two BCD products: (1) *_bcd.fits which is the standard calibrated BCD and (2) *_fbcd.fits which is a “filtered” bcd product designed for point sources. The fbcd is produced by subtracting off a median of the surrounding DCEs as a function of time per pixel. This filtering technique significantly mitigates the accumulation of stimflash latents and the residual background drifts due to variations of the slow response as a function of time. The application of the median filter removes the background from both the sky and the residual detector

effects (i.e., there is a loss of information about the extended background level in the field). **Early tests show that the application of a median filter maintains point source calibration for scan maps of fields with uniform backgrounds, but the fbcds do not preserve calibration for extended sources or for bright ($> \sim 0.5$ Jy) point sources within complex emission regions. For extended and/or bright sources, you may achieve better results with offline custom filtering using the GeRT (see section 7.4).**

4.3.2 S13 updates

Starting in mid-November 2005, the current version of the pipelines in SSC parlance, is the “S13” version. Any campaign taken after that date will be automatically processed with S13. With this pipeline release, earlier campaigns will be reprocessed with S13 as soon as possible after the release, probably in early 2006. (MIPS generates a lot of data, and it takes time to reprocess it.) Certainly initially, most of the data accessible from the Archive is still processed with S12 or S11. The next version of the pipelines, S14, is due in Spring 2006, and may or may not similarly result in a reprocessing of the archive. A history of significant pipeline changes is available on the SSC website.

The S13 version of the pipeline included the following improvements over S12:

1. New calibration factor for 70 (702, change of 11%) and 160 (44.7, change of 6%).
2. New header keywords for predicted backgrounds and an indicator of a warm MIPS campaign.
3. Improved SED calibration files (IC and response function).
4. SED Post-BCD Products can be made as part of the MOPEX package. They include: On and Off source mosaics, uncertainty and coverage maps and extracted spectrum/a. Also, the WCS keywords were not populated accurately prior to S13 for SED. (We were pointing at the correct place, but the pointing software for SED was under development.)
5. More flexibility in filtering. In particular, switched the order of column filter and high-pass time filter for 70 microns for default processing.
6. Updated the GeRT to allow for multi-thread processing and compatibility with Linux and Mac. (GeRT in testing now, to be released in early 2006.)
7. A 5 arcsec pointing error at 160 microns has been fixed.
8. Some radhit parameters have been optimized for 160 microns.
9. Making std error image for post-BCD processing (for good coverage observations, std images are better than unc images for source extraction).
10. Fixed bugs associated with propagation of NaNs.

The S12 version of the pipeline included the following improvements over S11:

1. SED support (additional calibration files).

2. Better errors calculated for filtered BCDs. (Those calculated in S11 were too large.)
3. FITS header keyword to track parameter files used in pipeline.
4. Use of ensembles for scan map AORs. (This groups together scan legs and allows a better stim interpolation and therefore better calibration.)

Should you wait for your data to be reprocessed under S13? For most science applications, the pre-S13 data is sufficient. The SED mode data saw some significant improvements, so it might be worth waiting for the SED reprocessing. Keep in mind reprocessing MIPS data can take many months.

The anticipated S14 updates to the Ge micron pipeline include more flexibility in stim interpolation, SED post-BCD processing, and TP mode pipeline support.

4.3.3 Things that aren't in the current pipeline

Possible flux non-linearities have yet to be fully quantified for MIPS-Ge, but are likely to be an effect at the <20% level. This information will be provided as it becomes available.

5 Post-BCD Pipeline Description

5.1 Introduction

This chapter, combined with the previous one, covers how your data get reduced, or what we did to your data between when it left the spacecraft and when you get it. *As of this writing, the BCD products, discussed in the previous chapter, are for the most part what you should start with when working with MIPS data.* In most cases, you can start with the 24 micron post-BCD products. For Ge data in particular, the post-BCD data products are a good way to get an overview of your data, but to do science, you should revert to the BCDs and make your own post-BCD products.

The Spitzer post-BCD tools can perform tasks including additional corrections for cosmic ray hits, illumination variations, cosmetics, and pointing refinement, as well as basic mosaicking of individual BCDs, source extraction, and bandmerging of point sources.

Technically, the suite of post-BCD software is more formally referred to as the “Advanced Data Products Software,” because the software is flexible enough to be used with more than just Spitzer data. However, in this context, we will simply refer to it as the “post-BCD” software.

The software for many of the post-BCD tools, along with copious documentation, is available at <http://ssc.spitzer.caltech.edu/postbcd/>. The post-BCD tools are available in a single package called “MOPEX.”

In summary, the steps of the post-BCD processing are Background Matching, Pointing Refinement, Basic Mosaicking, Outlier Detection, Astronomical Point Source Extraction (APEX), and finally, Bandmerging of Point Sources. We refer you to the manuals available on the post-BCD website for the nitty-gritty of how to run the software; the rest of this chapter addresses MIPS-specific issues and concerns. Suggested namelists for certain situations are given on the SSC MIPS website and in the data analysis cookbooks.

5.2 MIPS and Pointing Refinement

The pointing refinement step looks for sources in common with 2MASS and uses these common sources to refine the coordinate information in the headers of the BCDs. Note that 2MASS wavelengths are much different than MIPS wavelengths!

It is not recommended that you use the offline pointing refinement tool for MIPS, since it requires much tedious parameter tweaking and a good understanding of the quality of astrometric source matches. It is important to note that the accuracy of the refined pointing keywords appended to each scan mode BCD FITS header by the SSC strongly depends on the number and quality of the 2MASS-to-24 micron source matches available. Please use these values with care if you by any chance replace the standard BCD WCS with these refined keywords

prior to mosaicking. If the mosaic turns out smeared (or sources appear double) then in all likelihood, the refined pointing is suspect and you will need to revert to the raw pointing.

In the end, if you do not plan to use these refined pointings, the mosaicker uses the raw image pointing reconstructed from the telescope boresight telemetry and a calibrated model for the scan-mirror. The blind pointing uncertainties of MIPS are currently $\sim 1.2_*$ for 24, $\sim 1.7_*$ for 70, and $\sim 3.9_*$ for 160 microns, all 1 sigma radial.

In S12 SSC pipeline operations, the pointing refinement pipeline will only run on 24 micron scan mode data using exclusively 24 micron point sources that are common with those from the 2MASS public catalog. It operates on the individual scan-legs of scan-mode observation in order to maximize contiguous sky coverage and hence the number of potential 2MASS matches. Earlier testing has revealed that 2MASS-to-24 micron point-source matches are very rare in a BCD frame. The online pipeline performs optimum registration of scan-leg mosaics using 2MASS astrometry if a sufficient number of matches exist, then, the refined (intermediate) scan-leg pointings are mapped into the WCS of each BCD frame. Even for large scans, the online pointing refinement pipeline may not yield reliable results (or nothing at all) since 2MASS-to-24 micron matches are far and few between at all galactic latitudes.

5.3 MIPS and Mosaicking/Outlier Detection

The mosaicking procedure first includes the projection of BCDs onto a common frame. The projection is done using a linear interpolation (other current options are drizzle and grid, and there are others in development) and takes into account the distortion corrections. The initial projection uses pixel masks for each BCD produced by the pipeline. Remaining pixels affected by cosmic rays that were not detected during the pipeline processing can be flagged using a multiframe spatial-temporal outlier detection (other options include single frame and multiframe spatial). MOPEX keeps track of these outliers in a “rejection mask” (*brmsk.fits) and these masks are used when the images are re-projected and mosaicked. (For the specific mosaicking parameters used when running MOPEX as part of the automatic pipeline at the SSC, please see the SSC website.) The final mosaic is oriented in the file such that the size of the image is minimized; it is generally maximized in the y coordinate, and you can really see this in long scan maps. This means that the mosaics are rotated in order to make the scan direction roughly along the y-axis.

Jailbars (see Section 6.3 below) can be seen in some of the MIPS-24 BCD frames, particularly at the beginning of a scan leg or in frames with saturated sources. By superposition, some of these jailbars are removed in the outlier rejection step of the mosaic construction, but sometimes they persist. The frames can be corrected by applying an additive correction to the affected columns (or portions of columns) at the BCD level, or you may choose to exclude the affected frames entirely from the mosaic construction.

5.4 MIPS and APEX

The extraction of point sources in MIPS images is done in the pipeline using APEX. At this time, running APEX in the automatic, hands-off mode has not been scientifically verified, so source lists are not provided as part of the Archive.

APEX requires as input a PRF (point response function). (Here we use the language common in the optics field; the point spread function [PSF] is before sampling by the detector array, and the point response function [PRF] is after sampling by the detector array. More information is available on the SSC website.)

As of October 2004, there is a tool to estimate the PRF as part of APEX. You can estimate the PRF from your own data, either from individual BCDs or from the final mosaic (if sources are too faint to be detected in individual BCDs).

The current version of APEX produces a list of detections, fitting all sources as point sources (including bright and extended sources). You need to identify visually the bright (creating false detections) and extended sources and measure their fluxes inside suitable apertures after subtracting surrounding point sources; best results for bright sources may be obtained by interactive aperture photometry. A future implementation of APEX will allow you to identify extended sources in a two-stage detection process. The “detect” module will compute shape characteristics of the detected objects and create an extended object mask image. APEX will avoid point source fitting of bright and extended objects and create separate point source extraction and extended-bright detection lists.

5.5 MIPS and Bandmerging

The resolution of MIPS varies so much from 24 through 70 to 160 microns that bandmerging becomes a difficult process which needs to be guided by the science goals. For this reason, the pipeline does not currently produce an automatic list of bandmerged sources. In the future, a merged list of 24 and 70 sources may be included in the automatically produced products. Currently, you can do this merging yourself; you can also merge MIPS-24 and IRAC data, though, again, be careful about resolution changes between wavelengths.

The bandmerge code expects input source lists of x and y coordinates defined on the same FIF (Fiducial Image Frame). Therefore, the same FIF should be used while mosaicking BCDs from MIPS bands to be bandmerged.

6 Data Details (“Gotchas” and Examples) – MIPS 24

In this chapter, we attempt to summarize the most common things you might encounter in your data. We have not attempted to cover all possible cases, so if you discover in your data something ‘interesting’ and not listed here, please do not hesitate to let us know.

Figure 6.1 and Figure 6.2 show examples of some of the effects in MIPS-24 data discussed in this chapter. Note that the Si pipelines are summarized in Section 4.2.

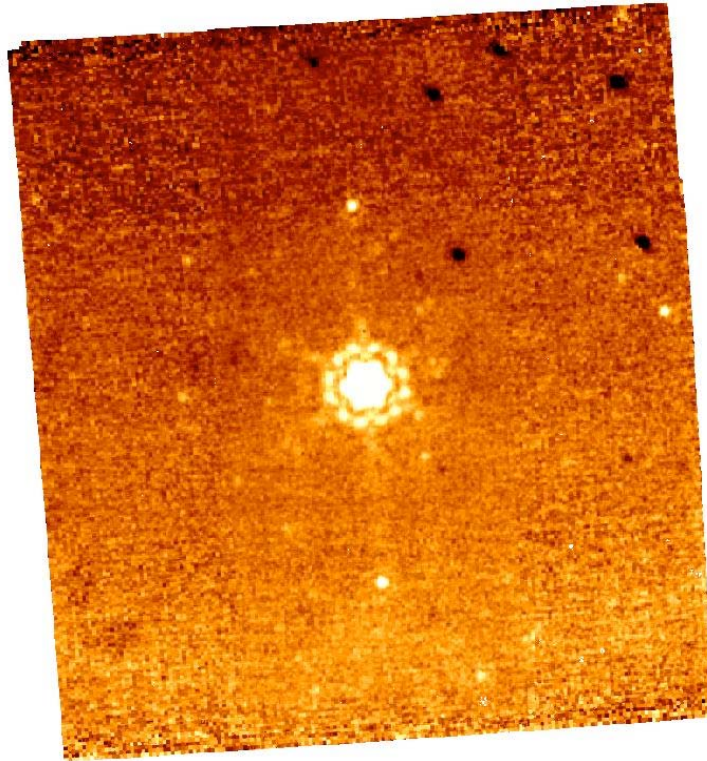


Figure 6.1: Sample MIPS-24 photometry mosaic product (several combined BCDs) from before the read-2 correction (see Section 4.2); the pipeline attempts to remove gradients across the field (such as the one seen here), but often gradients across the array at the 1-2% level remain. Also, note the dark spots (from pick-off mirror contamination, primarily in upper right), and the bright latents (above and below the bright source in the center). The specific pattern of the dark spots as portrayed here comes from the movement of the telescope+scan mirror during the photometry dithers.

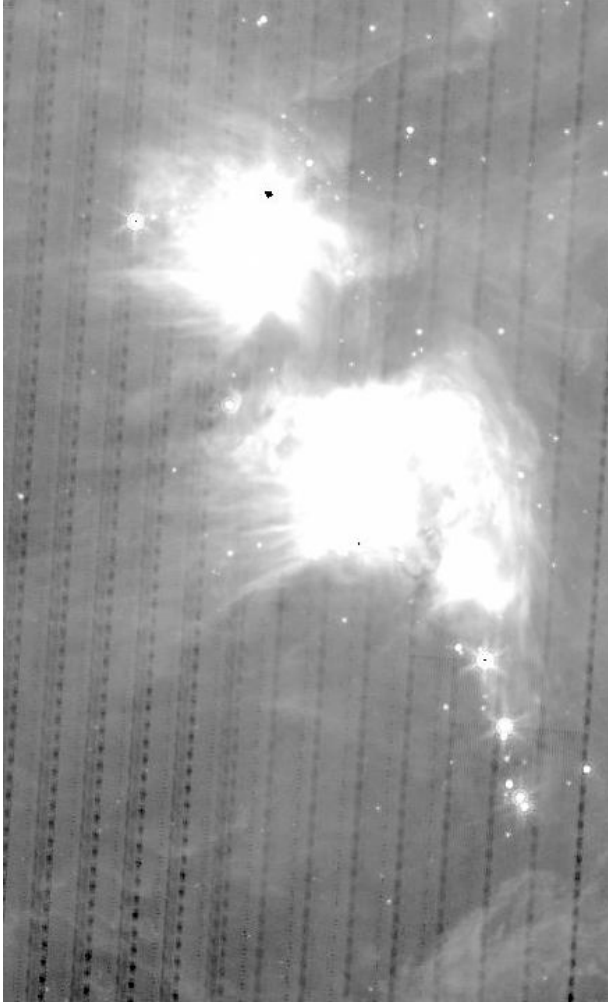


Figure 6.2: Sample subsection of MIPS-24 scan map. Note dark latents from bright objects.

6.1 Pick-off mirror contamination and systematic pointing: practical information

There is some contamination on the pick-off mirror (POM) that feeds MIPS. These dark spots appear to move with celestial objects during scan mirror moves (dithers). The darkest, most well-defined spots are 3-4 pixels across and are ~15-20% dimmer than surrounding pixels; they are located primarily in the upper right of the 24 μm array; see Figure 6.1, Figure 6.3, and Figure 6.4. There are also diffuse features that have a ~1-5% effect. A map of all of the spots seen during normal scan mirror moves based on 24 micron observations is in Figure 6.5. These spots appear to be stable; there is no evidence for “growing” or “jumping” spots.

As a result, the 24 μm flats depend on the scan mirror position and scan rate; the specific pattern of the spots depends on exactly what observing mode was used. We started the process of obtaining a complete library of flats for each scan mirror position, but this is complicated by the fact that the scan mirror doesn't

reproduce its position exactly from campaign to campaign; the spots appear to move slightly (<0.5 arcsec) for each campaign. There is also limited evidence for changes within a campaign. Scan mirror position dependent flat fields are applied to the data (when `PRIMEARR=1`) as part of the pipeline, but until we build up a sufficiently large library of flat fields for each scan mirror position in each mode, the spots may not be in the correct location for your data. With the S12 version of the pipeline, we will be matching the spot positions in each BCD to a library of synthesized flats based on real observations centered to 0.1 pixel for each BCD. Note that under S12 (and later), spots should be corrected in $\sim 99\%$ of frames; however, broad gradients may be introduced by flat variations between campaigns. Figure 6.6 shows the results of dividing a mismatched position-dependent flat from the data; if this happens to you, please notify the SSC Helpdesk (help@spitzer.caltech.edu). It's likely that the whole rest of the campaign is also affected, but it may very well be that you will have to wait for formal reprocessing for the spots to be removed properly. If you have enough data, you can create your own flat field for every scan mirror position (using keywords `CSM_PRED` and `CSM_RATE`), and this may be the best solution in general.

The fact that the scan mirror does not exactly reproduce its position has implications for the pointing; the pointing for any one campaign can be systematically offset by about 0.5 arcseconds in either direction. We are monitoring this systematic pointing offset; you can fix this effect by manually comparing a source list to 2MASS sources and editing the `CRVAL1` and `2` header keywords. Note that a list of 2MASS sources is one of the products served to you by the Archive. You can also use Spot to overlay a source list on your image to check for small systematic offsets in pointing.

As noted in Section 3.3.3, 24 micron data are obtained even during Ge photometry observations; these “non-prime” data necessarily use different scan mirror positions than when the 24 micron array is prime. Although scan mirror position-dependent flats are used for primary data, until recently, non-prime 24-micron data typically were not correctly flat-fielded because our library of scan-mirror dependent flats did not include these different scan mirror positions. We are working on improving this library.

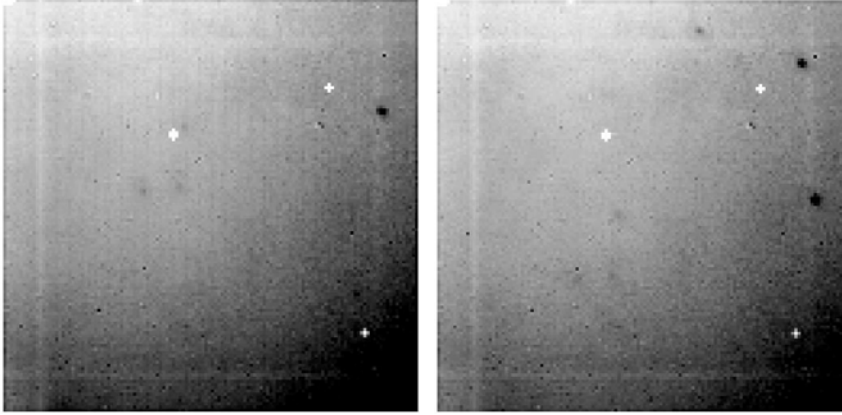


Figure 6.3: Two MIPS-24 flat fields at two different scan mirror positions. Note bad pixels (masked out and white) and dark spots from pick-off mirror contamination. The dark spots have a depth of about 20% and move when the scan mirror moves; see text. The gradient in the flat varies from 1.1 in the top left corner to 0.85 in the bottom right.

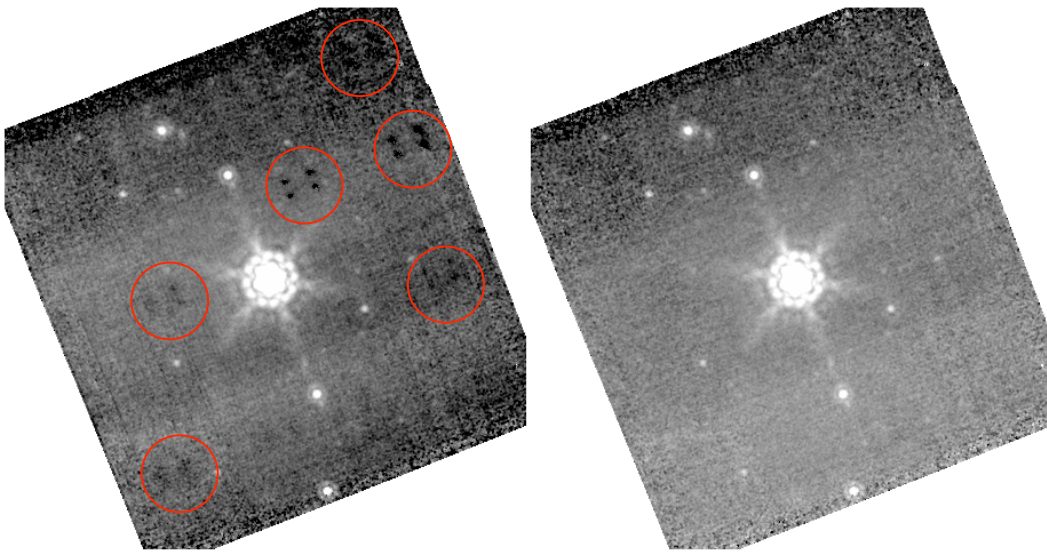


Figure 6.4: Pick-off mirror spots before (left, circled in red), and after (right) using scan mirror position dependent flats on a calibration star observation.

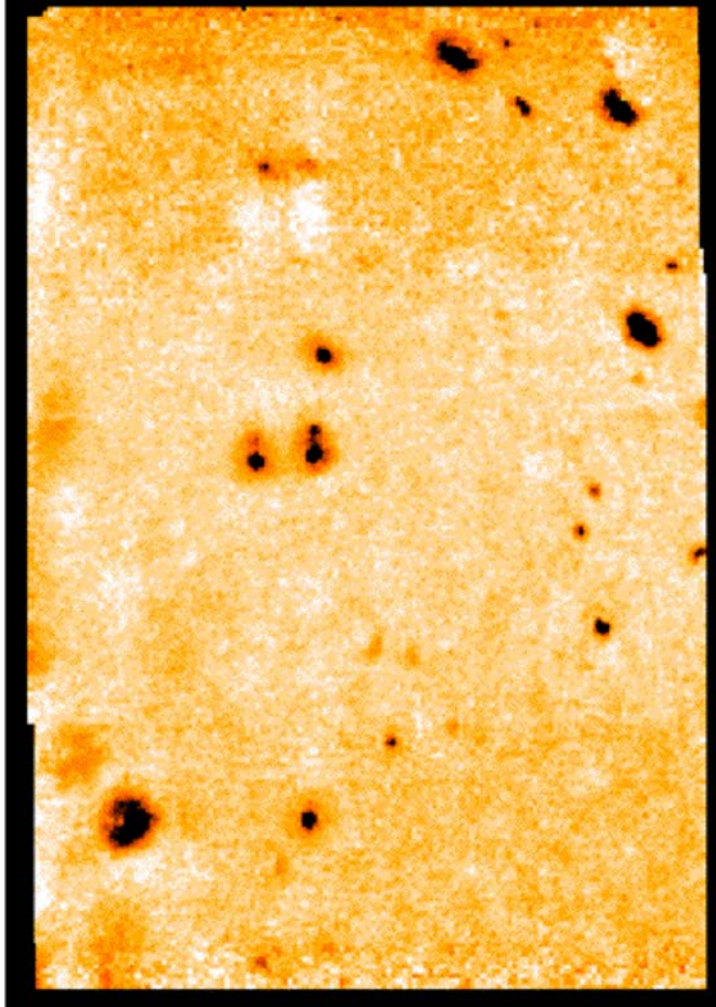


Figure 6.5: Map of the spot locations based on 24 micron observations.

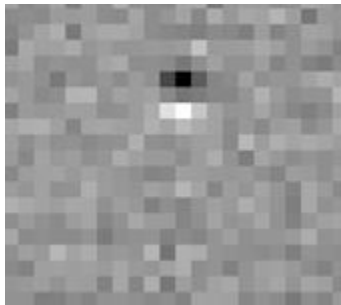


Figure 6.6: Results of dividing mismatched position-dependent flat from the data – zoom in on just one spot.

6.2 *More information on spot positions: for the truly dedicated*

Figure 6.7 shows the pointing offset in the Y-direction in the BCD frame as a function of campaign number. The variation is due to an intra-campaign wobble

in the scan-mirror, i.e., its on-board position does not repeat in the manner expected from a ground-test model. The pointing offsets are relative to campaign number 17. Offline analysis has shown that this campaign has very good absolute pointing, so that correcting the BCDs in any other campaign using the appropriate offset will get you to within an absolute pointing accuracy determined more-or-less by the quoted offset uncertainty.

The offsets in the Figure were computed by centroiding on a characteristic dark “spot” caused by debris on a pick-off mirror. The position of the spot changes in the Y-direction as the mirror rotates about its axis. The measurements were performed on stacks of 24 μm photometry mode BCD frames binned as a function of scan-mirror angle. The relative Y-positions of this spot (relative to our best-absolute pointing campaign; here number 17) were derived by performing a weighted average over all available mirror-angles for the campaign of interest. The associated uncertainty is purely due to spot centroiding error (typically one-tenth of a 24 μm pixel). More specifically, the mean spot position offset for a campaign i , relative to a campaign A with best absolute pointing known *a priori*, is given by

$$\langle \Delta Y \rangle_i = S_y \frac{\sum_j^{N_j} \frac{1}{\sigma_{i,j}^2 + \sigma_{A,j}^2} [Y_{i,j} - Y_{A,j}]}{\sum_j^{N_j} \frac{1}{\sigma_{i,j}^2 + \sigma_{A,j}^2}},$$

with uncertainty

$$\sigma_{\Delta Y} = S_y \left[\sum_j^{N_j} \frac{1}{\sigma_{i,j}^2 + \sigma_{A,j}^2} \right]^{-1/2},$$

where j is an index over mirror-position, the $\sigma_{i,j}$ are centroiding errors, S_y is the (24 μm) Y-axis *pixel-scale*, and the sums are over the N_j mirror positions for which measurements for campaigns i and A are available.

These corrections are such that if you had a BCD whose position angle was exactly zero, i.e., whose Y-axis was aligned along the declination axis, you simply add the above offset to that BCD’s declination. For non-zero position angles, a correction to both RA and Dec is needed and it comes down to a spherical trigonometry problem. No doubt the latter will always apply. But don’t despair; the offset corrections in the above plot will be applied to all SSC data products, for all MIPS modes, in subsequent campaign reprocessing beginning with the S13 pipeline version.

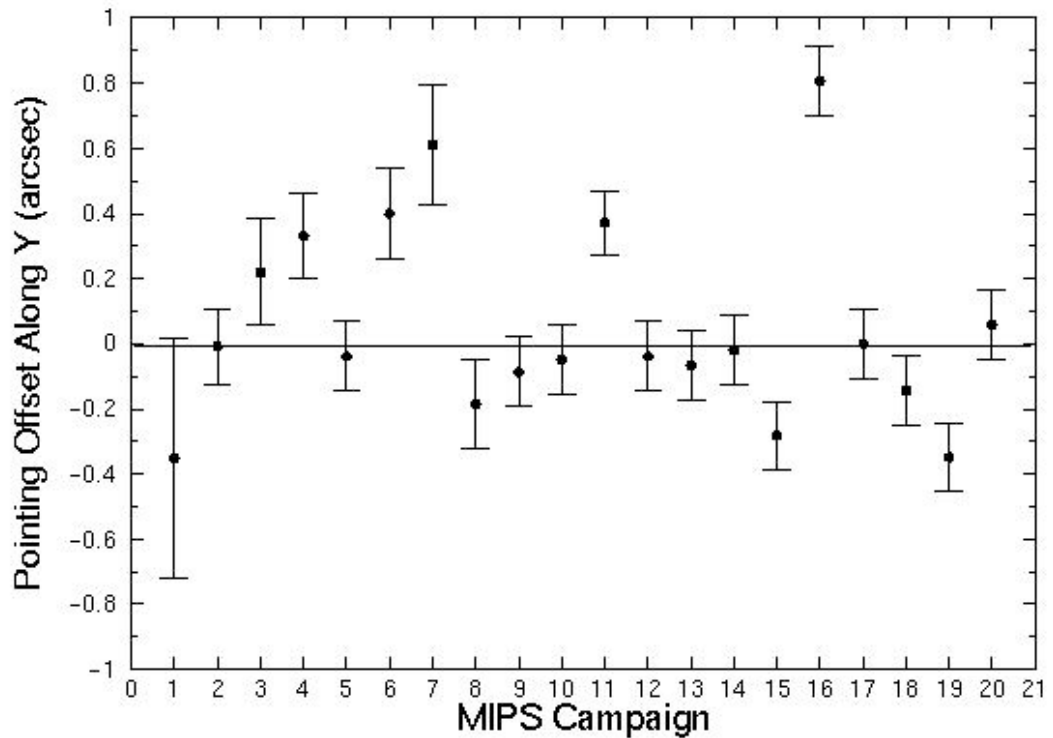


Figure 6.7: Spot position as a function of time; see text.

6.3 Jailbars

When a pixel is saturated, a responsivity change occurs in the corresponding readout. This results in a “jailbar” pattern occurring every 4th row/column for saturated sources (including some cosmic rays); see Figure 6.8. Only the portion of the array read out after the saturated source is read is affected. Typical effects of jailbars from point sources saturated only in the core produce a decrease in the flux of affected pixels at about the 2 MJy/sr (50 microJy/arcsec²) level, but the magnitude of the effect may vary with source flux.

For extended sources, often the saturated regions will cover all 4 or more contiguous readouts and thus an altered responsivity level is seen but no obvious jailbars.

Occasionally, one may see strong jailbars where there are no apparent sources. We believe this effect is due to cosmic ray hits.

Faint jailbars are often seen in lower-coverage regions of photometry mosaics where the dither pattern stacks the jailbars.

Many of these effects can be mitigated in the post-BCD stage using outlier rejection.

The fix for strong jailbars caused by saturated sources is *additive* – we recommend that you adjust the appropriate (portion of) the column additively to match the median level of the unaffected region of the column; see Figure 6.10-

Figure 6.11. However, weak jailbars appear to be *multiplicative*. Weak jailbars *should* flatfield out, but they often do not; self-calibration via dividing by the median of the affected frames often decreases the jailbar contrast (see section 6.13, and Figure 6.21).

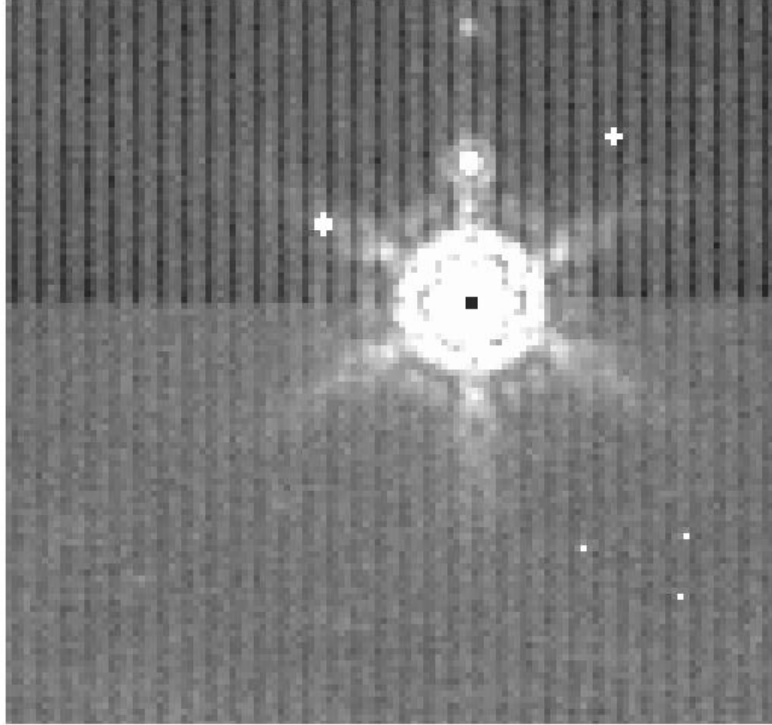


Figure 6.8: Example of “jailbar” effect from a saturated point source; note that the jailbars are stronger after the bright object. Bright latents (above the source) can also be seen. The central pixel of this bright object is hard saturated (no replacement is available), so it appears black.

6.4 Latents

There are three types of MIPS-24 latents: (a) ~0.8% bright latents that last from seconds to 10s of seconds, decay exponentially, look like PSFs, are easily recognizable by eye, and are flagged (but not corrected) by the pipeline; (b) ~2% dark splotchy effects from very bright objects (>50 Jy) that last for hours; and (c) 0.5% bright latents from extremely bright objects that can last for days. (Saturated sources will also produce cosmetically ugly “jailbars” (see above), but these are easily recognizable.)

6.4.1 Short-lived bright latents

These are the easiest to recognize by eye or automatically because they always occur in the in-scan direction, and the pipeline does in fact flag them in the mask file (though the pipeline does not remove them). Examples of this effect can be found in Figure 6.9, as well as Figure 6.1, Figure 6.8, and Figure 6.10.

Bright latents are typically not removed by outlier rejection in scan mode because the scan mirror produces repeated overlapping patterns. This is why you may see a trail of latents (often on both sides of a bright source) along the scan direction, particularly for fast scans.

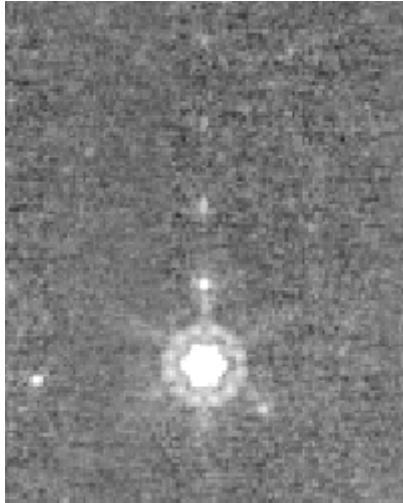


Figure 6.9: Example of short-lived bright latents – note trail of bright dots above the bright source.

6.4.2 Dark latents

Examples of dark latents from bright sources can be found in Figure 6.2, Figure 6.10, Figure 6.11, and Figure 6.13. This reduction in response of 1-2% comes from very bright sources, those >50 Jy. Low-level dark latents have been seen for sources as low as 18 Jy. They can last a long time, with a timescale of about 10 hours. If your observations have these features, it may be a result of a bright object seen in observations prior to yours. The impact of this is usually reduced by redundancy (e.g., additional dithered frames). If you encounter these kinds of latents in scan mode, because the latents last longer than the maximum length of an AOR, they are stable and can be removed using your own data, called self-calibration (see below and section 6.13). If you have these kind of latents in data taken in photometry mode, the pattern of latents may be different (because the dithers are different), and you might not have enough data to self-correct it. (However, see section 6.13.)

The effects of dark latents AND any residual but static imperfections in the flat fielding can be removed quite effectively by division of each BCD affected by dark latents by a normalized median of all of the BCDs affected by the dark latents within the AOR (excluding very bright pixels); see Section 6.13. This effectively gives an improved flat field and is generally recommended in regions of low background where subtle (1-2%) effects may be important to remove. After correcting the BCDs, you then have to make a new mosaic (using the SSC's MOPEX or other software).

The dark latents are removed by thermal anneals, which are a rare event for the 24 micron array, and are generally only done at the start of a campaign.

Currently, we try to limit the impact of these latents by manually scheduling already-known bright sources (known to be bright from 25 micron IRAS data) at the ends of campaigns.

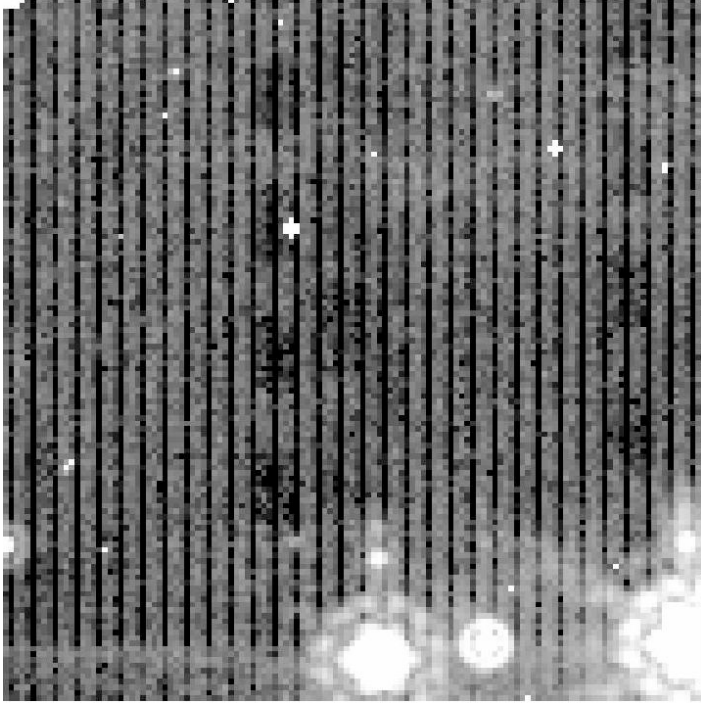


Figure 6.10: Initial BCD affected by bright sources; note “jailbars,” bright (point-like) latents, and dark (splotchy) latents.

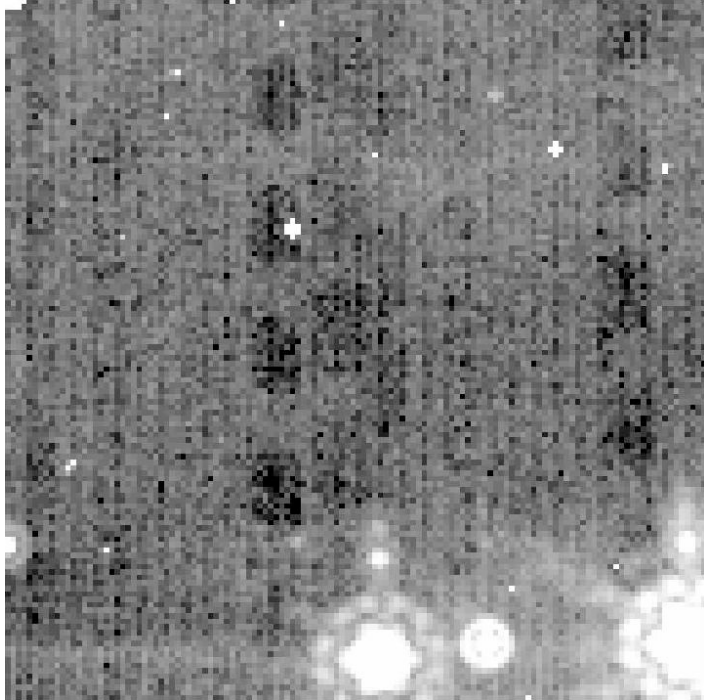


Figure 6.11: BCD after additive jailbar correction.

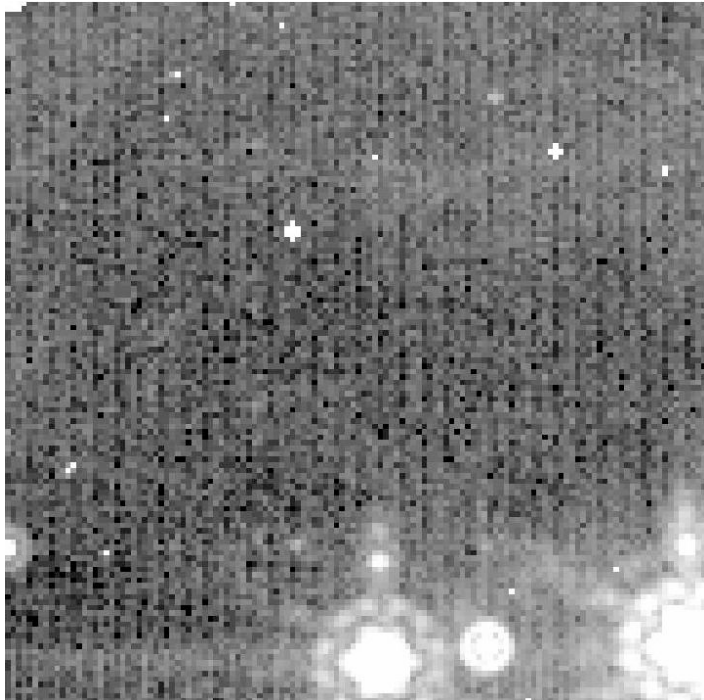


Figure 6.12: BCD after "self-calibration" to correct dark latents.



Figure 6.13: Example of dark latents all by themselves. Even trails from slewing the telescope over the bright object can also clearly be seen.

6.4.3 Long-lived bright latents

Finally, examples of long-lived bright latents can be found in Figure 6.13 and Figure 6.14, as well as Figure 6.21. These bright 0.5% latents remained for the duration of the week-long instrument campaign!

Just like for long-lived dark latents, the impact of these latents is usually reduced by redundancy (e.g., additional dithered frames, inherent to MIPS observing modes). If you encounter these kinds of latents in scan mode, because the latents last longer than the maximum length of an AOR, they are stable and can be removed using your own data, called self-calibration (see below, and section 6.13). If you have these kind of latents in data taken in photometry mode, the pattern of latents may be different (because the dithers are different), and you might not have enough data to self-correct it. Just as above, you can remove these effects by dividing each of the affected BCDs by a normalized median of all of the affected BCDs (excluding very bright pixels). This effectively gives an improved flat field, and is generally recommended in regions of low background where subtle (1-2%) effects may be important to remove. After correcting the BCDs, you then have to make a new mosaic (using the SSC's MOPEX or other software).

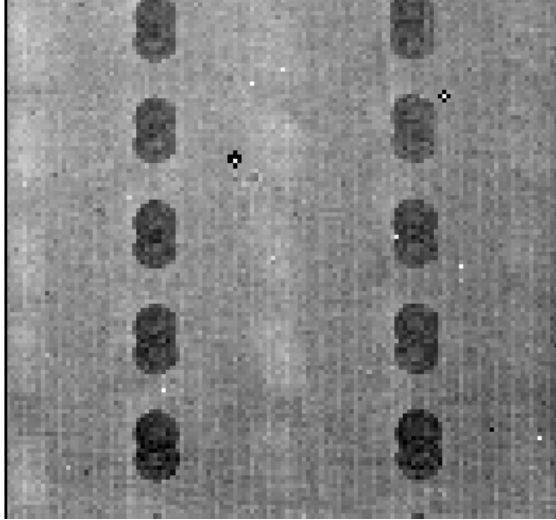


Figure 6.14: Example of long-lived bright latents with newer dark latents.

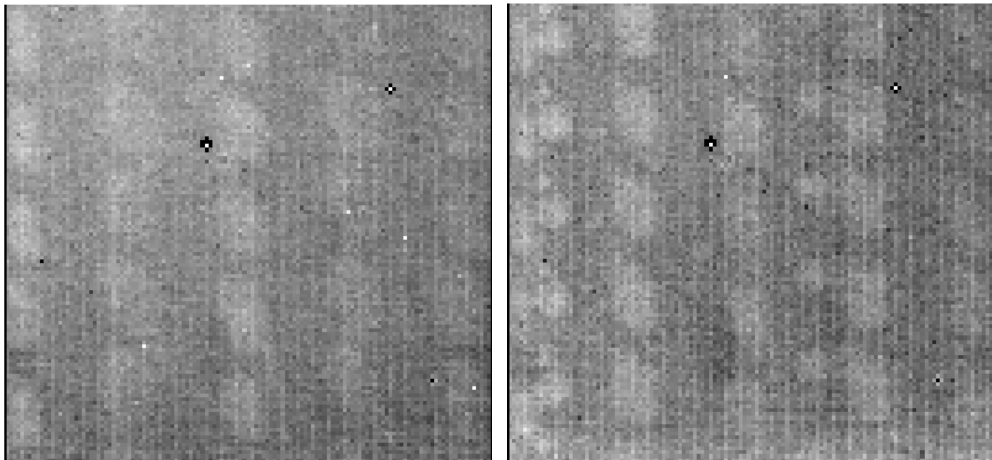


Figure 6.15: BCDs from AORs later in the campaign where the data in Figure 6.13 were obtained. Note that the dark latents seen above have turned into bright latents here. The figure on the right has additional bright latents obtained in still later observations.

6.5 First and second DCE effects

The first DCE of every commanded sequence of observations (e.g., data with the keyword DCENUM=0) have a shorter exposure time and are depressed in response by 10-15%. The photometry AOTs are designed such that these “extra” frames can be discarded. Although there could be useful information in these frames, they are omitted from the automated post-BCD mosaics. You will be sent all BCDs (including those with DCENUM=0), so if you reconstruct the mosaics, you should avoid using the DCENUM=0 frames.

If you get a mosaic that looks like Figure 6.16, then you have indeed accidentally included these first DCEs, and you should omit the DCENUM=0 frames. You can identify these from the filenames alone; see Section 3.2.1.

In addition, the second and even third DCE/BCD (DCENUM=1, 2) appears to have a somewhat reduced signal ($\sim 2\%$) and often enhanced jailbars compared to the rest. For now, these second DCEs are included in the automatic mosaics, but if you have enough data, you might consider rejecting these as well. We are anticipating that a future version of the pipeline will account for DCENUM dependence so that all frames are well-calibrated.

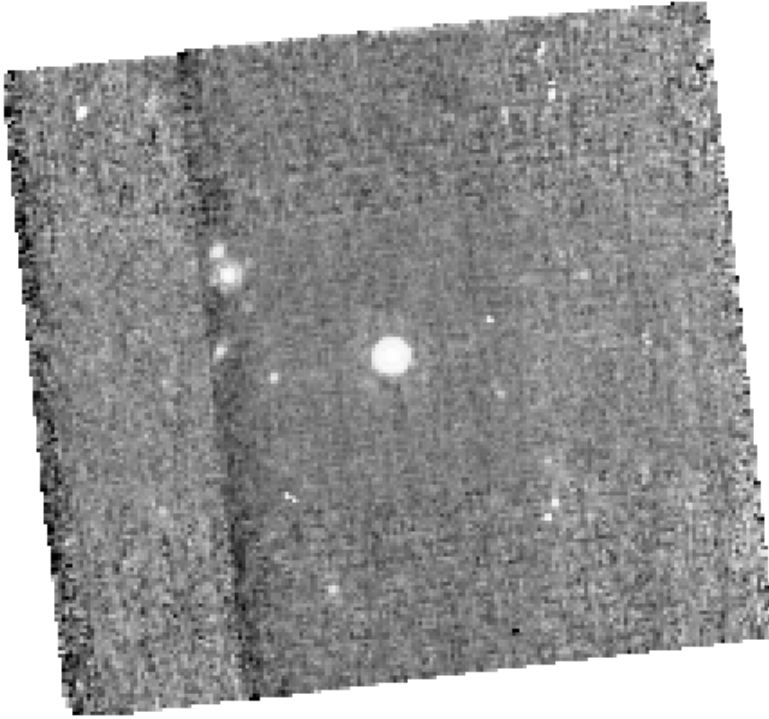


Figure 6.16: First DCE effect— **DON'T DO THIS!** See the gradients on the left? To avoid these, drop the DCENUM=0 frames. See Section 6.5.

6.6 Post-anneal slow response drift

Figure 6.17 shows the median flux of each BCD (after rejection of pixels affected by cosmics and sources) for the two AORs of the ELAIS-N1 deep 24 micron observations. The background of the region observed is uniform. The observation is in photometric mode, using the offset position just to observe a more extended field. Every ten BCDs, a bias frame has been taken, which also resets the detector.

The first AOR shows a clear monotonic increasing trend. The second AOR, which has been taken a few hours later after observing a bright source, is more stable (there are however some latencies in the BCDs from this sources which have been corrected with a median stack).

This analysis will be discussed in more detail in Fadda et al. (2006, in preparation).

This effect is at the level of less than $\sim 1\%$, and lasts for ~ 3 hr timescale.

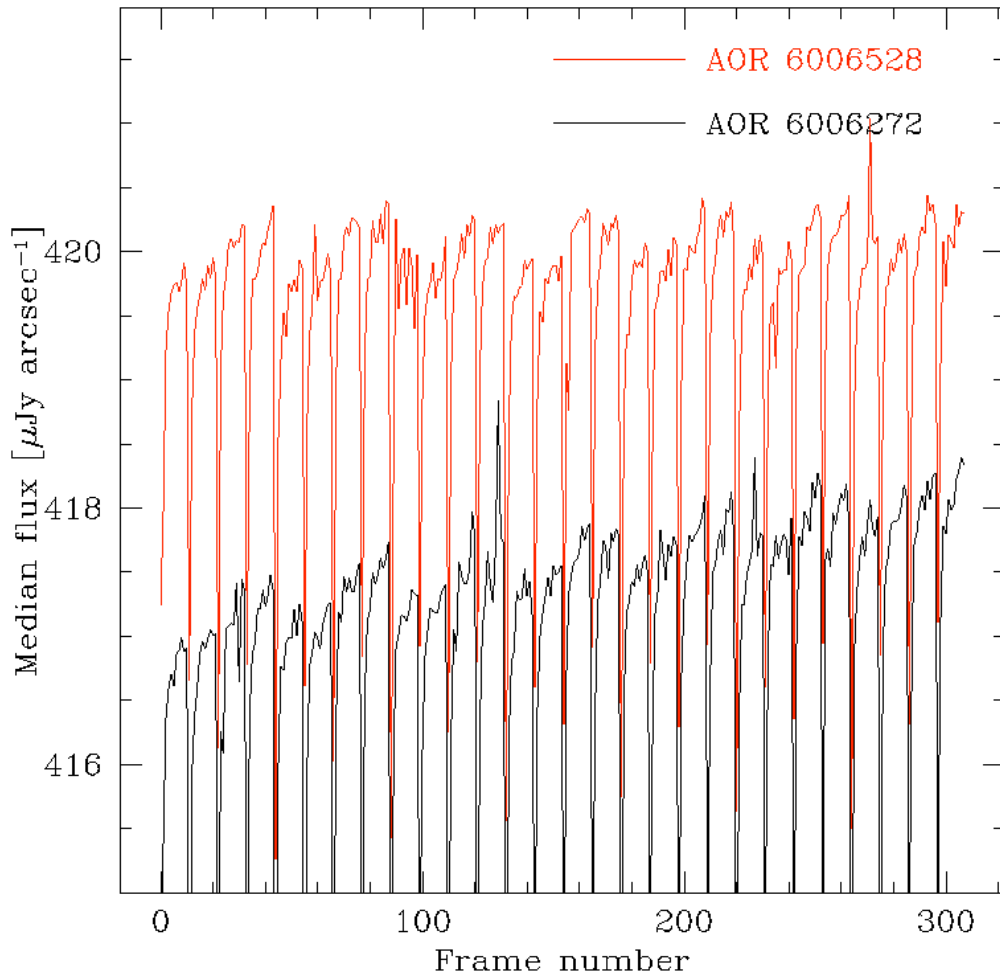


Figure 6.17: Evidence of slow response drift in two ELAIS-N1 deep 24 micron fields.

6.7 Bright sources and droop correction

In order to correct properly for the droop effect, one needs an accurate estimate of the total flux incident on the array. If part of the array is saturated, one doesn't know the total flux, and the part of the array that is saturated is likely to contribute significantly to the total flux. The pipeline attempts to correct for these kinds of effects as best it can, but in some cases where the array is really saturated, the droop cannot be calculated properly, resulting in a DC offset to the whole array for that frame.

If your observation includes very bright sources, you may have to manually correct that frame for this DC offset.

6.8 Ghosts and glints

Ghosts and glints are rarely seen in MIPS data.

To date, one glint has been seen 1.5 degrees from the center of a scan map as a result of a very bright source – a source of >1500 Jy created a diffuse ghost of 12 Jy. When a bright source is at or just off the edge of the array, there are linear glints that appear in the frame.

Redundancy (e.g., additional dithered frames) and median-combining frames

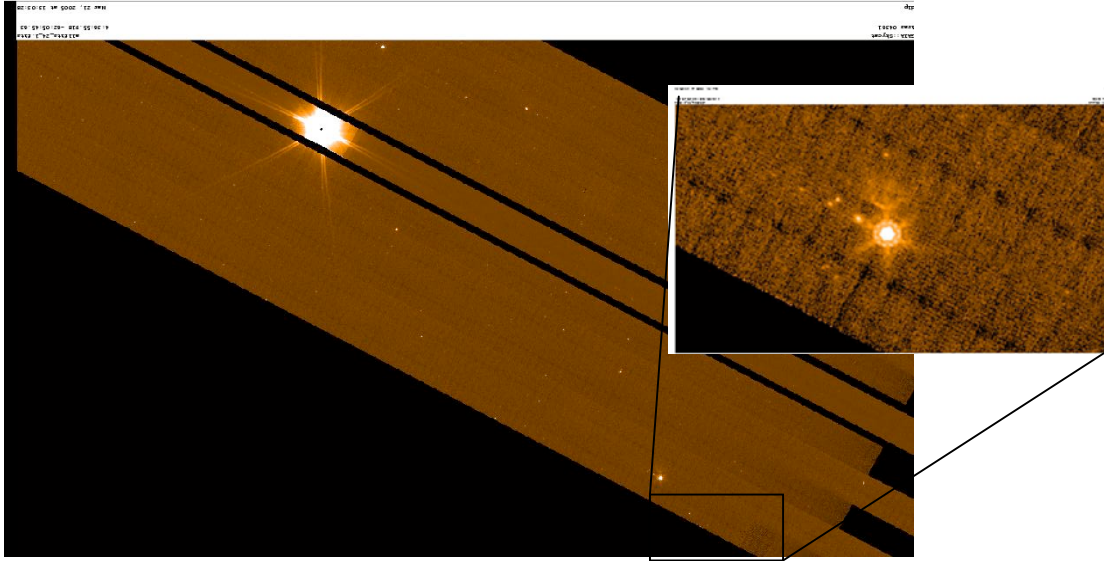


Figure 6.18: Very rare glint – fake ~12 Jy source seen ~1.5 degrees from ~1500 Jy source.

6.9 Zero-level offset

Occasionally, there is a zero-level offset in a single BCD frame, e.g., the whole frame appears brighter than others; see Figure 6.19. This is not yet understood, and perhaps it is due to a bright cosmic ray. If you see this in your data, you can correct it with an additive offset to that frame, or you can use background matching in MOPEX if there is sufficient overlap with adjacent BCDs.



Figure 6.19: Example of single frame with zero-level offset. No background matching was performed in creating this mosaic.

6.10 Distortions

The distortion at 24 microns is consistent with what was expected pre-launch. The 24 μm photometry can vary by about 2-10% across the array for data prior to the distortion correction. The BCD pipeline puts the distortion keywords (see Appendix for a list of the keywords) into the header, but does not correct for the distortions. The Post-BCD pipeline does in fact correct for the distortions such that the mosaics are resampled to have a default pixel size on the sky of 2.45×2.45 arcsec. The photometry part of MOPEX can do single-frame photometry and takes into account distortion on the individual frames.

6.11 Large- and small-scale gradients

For large scan maps, we have noticed a slow large-scale gradient across the entire map, which is along the direction of a scan leg. Since we scan along directions perpendicular to the ecliptic plane, this may very well actually be real, physical variations in the zodiacal light. However, sometimes the gradients do not match in adjacent scan legs. Some fraction of this effect may be due to residual read-2 effects.

Gradients are also seen within individual 5×5 arcmin BCDs, but despite being in the scan direction, these are not likely to be astronomical in nature. Some may be due to poor flat-fielding, and can be corrected with self-calibration (see section 6.13). However, systematic gradients are seen as a function of scan mirror position, especially in photometry mode, which uses the largest range in scan mirror angle. These may be due to scattered light changes as a function of scan mirror position. These are likely to be additive. Additional analysis is pending.

6.12 Asteroids!

Finally, as another common “gotcha” to list here, there are many, many asteroids to be found, even in observations obtained some considerable distance from the ecliptic. Beware of 24 micron sources without short-wavelength counterparts, especially near the ecliptic plane! Most of the point sources in Figure 6.20 are asteroids.

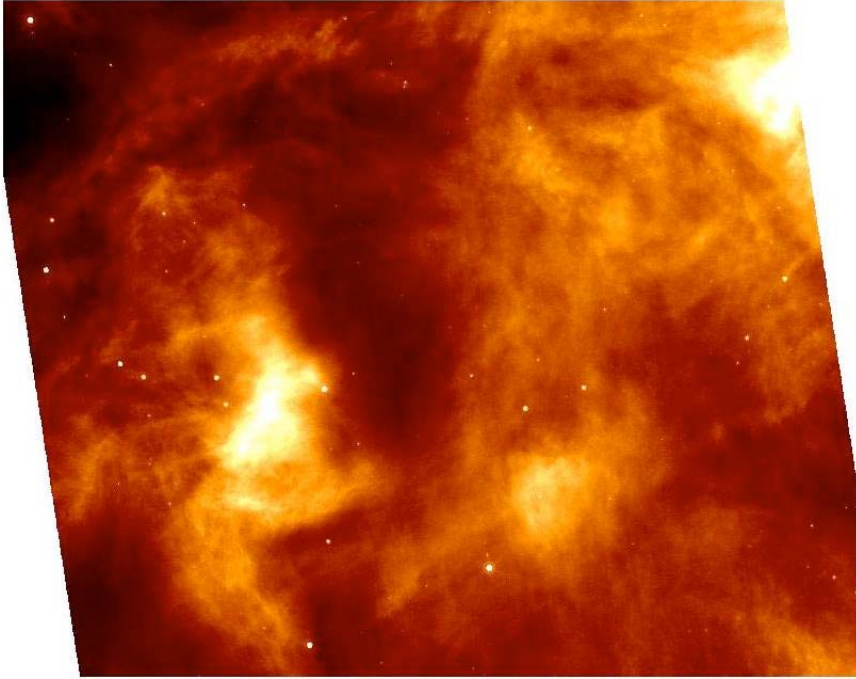


Figure 6.20: Beware of asteroids! Most of the point sources in this frame are asteroids.

6.13 Example: Self-calibration

To correct persistent effects, including long-term latents, low-level jailbars, and gradients, you should use your own data to self-calibrate.

First, assemble a list of BCDs without the very bright sources but with the persistent effects. If the latents are caused by your own data, make sure to separate BCDs before and after the offending bright sources. For some data sets, you may want to include the non-prime BCDs.

Second, take the median of the list(s) of BCDs and normalize it. Then, divide all affected BCDs by the normalized median. Note that the S12 pipeline (and later) will provide a non-normalized median of entire AOR as a data product, `bmed.fits`.

Finally, make a new mosaic from your modified BCDs. See Figure 6.21, Figure 6.22, and Figure 6.23 for example “before” and “after” images.

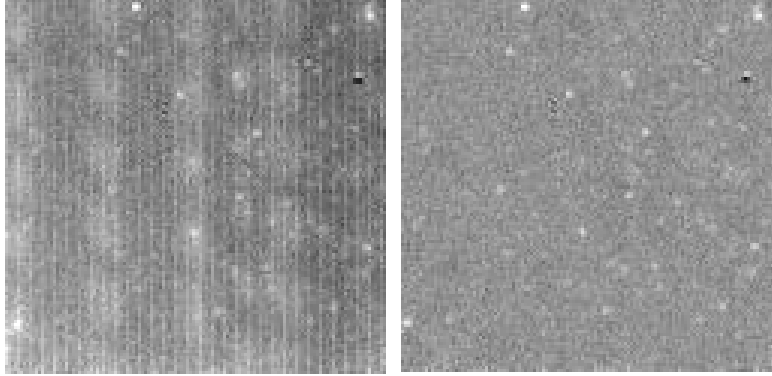


Figure 6.21: Example mosaic before (left), with long-term bright latents and weak jailbars, and after (right) self-calibration, where those effects are well-corrected. Note that the flat fields in this example did not match the spot positions in the data very well (upper right).

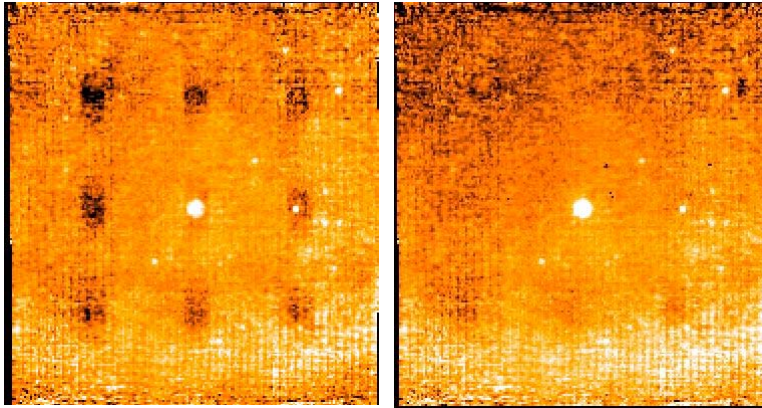


Figure 6.22: Example mosaic before (left), with long-term dark latents, and after (right) self calibration of photometry data using non-prime data.

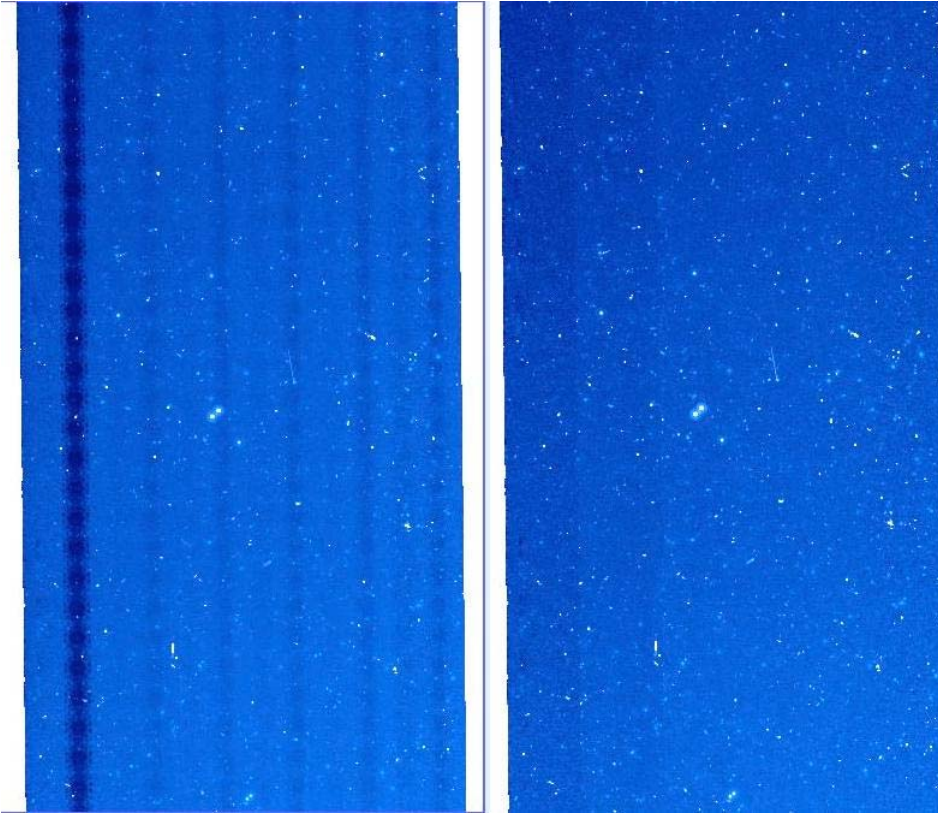


Figure 6.23: Another example of self-calibration removing dark latents, this time in a large scan map. Left is before, right is after.

6.14 Example: NGC 300

Figure 6.24 shows a 24 micron scan map of NGC 300, rotated to have north up. (This object is also used for some Ge examples in the next chapter of this document; the corresponding science paper is Helou et al. 2004, ApJS, 154, 253.) The Figure is a mosaic of the default output BCDs, and is a degree long. The gradient across the entire scan map is apparent at a level of 1.5%, and becomes brighter as the ecliptic latitude decreases. Note also that the POM contamination has been completely removed due to the use of scan-mirror-dependent flat fields.

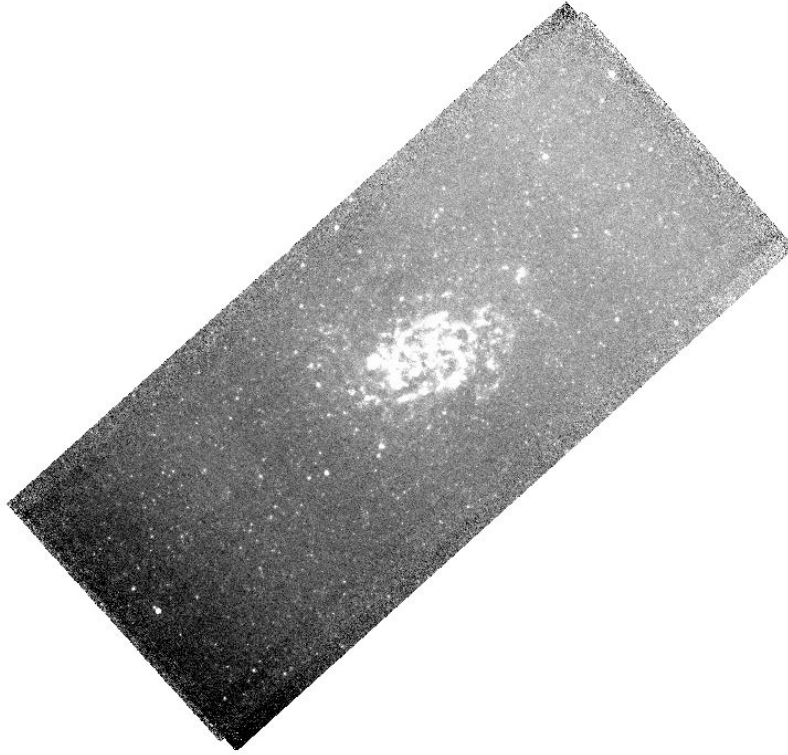


Figure 6.24: NGC 300 in 24 microns, rotated to have north up. The gradient across the entire scan map is evident, and is most likely a real variation in the Zodiacal light.

6.15 Additional examples

Additional examples of 24 micron processing can be found on the SSC website; see the data analysis cookbooks.

7 Data Details (“Gotchas” and Examples) – MIPS Ge

7.1 Introduction

All traditional photoconductors, such as the MIPS Ge:Ga unstressed and stressed detectors, show multiple time constant response. In addition, they can exhibit spontaneous spiking and non-monotonic response characteristics (the “hook”). For much more discussion, see section 8.1.3.3.1 in the SOM 6.x. The result is a slow increase in detector response lasting tens of minutes (MIPS 160 μm detectors) to hours (MIPS 70 μm detectors). MIPS takes advantage of the fact that the fast generation-recombination response (fast response) of the detectors is inherently different than the longer term response by using the scan mirror to modulate (chop) the source signal on timescales of a few seconds, keeping measurements mostly confined to the fast response regime. Frequent use of on-board calibration sources (called stimulators, or stims) additionally allows tracking of the long-term drifts in response.

Note that the Ge pipelines are summarized in Section 4.3, including differences between S12 and S13 pipelines. As of this writing, most of the data in the archive are still processed with S11 or S12. Most observers (with any Ge data) will want to apply techniques discussed here to their data. For bright sources, you can use the unfiltered mosaic. For fainter sources, consider the fbcd product as a quick-look at your data and do your own filtering. If in doubt, err on the side of caution and redo the filtering and the mosaics yourself.

7.2 High-level summary

Ge:Ga processing is fundamentally different, but not necessarily more complicated or difficult than any other data processing. The basic processing steps are the following. Note that items 1 and 2 are done for you in our pipelines; you will most likely only have to spend time with items 3 and 4:

1. Fit slopes to ramps to make slope images. (See SOM for more discussion.)
2. Calibrate slope images. (See section 9.5 for more discussion.)
3. Correct for residual instrumental effects.
 - a. High-pass median time filter per pixel to remove residual variations of the slow response as a function of time. (This means: subtract the median value of the neighboring BCDs on a per pixel basis as a function of time.)
 - b. Column filter at 70 microns to remove residual stim latents. (This means: subtract median value of each column from every column since stim latents are correlated by column.)

- c. Since the automatically-produced (“online”) filtered mosaics are optimized for point sources, not for extended regions (i.e., the background is removed by filtering), *bright point sources can bias the filtering*. To maintain the calibration of bright point sources, do the filtering offline in two passes. Identify bright sources ($>\sim 0.5$ Jy) in the first pass, then mask and re-calculate the filtering corrections (offline 2-pass filtering examples below).
4. Co-add images to make mosaics. (Can be done entirely with MOPEX.)
 - a. Correct for array distortion.
 - b. Interpolation of frames onto fiducial sky frame.
 - c. Outlier rejection based on redundancy.
 - d. Re-interpolation of frames.
 - e. Coadd final frames.

7.3 Point vs. extended sources, or why there are 2 BCDs

The goal of BCD pipeline processing is to produce the best possible data products that can be derived from automated processing. Currently, the SSC produces two BCD products: (1) bcd.fits which is the standard calibrated BCD and (2) fbcd.fits which is a “filtered” bcd product designed for point sources. The fbcd is produced by subtracting off a median of the surrounding DCEs as a function of time per pixel. This filtering technique significantly mitigates the accumulation of stimflash latents and the residual background drifts due to variations of the slow response as a function of time (see below for more information). The application of the median filter removes the background from both the sky and the residual detector effects (i.e., loses information about the extended background level in the field). **Early tests show that the application of a median filter maintains point source calibration for scan maps of fields with uniform backgrounds, but the fbcds do not preserve calibration for extended sources or for bright ($>\sim 0.5$ Jy) point sources within complex emission regions. For extended and/or bright sources, you may achieve better results with offline custom filtering using the GeRT (see section 7.4).**

Figure 7.1 shows a flowchart of possible analysis steps, discussed in much more detail below. A mosaic constructed from some sample unfiltered MIPS-70 scan map data appears in Figure 7.2; a mosaic constructed from the same data but filtered is in Figure 7.3. The dark horizontal (in-scan) stripes are fast/slow response variations, which are removed from the data using a temporal median filter per pixel in the current automatic pipeline. The bright vertical stripes are stim latents, which were removed manually after the pipeline using column median filtering (which is part of the S11 pipeline). These sample FLS data date from early in the mission, e.g. they were taken with the old bias settings (see “stim latents” below). Your data were almost certainly taken with the new bias setting, so the magnitude of both of these effects should be lessened.

To the BCD level, our pipelines yield quantitatively similar results to those described in Gordon et al. (2005, PASP, 117, 503).

Real-life specific examples of extended source work with MIPS can be found, for example, in the ApJS special issue; see, e.g., the paper by Engelbracht et al. (2004, ApJS, 154, 248) on NGC 55, Helou et al. (2004, ApJS, 154, 253) on NGC 300, and/or Regan et al. (2004, ApJS, 154, 204) on NGC 7331.

7.4 The GeRT

In Spring 2005, the SSC released the GeRT on the “contributed software” portion of the SSC website. (The initial release only works on Solaris platforms, but copies that work on other platforms are anticipated for early 2006.) Most people will find the archived BCD products (filtered or unfiltered) are suitable for their needs, but with the GeRT, you can either “clean up” the BCDs, or reprocess the raw data. Examples of cases in which reprocessing from scratch would be important include the following: (a) the online stim calibration was not done optimally, e.g., extrapolated stim calibration or stim calibration corrupted by bright emission regions; (b) important new or updated calibration files and/or pipeline corrections not yet available online but important for a specific case; (c) optimization of the pipeline parameters for non-standard data and/or specific science applications for expert users.

7.5 Recommended steps for looking at your data

1. Using the BCDs, look at the online default postBCD mosaics (*msaic.fits).
 - a. If this msaic.fits file is ok, then you’re done, and you can start doing your science.
 - b. If this msaic.fits file has bad outlier rejection, remake the mosaic from the online BCDs (using MOPEX).
 - c. If this msaic.fits file has streaks/artifacts, then check the filtered mosaic (*mfilt.fits).
2. Look at the online filtered mosaic (*mfilt.fits), which was constructed from the filtered (*fbcd.fits) files.
 - a. If this mfilt.fits file has bad outlier rejection, remake the mosaic from the online *fbcd.fits files (using MOPEX).
 - b. If this mfilt.fits file has negative sidelobes, do 2-pass filtering offline starting with the BCDs and adjust the filtering window based on the extent of the source.
3. If stim response artifacts are present due to bright sources, then reprocess from scratch (the “raw” data) yourself (using the GeRT) and make new BCDs by masking out bad stim frames/pixels. You should correct for any multiplicative stim-response effects first and then correct for the residual additive slow response drifts via filtering.

The choice of filtered vs. unfiltered BCDs depends on your scientific goals. Extended absolute background measurements should be made from the unfiltered BCDs. For point sources and small extended regions, you can use filtered products (optimized for your source, if necessary).

7.6 Note on point source photometry

Since the small field photometry AOTs do not dither with offsets much larger than the size of the MIPS-Ge PSF, temporally filtered fbc data will underestimate the true point source flux values (by roughly about 10%). We recommend that you mosaic both the filtered and non-filtered data to determine whether or not additional offline processing is needed. You may find that the offline techniques described here significantly improve your data products.

To maintain point source calibration, it's possible to mask out the point sources before filtering. If you don't do that, we recommend that you measure the point sources before and after filtering to check its impact on the flux calibration.

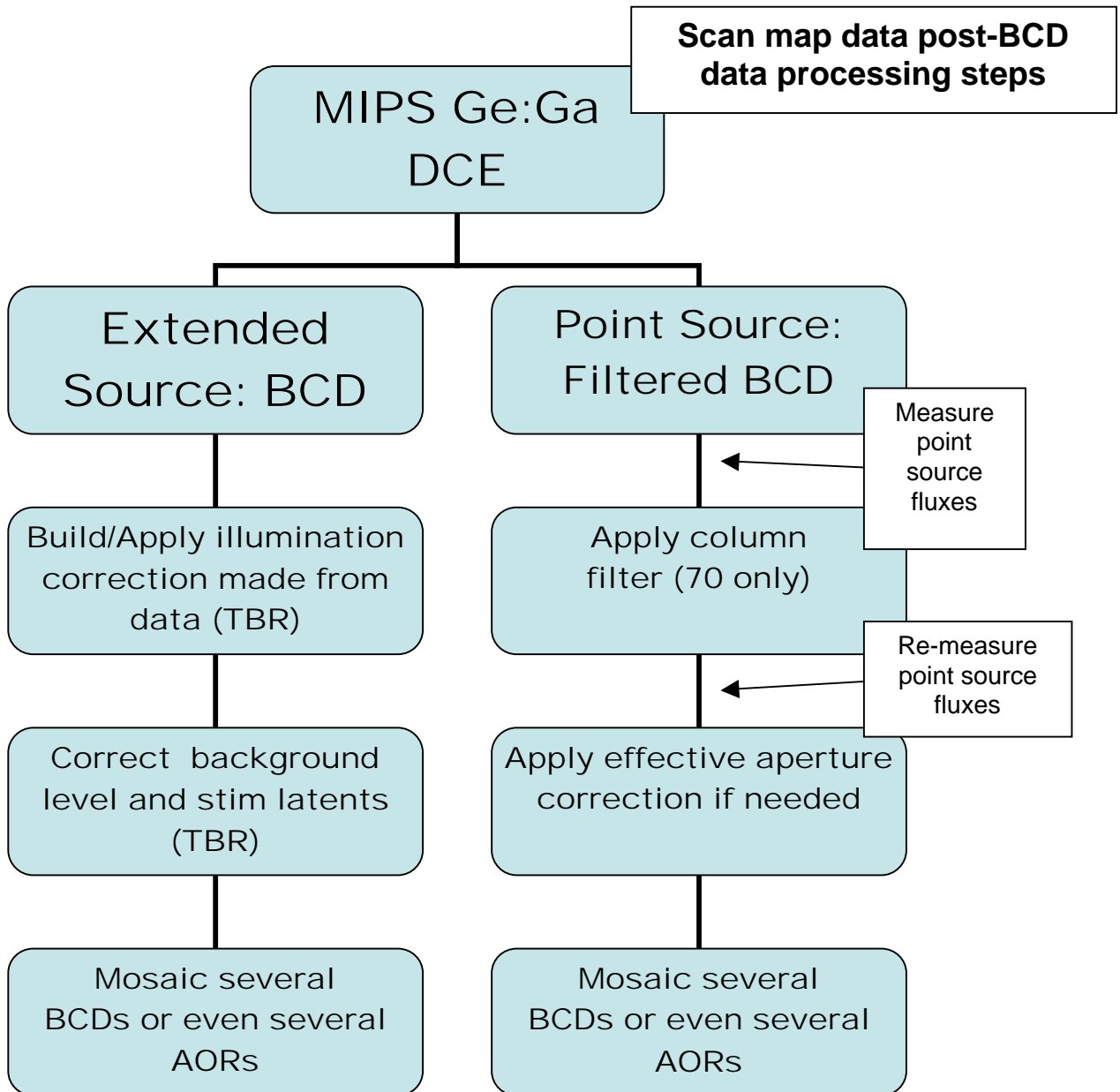


Figure 7.1: A flowchart describing possible pathways for analysis of scan map post-BCD Ge data processing. If your source of interest is not detected or higher S/N is required, then we recommend doing the steps above, otherwise the default BCDs may be sufficient. For extended sources of intermediate sizes, you may not want to correct for the slow response via an illumination correction but instead by an additive correction to the background.

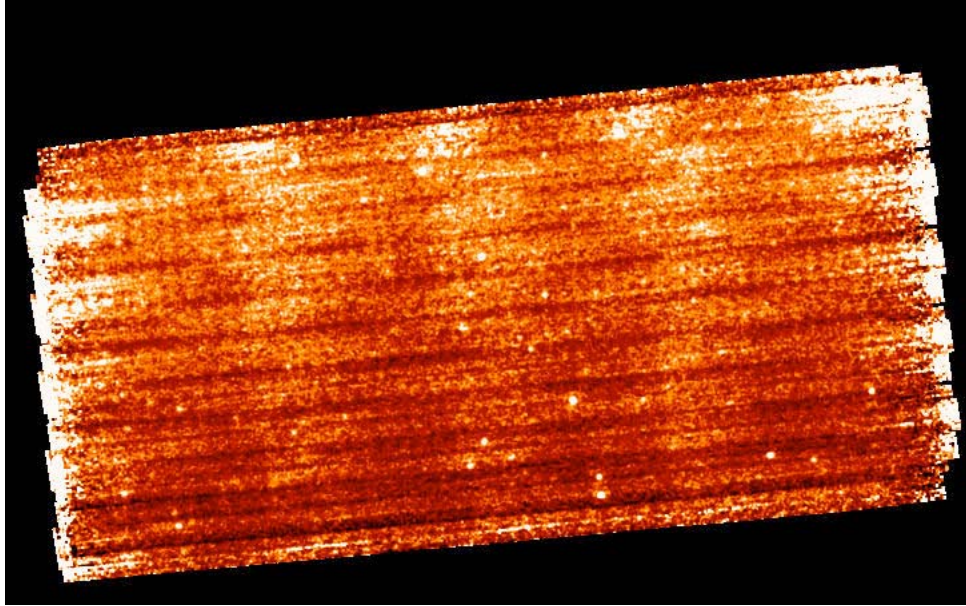


Figure 7.2: Default mosaic from 4 AORs of unfiltered MIPS-70 BCDs. The dark horizontal (in-scan) stripes are fast/slow response variations, and the bright vertical stripes are stim latents.

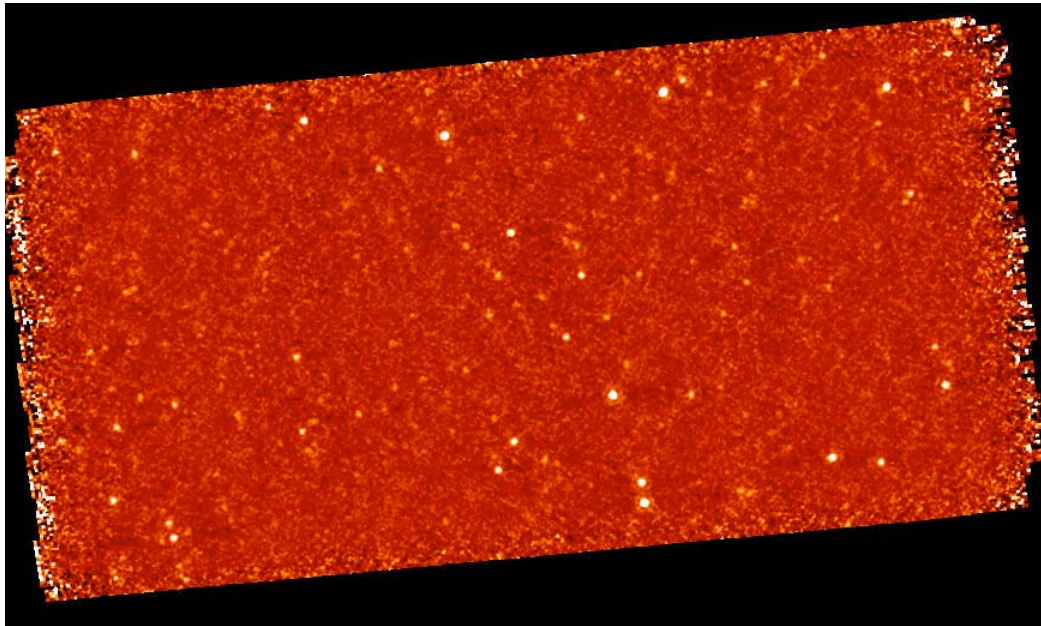


Figure 7.3: Default mosaic from filtered MIPS-70 BCDs, constructed from 4 AORs.

7.7 Error images

The error images currently provided with the BCDs are rough uncertainty estimations and do not include all of the systematic effects associated with the

Ge:Ga detectors. These error images also do not include the absolute flux uncertainty estimated to be about 20% for MIPS-70 and 160. The uncertainties include an empirical error on the slope calculation based on the dispersion of the data along the ramp, an estimated 5% uncertainty on the individual measurements of the stimflash signal, and the errors associated with the DARK and IC (illumination correction) calibration files. The errors on the calibration files represent the dispersion of the calibration DCEs about the median value (per pixel).

Note that the *bcd.fits and *fbcd.fits errors are inaccurate for S11. The BCD uncertainties are underestimated and the fBCD uncertainties are overestimated. This is fixed for S12 (and later) data products.

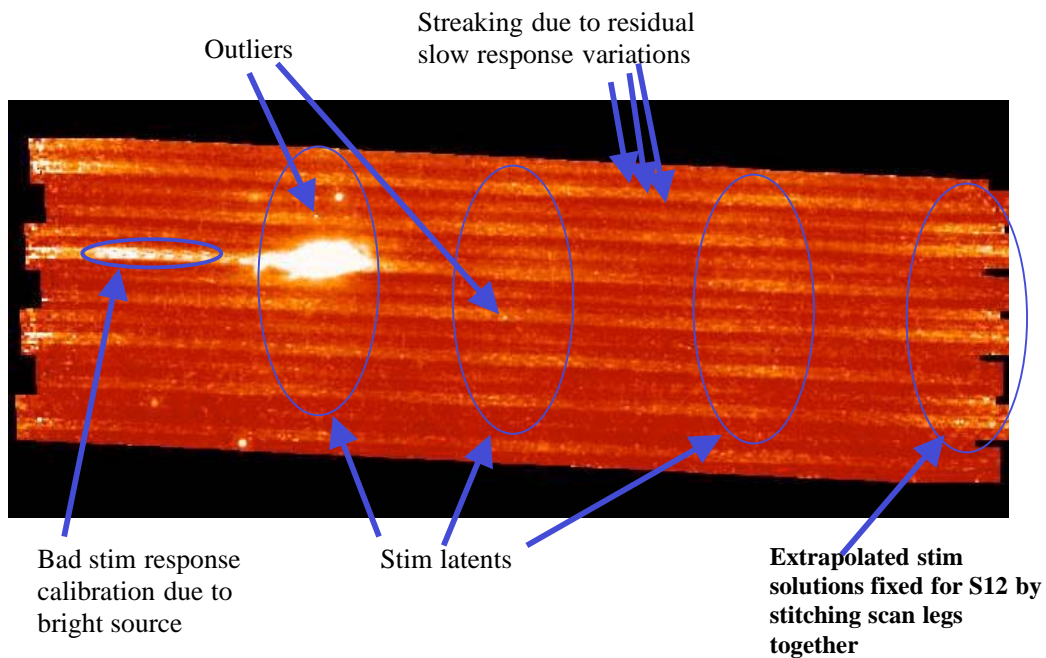


Figure 7.4: Examples of several of the most common MIPS-70 artifacts; see next several sections for more discussion. Note that these data are pre-bias change data processed under S10. (These data are NGC 7331, from the SINGS Legacy team.)

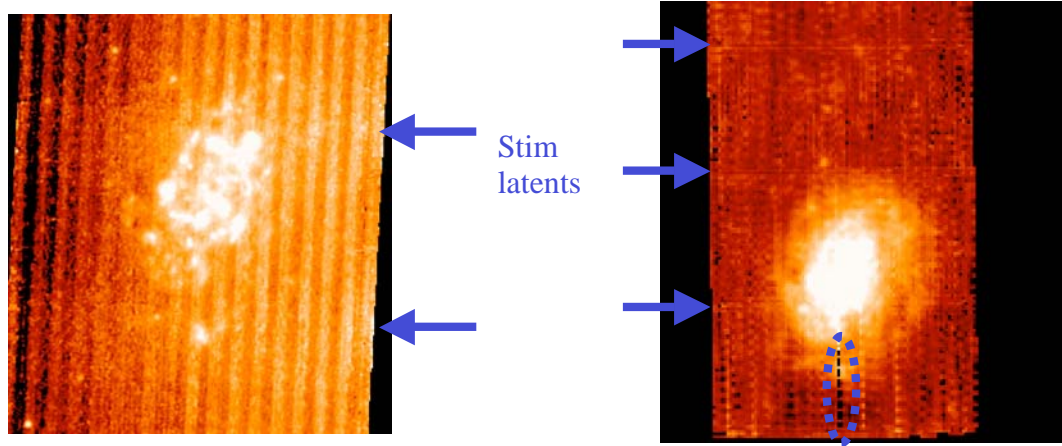


Figure 7.5: Automatically-produced mosaics of NGC 300. Left is 70 microns, and right is 160 microns. Stim latents are indicated. On the left, the vertical streaking is from residual slow response drifts (columns 5-9 are most affected at 70 microns). On the right, the dotted blue oval indicates a changed response in the stim calibration that comes from the bright source.

7.8 Variations of the slow response

MIPS-Ge data are calibrated using the stimulator flashes (or “stims”) to track the variation of the short-term response of the detectors; see SOM for more information.

The stim flashes are designed to track the responsivity drift of the Ge detectors. Since we measure the stim minus background signal, the calibration most accurately tracks the response to a step function, i.e., the fast response. The stim flash calibration does not completely remove long-term transients for the MIPS-Ge detectors. The effects are most noticeable before the bias change for MIPS-70 (e.g., dark horizontal stripes in bottom of Figure 7.2). The effects are not as noticeable for MIPS-160 due to short time constants for the stressed 160 micron detectors. For point source science, this effect can be removed using a temporal median filter (e.g., for scan data).

The variation of the drift in the slow response affects the ability to accurately measure the true background level. For point sources, the long-term drifts can be treated as an additive effect (i.e., subtracting off a temporal median). The long-term drifts affect the actual response from the background, suggesting a multiplicative correction may be needed for large extended regions. For large extended sources, we recommend that observers take enough off-source data of the surrounding background so that the total extended source flux can be estimated.

7.9 Stim latents

For data taken in IOC/SV or the first 4 MIPS campaigns in nominal operations, the bias setting of the 70 μm array was set at a level that attempted to increase the

sensitivity of both sides of the array, but a consequence was that the stimulator flashes left latents in the data. For bright sources, this is less of a concern than for extended regions or long integrations built up from short exposures (e.g., in photometry mode). The stim latents and variations of the slow response as a function of time can be mitigated by median filtering the data, if you are only interested in faint point sources.

The amplitude of the stim latents depends on background and appears to increase with the time since anneal. The stim latents linger longer for 70 microns than 160 microns, since the decay time constants associated with the stim latents are larger at 70 microns.

Data taken after the bias change (MIPS-5 or later, after 14 March 2004) should still see these effects, but at a much lower level.

7.10 First DCE effects, or corrupted stim-minus-background measurements

As mentioned above, long-term transients are tracked using the stim flashes. In scan maps, necessarily the first set of DCEs has an extrapolated stim calibration since there is no background for the first DCE. The number of DCEs suffering this effect varies as a function of scan speed; see Table 7.1. Of course, this implies that these first DCEs are of lower reliability; except for fast scan, these DCEs are generally part of the “overscan” region, and do not count for coverage of your requested area. This also means that you should not just grab all of the DCEs and blindly work with them, especially when you have scans over bright regions or scans that end in bright regions; see Figure 7.6, which shows a portion of a fast scan over a bright region. The artifacts apparent in the left panel are largely omitted in the right panel when the DCEs with extrapolated stims are dropped. Note that the white streak in the right is still a bright object artifact, but the effects of the bright object are substantially reduced in the final product on the right.

Conversely, however, the trailing DCEs have plenty of stim flashes, and are quite reliable.

DCEs with extrapolated stim solutions can automatically be rejected by the SSC mosaicking software MOPEX. There is a bit in the bmask which indicates extrapolated stim solutions so that you can tell software to ignore those frames.

For S12 and later, data will be processed on an AOR basis instead of a scan leg basis, which will minimize the number of DCEs with extrapolated stim solutions.

Table 7.1: Number of DCEs with extrapolated stim calibration.

Scan speed	Number of DCEs with extrapolated stim calibration
Slow	First 12
Medium	First 26
Fast	First 34

Bad stim calibration can occur not only for extrapolated solutions, but in cases where the background DCE for the stim is on a bright region, which due to the latents from the source, can yield a bad stim-background measurement. You should try to avoid this when planning your observations (e.g., by taking a long enough scan to get enough background). You may need to correct these cases by deriving a correction based on the surrounding valid stim-background measurement; in some cases, the observation may not produce optimal results. This is a difficult problem, and if you think you have encountered it, your data may not be easily calibrated. Consider using the GeRT.

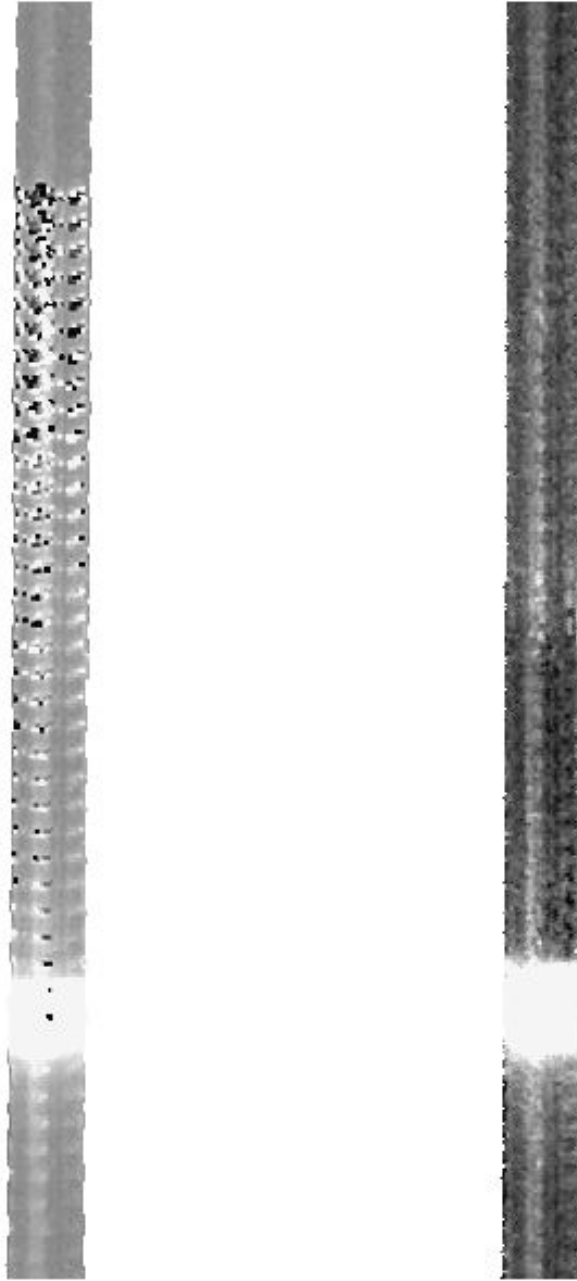


Figure 7.6: Effects of extrapolated stim calibration. On the left, the artifacts from an extrapolated stim are clearly apparent; on the right, the DCEs with extrapolated stims have been omitted.

7.11 Electronic non-linearities

The electronic non-linearities for the MIPS-Ge detectors are corrected for in the online pipeline. However, spurious electronic non-linearity solutions for a few unstable pixels on the top row of the 70 micron detector can yield artifacts in the mosaics. The recommended solution is to make sure you have the most recent pmask downloaded from the SSC website, and make mosaics with this updated

pmask, ignoring these pixels (use the pmask rejection parameter=16648). This is fixed starting in the last half of S11 reprocessed campaigns.

7.12 Flux non-linearities

The flux nonlinearities for the MIPS-Ge detectors have yet to be fully quantified. These nonlinearities represent the differences in the flux conversion factor as a function of source flux. Currently, the SSC assumes a constant flux conversion factor for all flux ranges; see Table 3.9. Early observations suggest that faint MIPS 70 micron sources (<100 mJy) have flux non-linearities that are a <20% effect. The level of flux non-linearities for 160 micron has not yet been quantified, given the small number of asteroid calibration observations that have been carried out to date. Analysis is ongoing, and we will update this document as information becomes available.

7.13 160 μm short-wavelength light leak

Signals on pure photospheres of stars at 160 μm are stronger than expected by about a factor of five. Review of the instrument design has revealed a weakness in the stray light control that could result in a short wavelength Ge:Ga response being detected in this band (due to scattering off a blocking filter).

For many types of observations, this light leak does not impact the data at all. Stars fainter than $m_J \sim 5.5$ mag will not be detectable in the leak above the confusion level. No compact extragalactic sources have m_J brighter than 5.5 mag. The leak signal for a star of $m_J = -0.5$ mag is equivalent to ~ 2.5 Jy at 160 μm . The parameter to consider for any given target is the 160 μm / 2 μm flux density ratio. For a Rayleigh-Jeans source, this ratio is 0.0001. Anything with a ratio larger than 0.004 will produce uncorrupted data, so most objects will not be affected. Sources with 160 μm fluxes more than a factor of 40 above that of a Rayleigh-Jeans source from 1 – 1.6 μm will have leak signals <10% at 160 μm . Galactic programs on star formation, ISM, etc., will likely be impacted.

For stellar observations, the strongest signal apparent in a 160 μm observation is likely to be the leak itself. Tests were performed using HD 163588, a K2III star which is routinely observed at 70 μm and has also been observed at 160 μm . Similar results are obtained for HD 36673 (Arneb), an F0Ib star, and for HD 87901 (Regulus), a B7V star. The leak is 15 ± 7 times as bright as the photosphere of a star.

Figure 7.7 and Figure 7.8 show example 160 micron images of a star and an asteroid, respectively. The asymmetry apparent in the stellar image is a result of the short-wavelength light leak. Note that the brightest thing here is actually the *leak*; the *star* is the asymmetry to the bottom right. Figure 7.10 provides another view of the spectral leak, compared to a galaxy this time.

It has been demonstrated that observations of bright point sources strongly impacted by the leak (stars) can be corrected to a high level using an empirical stellar PSF and careful deconvolution (see, e.g., Stapelfeldt et al. 2004, ApJS, 154, 458). Best results will be obtained with observations for which proper

planning and data acquisition was made to allow a good characterization of the leak signature for the object brightness and color. For example, plan to obtain identical observations of “calibrator” stars of similar type and brightness to your target stars, but without long-wavelength excesses.

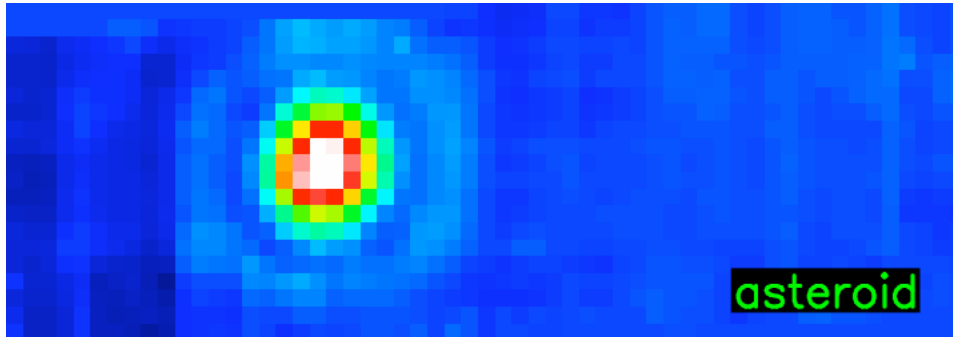


Figure 7.7: 160 micron image of an asteroid; compare to next 2 figures. Note that this PSF is more symmetric than the stellar one in the next figure.

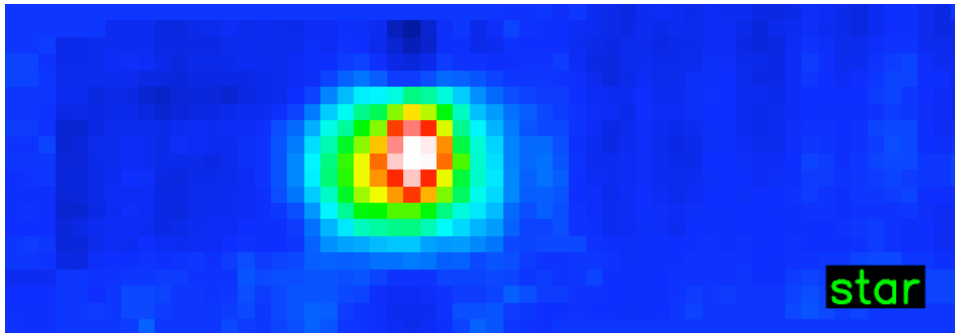


Figure 7.8: 160 micron image of a star; compare to previous and next figure.

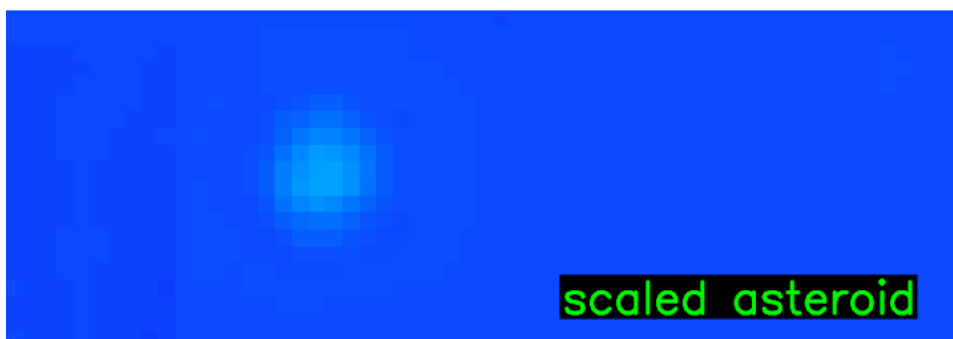


Figure 7.9: Scaled asteroid – this is the brightness of the photosphere compared to the leak. (Compare to previous two figures.)

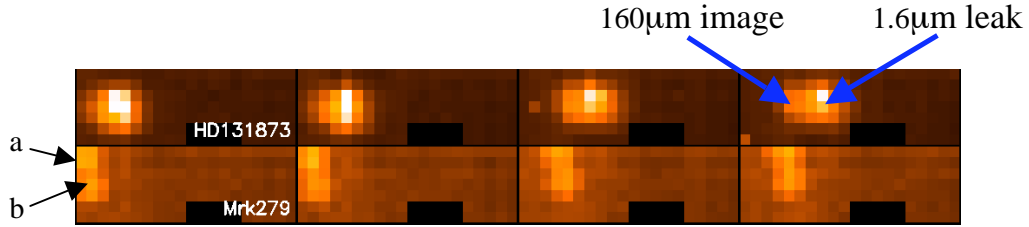


Figure 7.10: Another view of the spectral leak. The top row is 160 μm photometry observations of a star, HD131873, a K4 III ($V=2.1$, 160 micron flux of 0.66 Jy); it has a Rayleigh-Jeans spectrum. The bottom row is Mrk 279, a double galaxy (components are indicated as a and b). This is an extremely red object! Dithers in both cases are identical. The relative offset of the stellar image and leak is a function of position on the array.

7.14 Offline Enhancements to MIPS 70 Fine Scale or 70/160 large-field

The observing strategy implemented for the MIPS-70 Fine Scale AOT and the 70/160 large-field photometry differs from both the MIPS default photometry and scan modes in that alternating on- and off-source DCEs are obtained during each cycle. The distance between the centers of the on- versus off-source positions is roughly $4'$. Consequently, the two fields of view overlap and the online pipeline currently creates a single mosaic consisting of both on- and off-source BCDs. The acquisition of the off-source frames provides the opportunity for additional offline post-processing. While in most cases the pipeline reduced BCDs are of good quality, we have found that the data can be improved to varying degrees by different methods of off-source “background” subtraction. However, *there is no general recipe* that works equally well for all types of observed sources and the observers are cautioned to carefully investigate the appropriate method for their particular datasets, especially in the case of bright and spatially varying extended emission.

Several offline approaches can be applied to clean up these data without filtering, which allows users to maintain proper calibration for extended sources. The best technique depends on the details of a particular data set. You can subtract the “off-source frame” from the preceding “on-source” frame (e.g., with IRAF) and mosaic the resulting difference images with MOPEX. You can take the median of the “off-source” frames, subtract the resulting median image from each “on-source” frame, and mosaic the resulting difference images. Or, you can do some variation/ expansion/ combination of these two approaches depending on the particular data set. In using any of these, watch out for sources in the “off-source” frames!

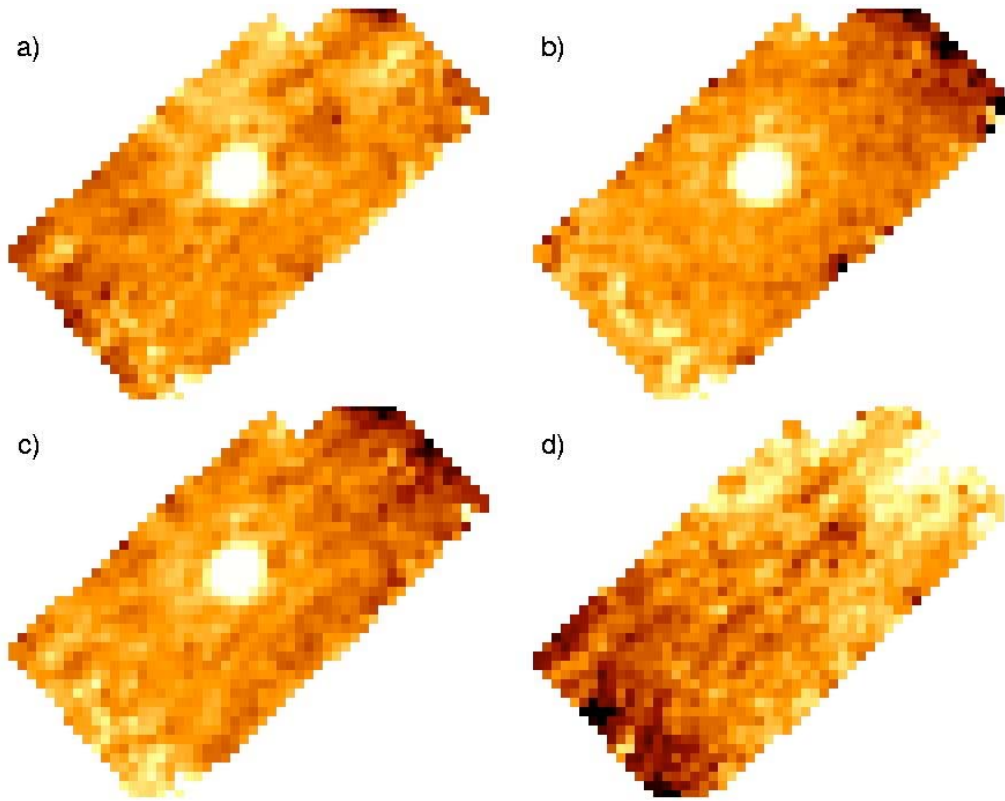


Figure 7.11: Examples of 70 micron fine scale reprocessing discussed in text.

Figure 7.11 shows examples of several cases.

- a) The mosaic of all on-source BCDs without any additional post-processing. On-source BCDs are the odd-numbered BCDs in each cycle (1,3,5,7). The even-numbered BCDs represent the off-source BCDs and additional stim and stim background observations.
- b) The mosaic of paired on-source minus off-source BCDs, i.e., for each on-source BCD, subtract the off-source BCD immediately following it. This method usually provides the visually smoothest mosaic. However, the noise is usually slightly increased over methods where the off-source BCDs are first combined before subtraction (e.g., case c).
- c) The mosaic of on-source BCDs after subtraction of the median-combined off-source BCDs from each BCD.
- d) The mosaic of all off-source BCDs.

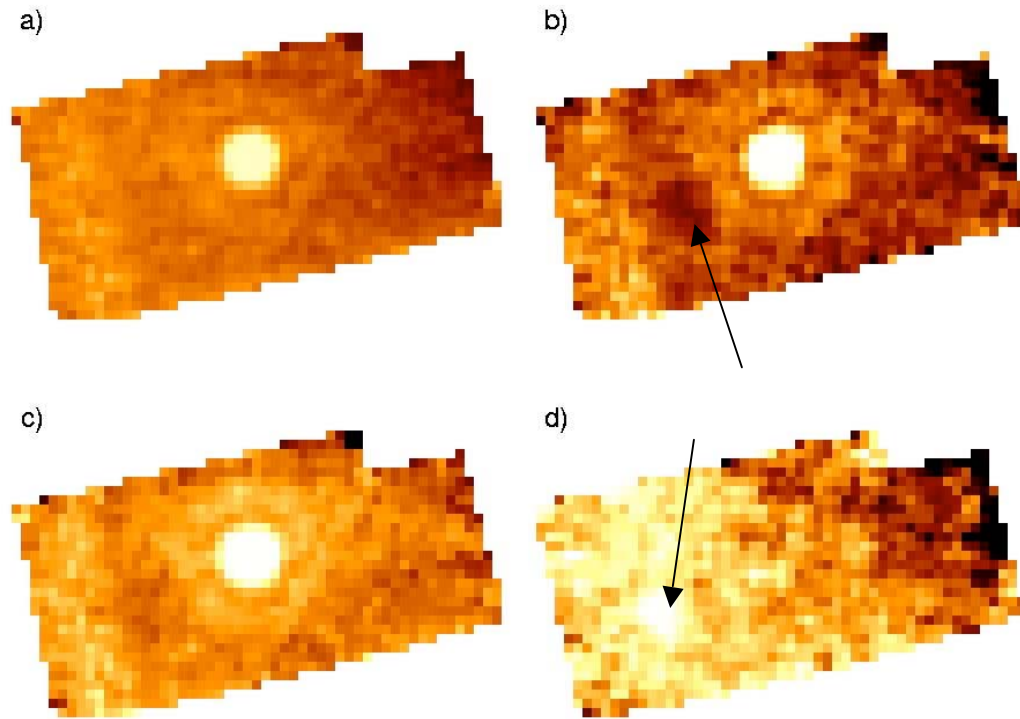


Figure 7.12: Examples of 70 micron fine scale reprocessing when there is a serendipitous off-source object; see text.

Before performing any off-source subtraction, we recommend that you *always inspect the mosaic of the off-source BCDs* to prevent introduction of off-source structure into the on-source mosaic. Figure 7.12 highlights the case where a serendipitous source is present in the off-source BCDs.

- a) The mosaic of all on-source BCDs without any additional post-processing.
- b) The mosaic of paired on-source minus off-source BCDs, i.e., for each on-source BCD, subtract the off-source BCD immediately following it. Notice that a dark residual is introduced due to the presence of the serendipitous source in the off-source BCDs.
- c) The mosaic of on-source BCDs after subtraction of the median-combined off-source BCDs from each BCD. Notice that the effect of the serendipitous source is reduced due to the median combination of the off-source BCDs (since the source is at slightly different array coordinates in each BCD).
- d) The mosaic of all off-source BCDs. Notice the serendipitous source present in the left half of the array.

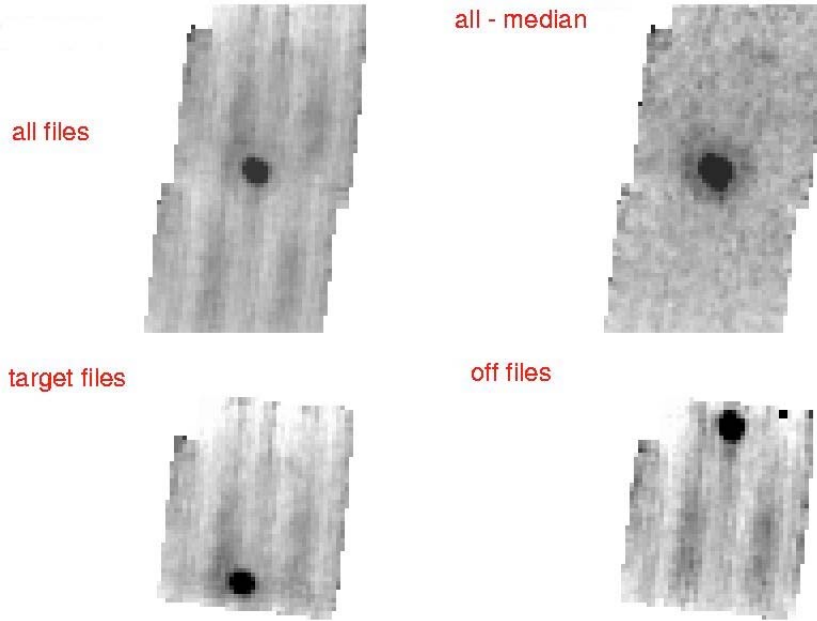


Figure 7.13: Applying the same technique to a small raster map observation; see text.

In the raster map example shown in Figure 7.13, the target was positioned so that it appears both in the “on-source” and “off-source” frames, hence neighboring “on” and “off-source” frames cannot be subtracted. Instead, all frames were median combined and the resulting image subtracted from each BCD.

7.15 Example: 70 micron faint point source survey

In this section, we describe how to reduce 70 micron data when you are interested in faint point sources. See also a graphical representation of this process in Figure 7.1.

Figure 7.14 shows a mosaic from one AOR of the extragalactic FLS verification field. It is made from the non-filtered 70 micron BCD products. The dark (horizontal) stripes at the bottom of the image are due to the variation of the residuals in the slow response. The bright (vertical) stripes at the top are due to stimflash latents.

Figure 7.15 shows a mosaic of the time-filtered BCDs (e.g. the *fbcd files). The drifts of the slow response and the majority of the stim latent artifacts are removed using the temporal filter data. While filtering scan data, point source calibration is maintained to within measurement errors.

If the stim latents in your data are significant, and vary significantly as a function of time, then you can make additional corrections to improve the removal of residual stim latent artifacts. Since there is a correlation of the stim latent signal with column, the simplest solution is to subtract the median value of each column from every fbcd image before mosaicking; see Figure 7.16 – note

that this is the first truly manual step in this process. This spatial filtering (along columns) will slightly bias point source calibration to weaker values by about 5%, given the large PSF of the 70 micron data. If you use this technique, we recommend measuring sources before and after column filtering and correcting for the systematic differences by applying the appropriate multiplicative scale factor (effectively an aperture correction) to the derived source catalog. (See Appendix or SSC MIPS website for IDL code example of column filtering for MIPS-70).

After correcting for the stim latent artifacts in the fbcDs, multiple AORs can be coadded; Figure 7.17 is 4 AORs processed in the same fashion and co-added. These data have noise properties that integrate down as roughly $1/\sqrt{t}$ for times less than about 500 seconds. Plan your observations to have redundancy!

Sample namelist files for the SSC post-BCD software are available on the SSC website.

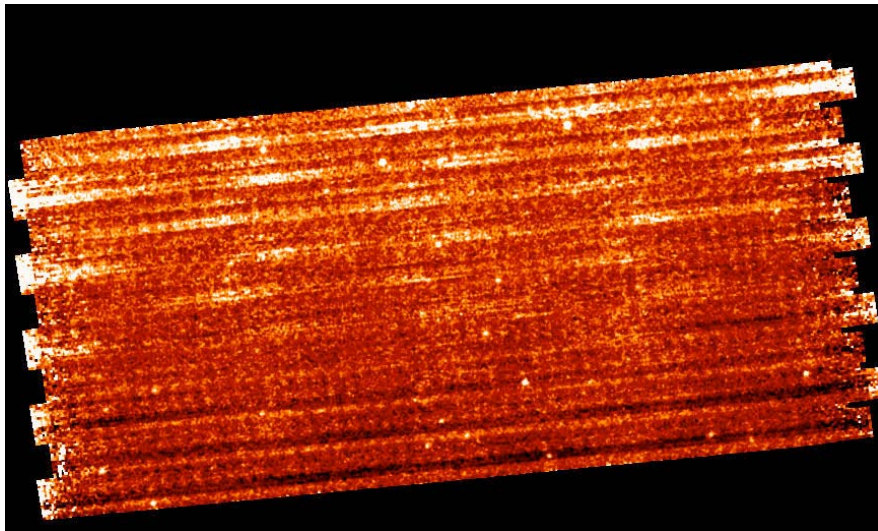


Figure 7.14: Step 1: mosaic of initial default 70 micron scan BCDs (1 AOR) from the extragalactic First Look Survey. Stim latents (white horizontal streaks) and slow response residuals (dark horizontal streaks) are apparent; see text.

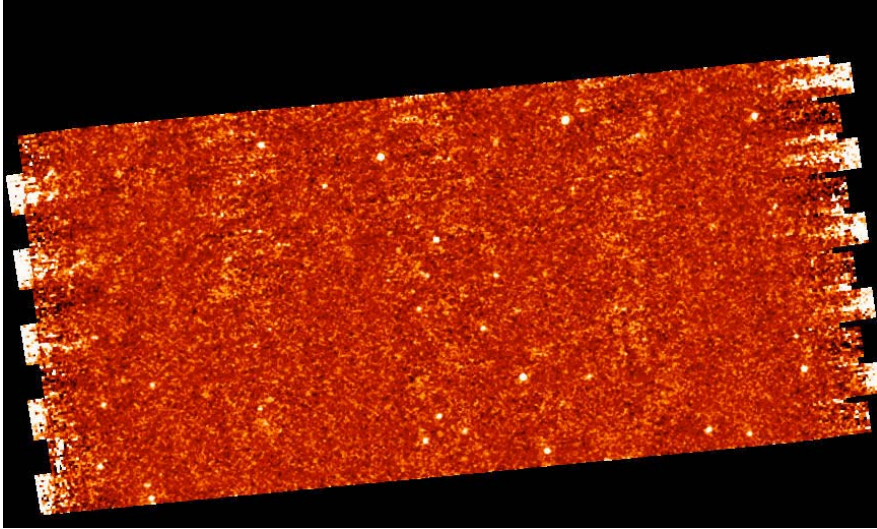


Figure 7.15: Step 2: mosaic of time-filtered 70 micron scan BCDs (e.g. using the fbcd files for 1 AOR). Variations due to slow response residuals have been corrected, though stim latents are still visible.

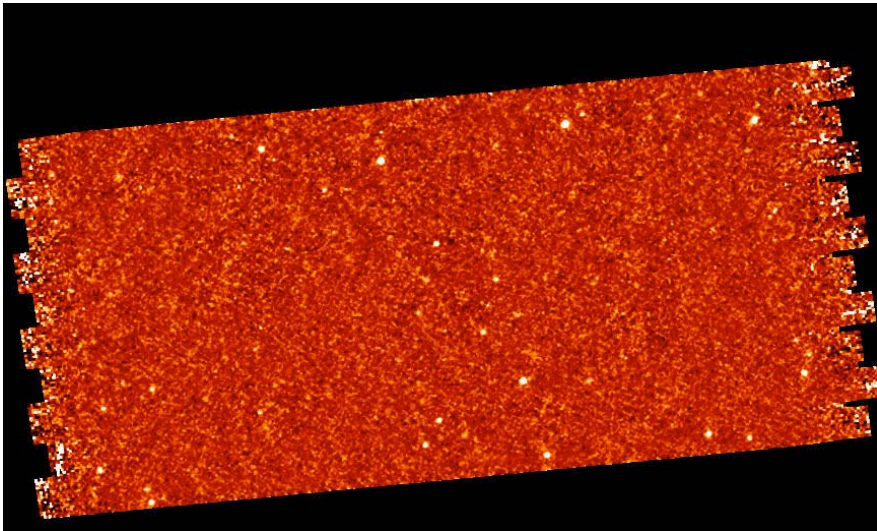


Figure 7.16: Step 3: mosaic of column-filtered 70 micron scan BCDs for 1 AOR.

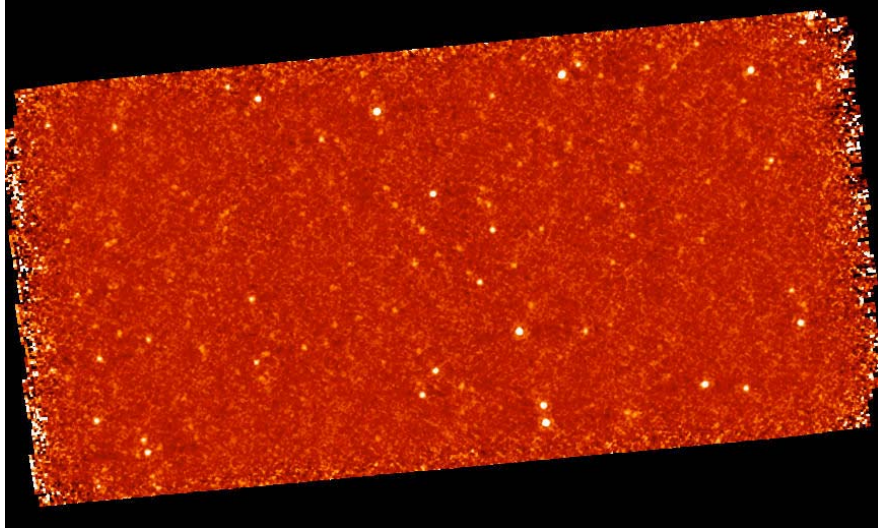


Figure 7.17: Step 4: mosaic of 4 AORs processed as above.

7.16 Example: 160 micron faint point source survey

Compared to the 70-micron array, the 160 micron detectors are generally better behaved due to the faster time constants – this means less filtering and/or custom-offline processing is required. Lack of redundancy is a major issue for most 160 micron observations (only 8x4 seconds in this example). Plan your observations to have plenty of redundancy!

Figure 7.18 is a mosaic of the standard non-filtered BCDs produced by the pipeline for the XFLS verification field. As with the 70 micron data, some responsivity streaks are visible in the in-scan direction, and some stim flash residuals are visible in the cross-scan direction. Figure 7.19 shows a mosaic of the filtered BCDs produced by the pipeline, e.g., the *fbcd files. This may be sufficient for most users interested in faint point sources.

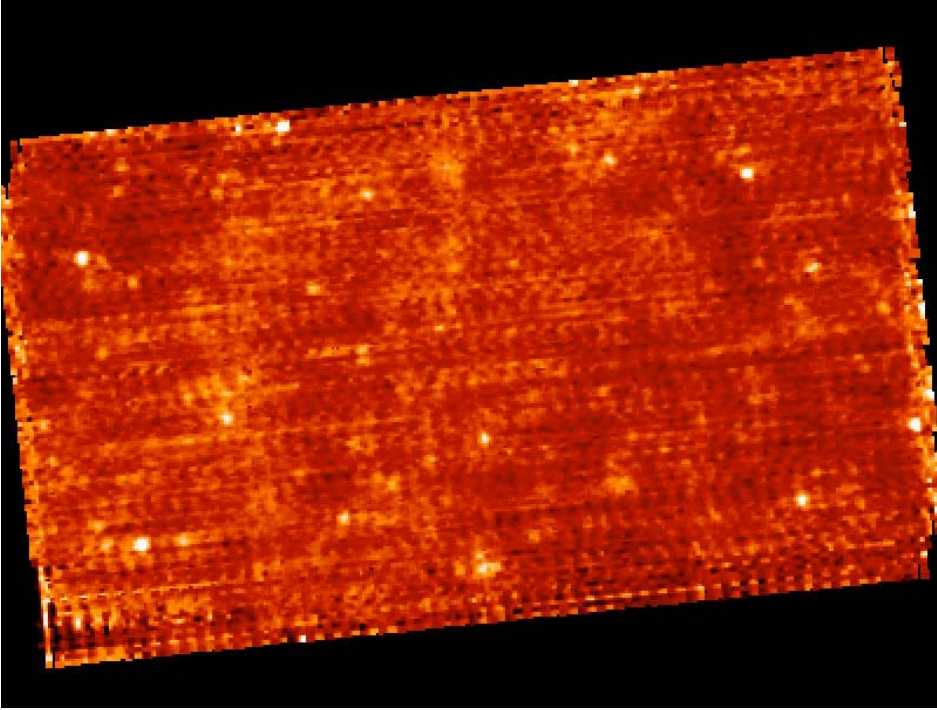


Figure 7.18: Mosaic of MIPS-160 default scan BCDs from the extragalactic FLS.

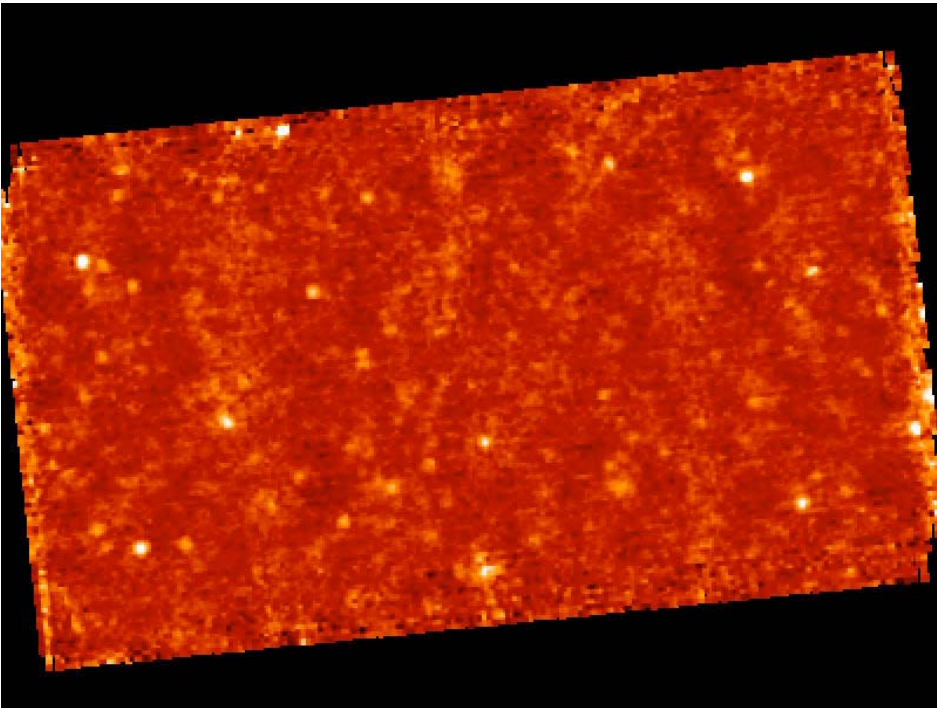


Figure 7.19: Mosaic of MIPS-160 filtered scan BCDs (*fbcf files).

7.17 Example: 70 micron bright extended source

In this section, we describe how to reduce 70 micron data when you are interested in bright extended sources. See also a graphical representation of this process in Figure 7.1. This example uses NGC 300; the corresponding science paper is Helou et al. (2004, ApJS, 154, 253). NB: The NGC 300 data as shown were taken before the bias change in March 2004. Data taken after the bias change may be sufficient for most purposes, without additional offline processing.

Figure 7.20 shows a 70 micron mosaic of NGC 300 made from the default non-filtered BCDs. The dark stripes at the left of the image are due to the variation of the residuals in the slow response. The bright stripes at the right are due to stimflash latents. Figure 7.20 also shows the mosaic made from the temporal filtered BCDs (*fbcd files). Although the drifts of the slow response and stim latents are removed, the filtering process removes extended source flux and introduces negative sidelobes near bright emission regions.

For extended sources, we recommend you use the default BCDs, not the filtered BCDs. **The filtering techniques are optimized for point sources and remove a significant fraction of the emission from extended sources.** For example, note how much the extended source flux changes in Figure 7.20 and Figure 7.21. To remove data artifacts for extended sources, observers need to observe enough off-source regions for good background subtraction. We recommend that observers linearly interpolate the measured background levels in the BCDs across the target on a pixel basis. The interpolated background corrections should be subtracted from the BCDs before coadding the data and making the mosaic. If there are not enough data to derive corrections with sufficient S/N on a pixel basis, then observers may find that background corrections derived on a column basis for 70 micron (or even a 1x8 readout region within the column) yield better results. The additive background corrections as described here have been shown to yield good results for extended galaxies. To derive the true sky level for extended regions, observers may want to consider TPM observations.

Sample namelist files for the SSC post-BCD software are available on the SSC website.

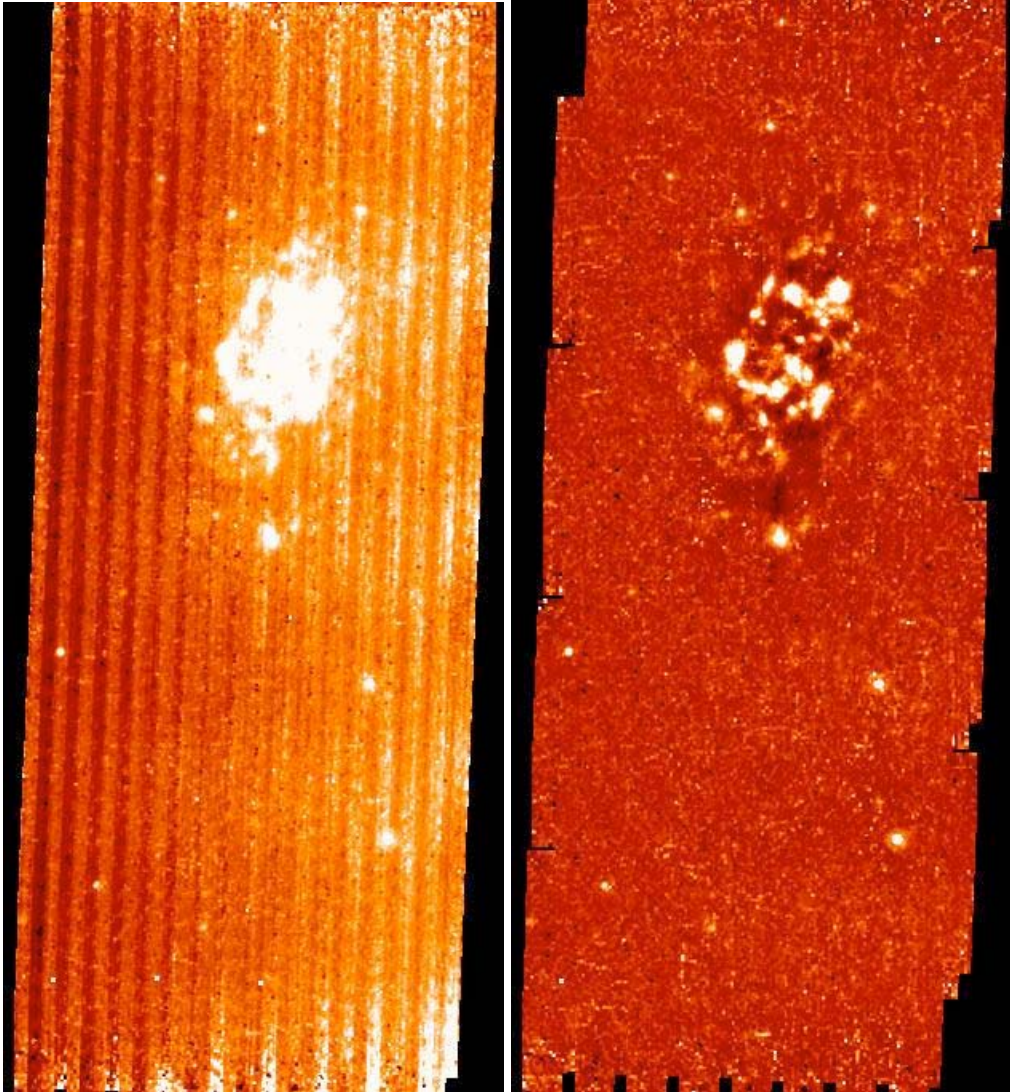


Figure 7.20: Mosaic of 70 micron BCDs from NGC 300: left is unfiltered and right is filtered (DON'T DO THIS!). On the left, note the variations in the background due to stim latents (bright) and the slow response residuals (dark). On the right, note the filtering process has removed extended source flux and introduced negative sidelobes near bright regions.

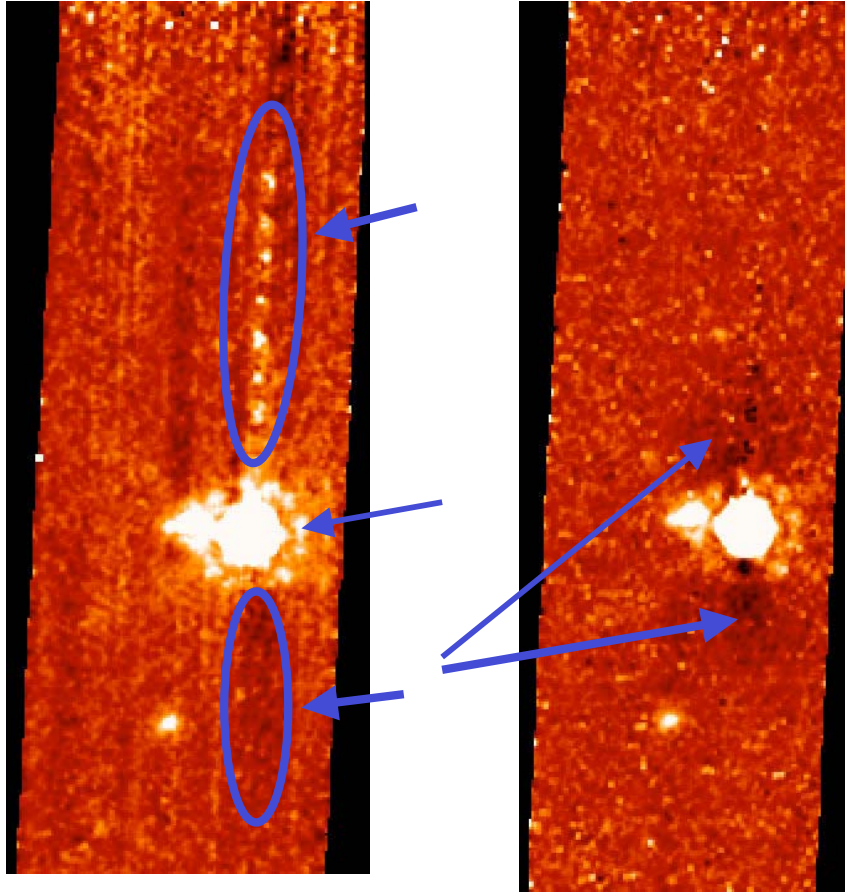


Figure 7.21: Another bright extended source: NGC 2798. Left is the BCD mosaic, and right is the filtered BCD mosaic. On the left, the top oval and arrow indicate where the stim calibration for some pixels is affected by the bright source. To fix this, you need a manual stim calibration, masking the bright source. The center arrow indicates the PSF itself. The bottom oval shows where trailing pixels after a bright source can be depressed due to a response effect from the bright source. On the right, the arrows indicate negative sidelobes introduced by the filtering. To fix this, you need 2-pass filtering and better outlier rejection.

7.18 Example: 160 micron bright extended source

In this section, we describe how to reduce 160 micron data for bright extended sources.

The standard 160 micron default, non-filtered reduction for extended sources may be good enough for most purposes; see Figure 7.22. You may be able to improve on the standard reduction by making a corrected illumination correction file from the data themselves and applying the correction before mosaicking. If the DCE after the stim is significantly brighter than following BCDs, you may not want to include this DCE in the mosaic, depending on the level of redundancy in the data set.

The use of median filtered data is *not recommended* for extended sources at 160 microns; see Figure 7.22.

A second example of a galactic object (the cluster L1228) on a bright background appears in Figure 7.23 through Figure 7.25. Again, constructing a mosaic from the filtered BCDs is *not recommended*; see Figure 7.25. The namelist used to produce these mosaics with MOPEX is available on the SSC MIPS website.

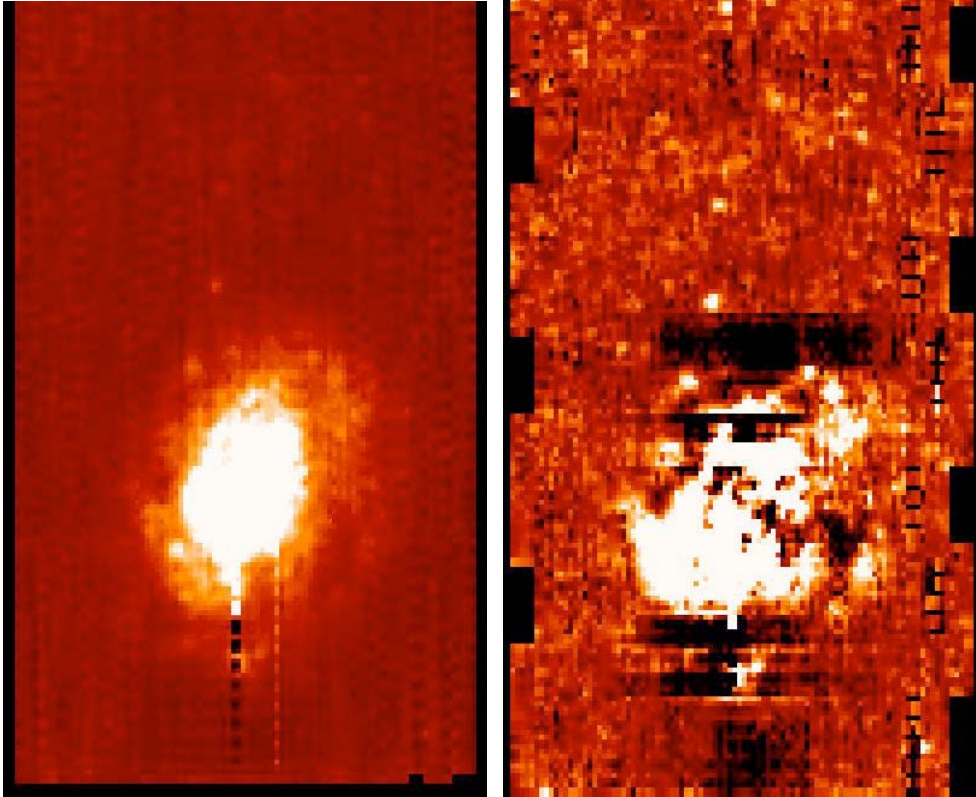


Figure 7.22: Mosaic of unfiltered (left) and filtered (right; DON'T DO THIS!) 160 micron scan BCDs of NGC 300. On the left, the dark and bright “dotted lines” are bright object latents. Note on the right among other things the dark sidelobes introduced by the filtering. See text.

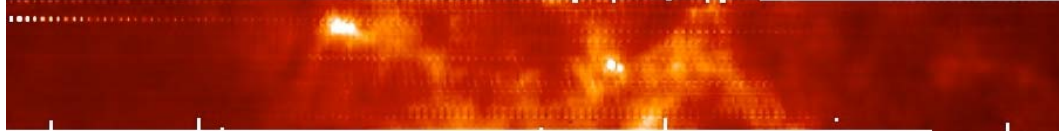


Figure 7.23: Scan map of the molecular cloud L1228 at 160 microns from the Galactic First Look Survey (2 degrees long). The image was created using MOPEX and the unfiltered BCDs, and illustrates how well the 160 micron array behaves on a relatively bright background.



Figure 7.24: As above, but using the filtered BCDs; the linear stretch is the same in both images. In this case the ‘damage’ on the intensity of the mosaic is not horrendous, but the flux level has been modified (see next figure below).

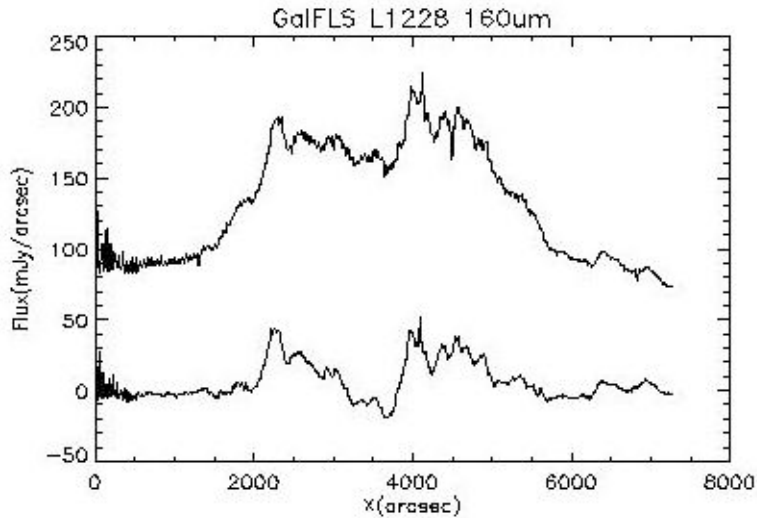


Figure 7.25: The integrated flux of the L1228 mosaic on the cross-scan direction along the scanning direction for the unfiltered (top line) and filtered (bottom line) BCDs. The flux density using filtered BCDs has dropped by nearly a factor of 3.

7.19 New examples using the GeRT

7.19.1 Trails of bright latents

Figure 7.26 shows examples of response corrections made via offline reprocessing with the GeRT. The “before” and “after” compares the automatically-produced (“online”) mosaic and the mosaic created from GeRT-reprocessed BCDs. With the GeRT, we removed stim pixels affected by the bright source and stitched the scan legs together. Variations in response can occur when the stim flash and/or stim_background DCE occurs on bright sources.

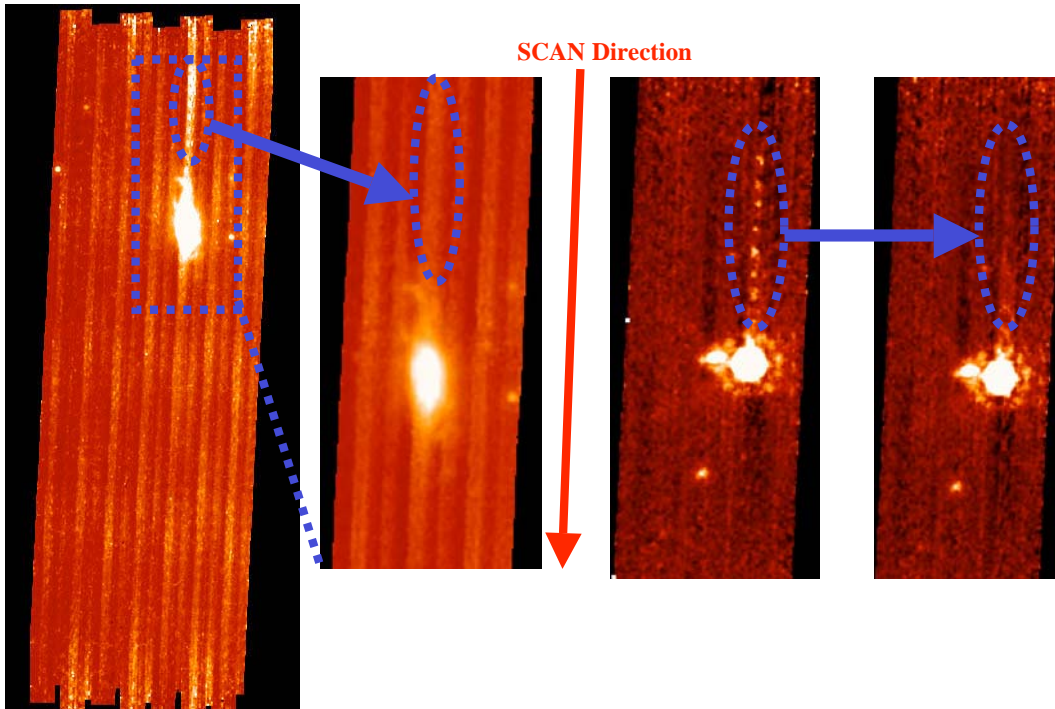


Figure 7.26: Examples of offline processing using the GeRT. Left pair of images is NGC 7331, and right pair of images is NGC 2798. Within each pair, the left is the automatically produced (“online”) mosaic and the right is after processing with the GeRT and remosaicking the BCDs.

7.19.2 Filtering the background behind a bright star

IDL routines that are packaged with the GeRT allow you to mask out a bright star and filter the background. Instructions for this come with the GeRT, but we summarize the steps here. The results can be seen in Figure 7.27.

1. Make input list of bcds and input mask files.
2. Start IDL, and set variables to be the RA and Dec of the source in decimal degrees:

```
IDL> ra0=288.13875
IDL> dec0=67.661667
```
3. Run Column filter ignoring pixels around input source position. This calculates the median value for each column, subtracts the value for each column for each BCD, and updates the BCDs in the input list (it overwrites the input BCDs).

```
IDL> bcd_column_filter, 'bcd70.lis', ra0, dec0
```
4. Make pixel-to-pixel additive correction. This calculates the median of each pixel for the data set to derive pixel-to-pixel additive corrections (ignoring the source and bad pixels), subtracts value from each pixel for each BCD, and updates the BCDs in the input list (overwriting the input BCDs).


```
IDL> bcd_time_filter, 'bcd70.lis', 'mask70.lis', ra0, dec0, /update,$  
pmaskfile='MIPS70_PMASK.fits'
```

5. Finally, re-mosaic the updated BCDs with MOPEX.

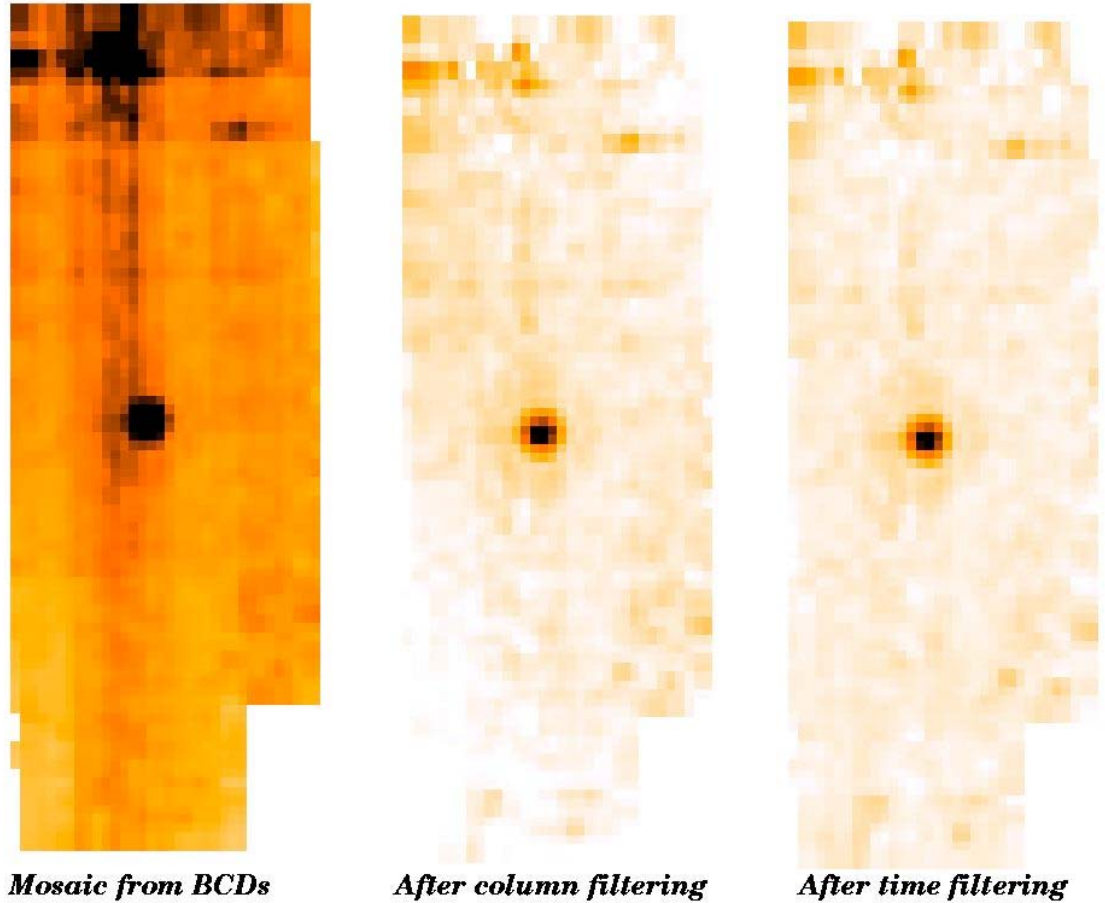


Figure 7.27: Example of use of column and time filtering routines packaged with the GeRT.

7.20 Additional Examples

Some additional examples are available on the SSC website; see the data analysis cookbooks. More cookbooks are planned.

8 MIPS-SED mode

MIPS-SED mode has been commissioned for uplink (e.g., Spot visualizations and spacecraft commanding are fine), and as of this writing, it is about to be commissioned for downlink. Because we are now taking science data in this mode, we have added this short chapter on MIPS-SED data. More extensive discussion will be added to future versions of this document.

The SED BCDs are fine to use right now, with a current flux uncertainty of up to ~20%. You currently need to combine the BCDs on your own; there are no tools available yet from the SSC for dealing with SED mode data.

To go one step further, you can also derive a simple median (or average) image from all the non-stim BCDs on the target, and a similar one from those off the target. The difference between the two coadded images is the sky-subtracted, 2-D image of the target. An example follows.

8.1 How to make simple coadditions of MIPS-SED BCDs

8.1.1 Chop/dither pattern

To correctly coadd MIPS/SED BCDs, you need to understand the pointing pattern on sky. Each SED observation is based on the following basic chop/dither pattern (i.e., the pattern when the number of cycles, N_c , is 1):

```

sky_position_#1
sky_position_#1 - STIM
target_position_#1
sky_position_#1
target_position_#1
sky_position_#1
target_position_#1
sky_position_#1
sky_position_#1 - STIM
(dithering via telescope nodding)
sky_position_#2
sky_position_#2 - STIM
target_position_#2
sky_position_#2
target_position_#2
sky_position_#2
target_position_#2
sky_position_#2
sky_position_#2 - STIM

```

where “target_position_#1” and “target_position_#2” refer to those telescope pointings for which the target is placed on the SED slit; the “sky_position_#1” and “sky_position_#2” are corresponding reference pointings acquired by chopping the MIPS scan mirror. The dither step size between target_position_#1 and target_position_#2 (or between sky_position_#1 and sky_position_#2) is about 5 detector columns.

If more than one cycle is requested ($N_c > 1$), this basic chop/dither pattern gets expanded as follows:

```

sky_position_#1
sky_position_#1 - STIM
target_position_#1
sky_position_#1
target_position_#1
sky_position_#1
target_position_#1
sky_position_#1
sky_position_#1 - STIM
[ target_position_#1
sky_position_#1
target_position_#1
sky_position_#1
target_position_#1
sky_position_#1
sky_position_#1 - STIM ] <--- [...] is repeated Nc-1
times
(dithering via telescope nodding)
sky_position_#2
sky_position_#2 - STIM
target_position_#2
sky_position_#2
target_position_#2
sky_position_#2
target_position_#2
sky_position_#2
sky_position_#2 - STIM
[ target_position_#2
sky_position_#2
target_position_#2
sky_position_#2
target_position_#2
sky_position_#2
sky_position_#2 - STIM] <--- [...] is repeated Nc-1
times

```

Therefore, there are a total of $2x(2 + 7xN_c)$ BCD images per AOR (or per raster point in the case of a raster map).

8.1.2 Make simple coadditions

The Spitzer post-BCD products will eventually contain properly mosaicked images by taking into account the actual pointing information as well as the uncertainty and coverage images. But until they become available, one can make simple image coadditions using only the knowledge of the chop/dither pattern summarized above. You can do this easily with IDL or IRAF. Here is an example of how to do this within IRAF.

List all BCD images at `target_position_#1` into a file named “on1,” those at `target_position_#2` into file “on2,” those at `sky_position_#1` into file “off1,” and

those at sky_position_#2 into file “off2.” Note that all the STIM images should be excluded.

[Hint: look at the headers, e.g., the following, to see what a BCD file is:

```
unix> ls SPITZER*_bcd.fits > files.list
```

then in IRAF, look into the header keyword

```
IRAF> hedit @files.txt STMFL_70 .
```

this prints out the 70um STIM flash keyword STMFL_70. Only STIM BCDs have non-zero values. You can compare the output with the chop/dither pattern described above. From here, you can easily cut and paste BCD file names into one of the “on1,” “off1,” “on2,” and “off2” files.]

Create a file named “coadd.cl,” which contains the following lines:

```
imcombine ("@on1", "on1.fits", combine="median")
imcombine ("@off1", "off1.fits", combine="median")
imcombine ("@on2", "on2.fits", combine="median")
imcombine ("@off1", "off2.fits", combine="median")
imarith ("on1.fits", "-", "off1.fits", "difave1.fits")
imarith ("on2.fits", "-", "off2.fits", "difave2.fits")
imcopy ("difave1.fits[1:21,*]", "dif1")
imcopy ("difave2.fits[1:21,*]", "dif2")
imshift ("dif2", "dif2s", 5.0, 0.0, boundary_type = "wrap")
imarith ("dif1", "+", "dif2s", "ave.fits")
imarith ("ave.fits", "/", "2.0", "ave.fits")
imcopy ("dif1[1:5,1:32]", "ave.fits[1:5,1:32]")
imcopy ("dif2s[13:16,1:8]", "ave.fits[13:16,1:8]")
imcopy ("dif2s[16:21,1:32]", "ave.fits[16:21,1:32]")
imrename ("ave.fits", "difave_mosaic.fits")
imdel ("dif1,dif2,dif2s", verify=no)
```

Finally, run this IRAF script you have just created.

```
IRAF> cl < coadd.cl
```

The coadded, sky-subtracted, 2-d source spectrum is called “difave_mosaic.fits.” Note that, if you have a mapping SED observation, the above procedure still applies, but to each raster point.

8.2 SED pointing history

The WCS keywords were not populated accurately prior to S13 for SED. We were pointing at the correct place, but the pointing pipeline routine for SED was under development.

We have made several updates in the spacecraft configuration files to adjust chop throw-related pointing parameters for the MIPS/SED mode. This section describes the history of these changes and their effects. Table 8.1 shows those campaigns in which we made these updates. In this table and the discussion that follows, “MC” means “MIPS campaign.”

Table 8.1: Timeline of MIPS/SED pointing updates.

Campaign	+1 arcmin chop	+2 arcmin chop	+3 arcmin chop	-1 arcmin chop	Remarks
Pre-MC19	None	None	None	None	Section 8.2.1
MC 19	None	None	Yes	None	Section 8.2.2
MC 21	None	Yes	Yes	Yes	Section 8.2.3
MC 23	None	Yes	Yes	Yes	Section 8.2.4

8.2.1 Pre-MC19

IOC and routine SED observations using the +1' chop throw all showed a good pointing for this chop throw. As a result, this +1' chop has been the default choice for our SED flux calibration. A mapping observation in MC16 with the +3' chop throw showed a possible pointing offset of about +2.4" (see Figure 8.1). (Note that we have defined the positive offset to be in the direction of increasing detector row number.) This prompted us to check the pointings of the other two chop throws in in MC19.

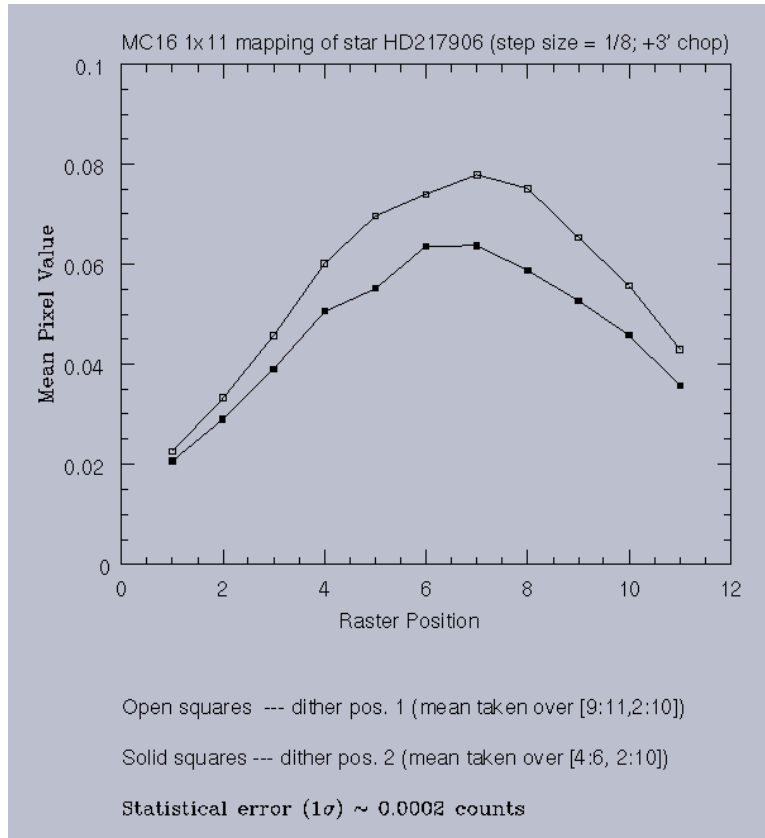


Figure 8.1: MC16 mapping of HD217906, suggesting a pointing offset.

8.2.2 MC19

In MC19, we made an adjustment to the pointing for the +3' chop throw, and we mapped a star across the slit with a step size of 1/8 of the slit width, with each of the following chop throws: -1', +2' and +3'. The results showed that the pointings were still off roughly by the following amount:

Chop Throw	Estimated Offset
-1'	+2.5"
+2'	+1.2"
+3'	+2.4"

See Figure 8.2 for supporting plots. Figure 8.3 is a plot of the relative flux difference between the +1' chop and the +3' chop for the bright star HD108903 observed in MC19. It indicates that the systematic flux difference between these two chop throws is on the order of 5%. This estimate is consistent with what one can directly estimate from the spatial profiles in Figure 8.2.

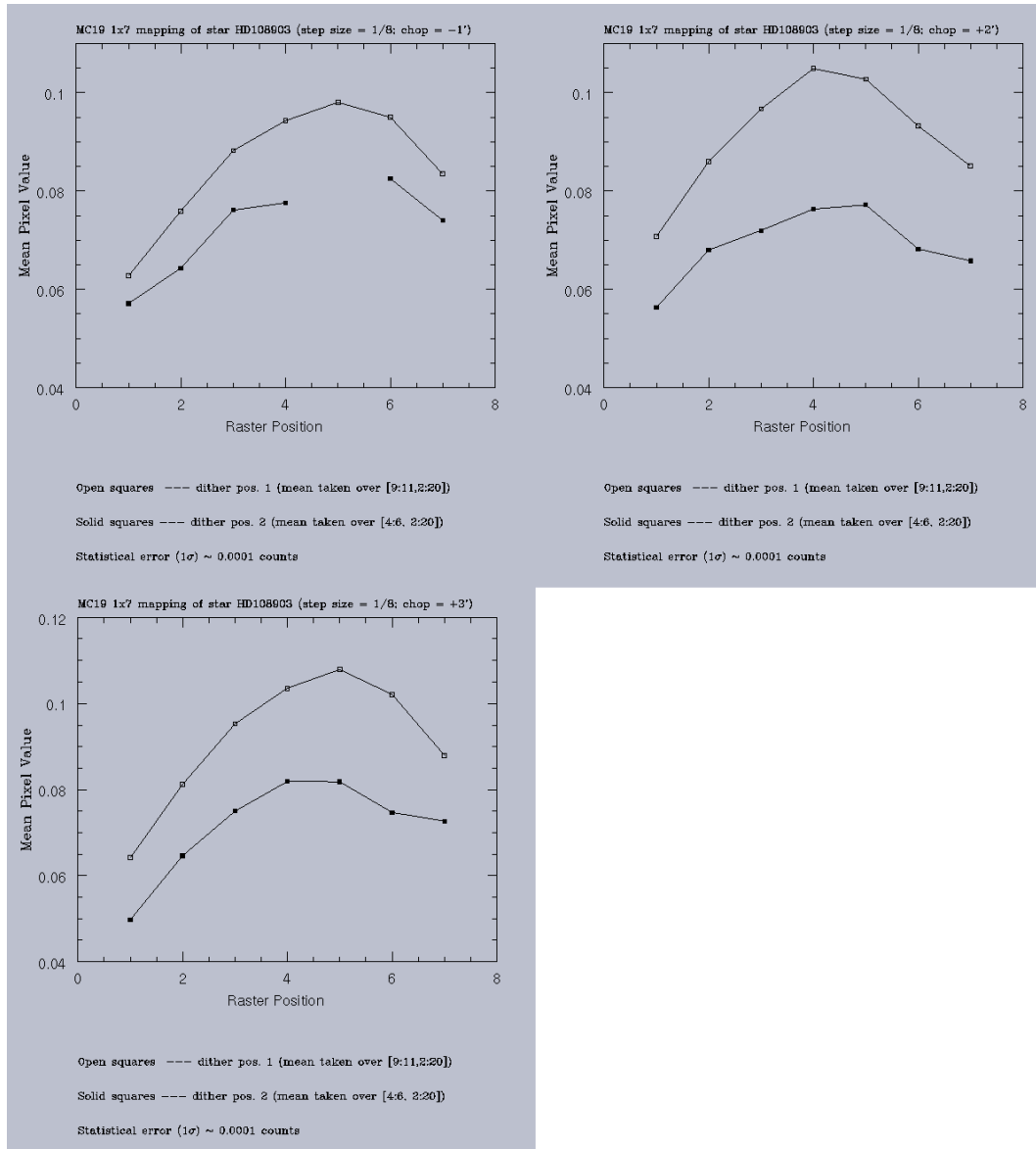


Figure 8.2: Plots demonstrating pointing offsets in MC19.

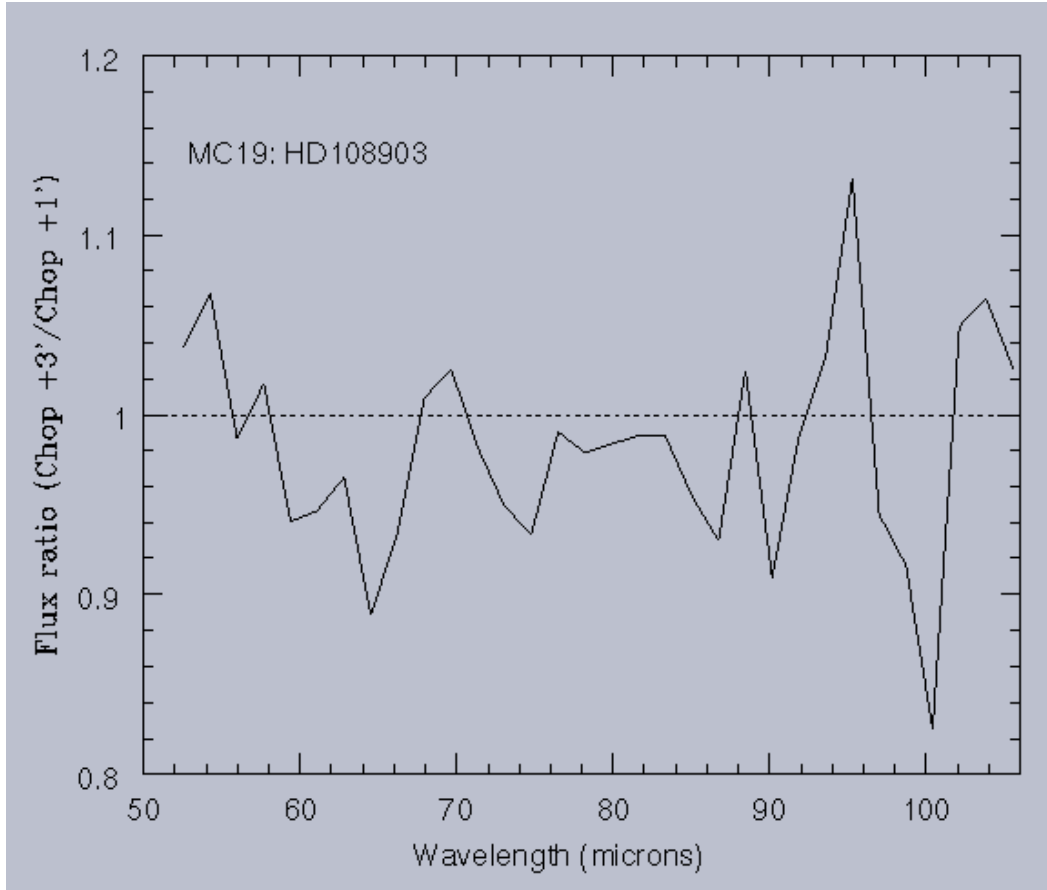


Figure 8.3: Relative flux difference between the +1' chop and the +3' chop for the bright star HD108903 observed in MC19. This indicates that the systematic flux difference between these two chop throws is on the order of 5%.

8.2.3 MC21

In MC21, we made adjustments to the pointing for the chop throws of -1', +2' and +3' with the goal to compensate for the pointing offsets found in MC19. Unfortunately the adjustments were probably made in the wrong direction, resulting in the following increased pointing offsets:

Chop Throw	Estimated Offset
-1'	+5.3"
+2'	+2.6"
+3'	+4.8"

See Figure 8.4 for supporting plots. Figure 8.5 shows the possible systematic flux differences between the +1' chop throw and each of the other chopping choices in MC21. In this case, the moderately bright star HD45348 was observed in a mapping mode that is not optimized for reaching adequate S/N ratios beyond ~70um. The panel (b) of Figure 8.5 indicates that fluxes near the blue end could be underestimated by 5%-10% in a chop throw other than the +1' one. Since

MC21 (and MC22) represents the worst pointings for the chop throws other than the +1' one, we expect smaller chop throw-dependent flux differences (on the order of 5% or less) for all the other campaigns prior to MC23.

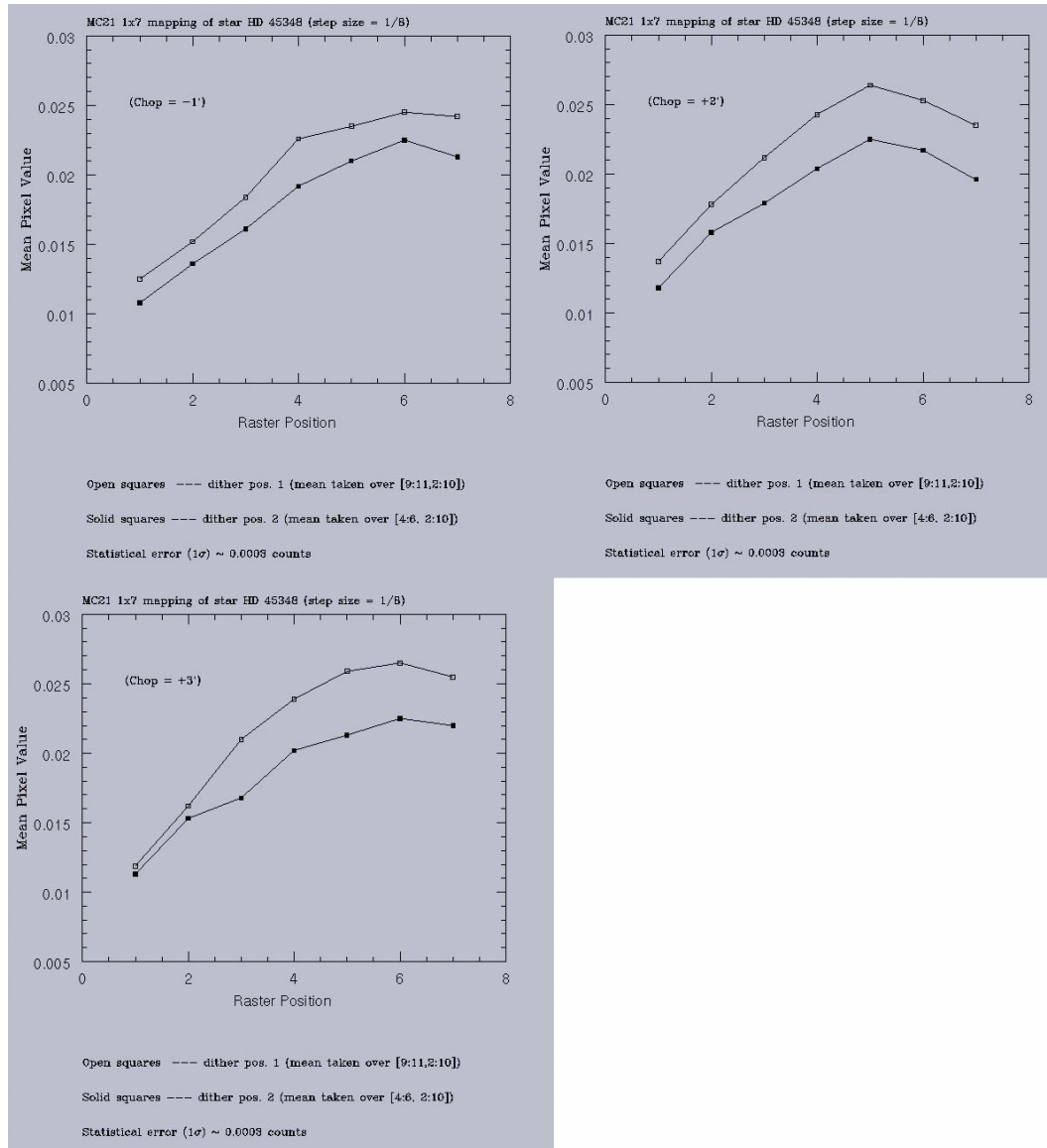


Figure 8.4: Supporting plots for MC21.

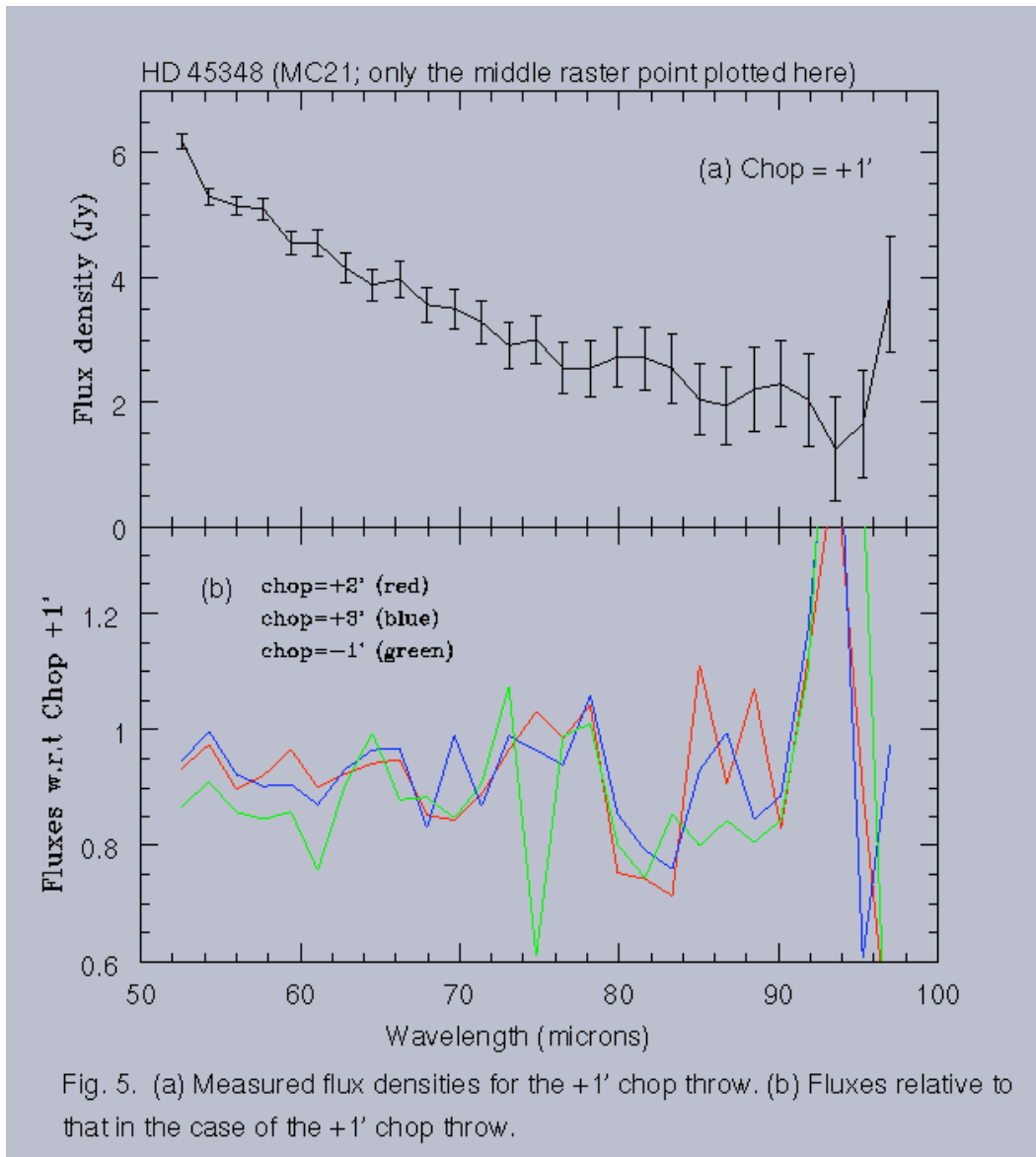


Figure 8.5: Possible systematic flux differences between the +1' chop throw and each of the other chopping choices in MC21; see text.

8.2.4 MC23

In MC23, we updated the pointing again for the -1', +2' and +3' chop throws. The mapping observations show the following offsets:

Chop Throw	Estimated Offset
-1'	~+0.0"
+2'	~+0.8"
+3'	~+0.6"

See Figure 8.6 for supporting plots. These offsets should be acceptable because the pointing jitter from the scan mirror could be as large as 1". We plan to add a plot here in a future version to show the magnitudes of systematic flux differences between various chop throws for observations obtained in and after MC23.

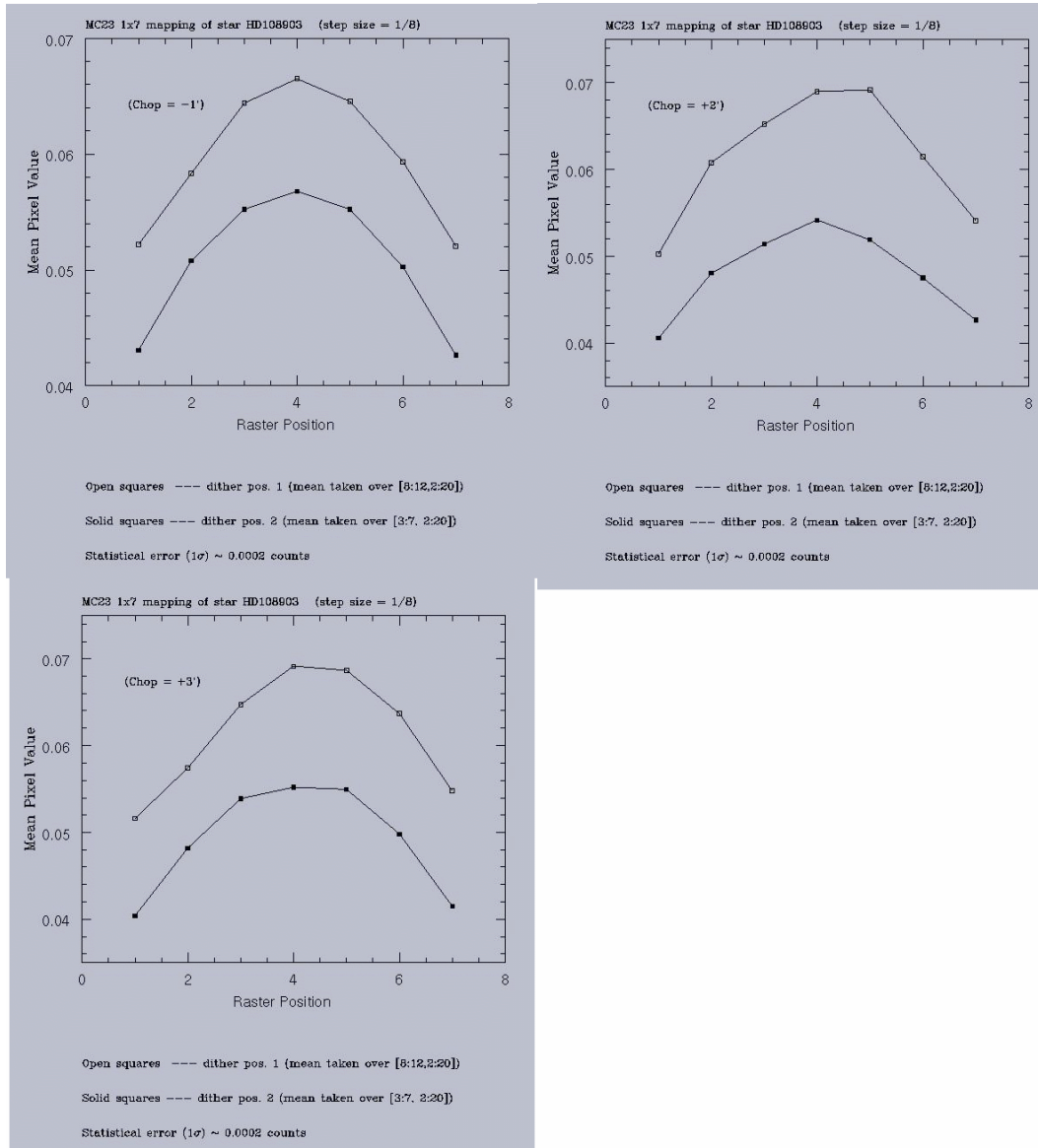


Figure 8.6: Supporting figures for MC 23.

8.2.5 Summary

We can summarize the above results in Table 8.2 below.

Table 8.2: Estimated pointing offsets.

Campaign	Estimated Spatial Pointing Offsets			
	+1' chop	+2' chop	+3' chop	-1' chop
MC 19 & earlier	0.0''	+1.2''	+2.4''	+2.5''
MC 21 & MC 22	0.0''	+2.6''	+4.8''	+5.3''
MC23 & after	0.0''	+0.8''	+0.6''	+0.0''

The fluxes of a point source are underestimated by a small percentage in some campaigns where the selected chop throw has a moderate amount of pointing offset. This effect is estimated to range from -5% for an offset of +/-2.4" (e.g., the +2' and +3' chops in MC19 and earlier campaigns) to -10% for an offset of +/-4.8" (e.g., the +2' and +3' chops in MC21 and MC22).

Note that a final test of all of these modes will take place as part of MC29, and therefore further updates to this information may appear in a future version of this document.

9 Calibration of MIPS data

9.1 *Uncertainties and Repeatability*

Current estimated uncertainty on point sources extracted from pipeline products is 10% for 24 microns, 20% for 70 microns, and 20% for 160. Additional analysis will achieve 5% at 24 microns, 10% at 70 microns. Extended source measurements have been consistent with these measurements.

Repeatability (as defined in the SOM) has been found to be excellent at all wavelengths – 0.4% at 24 microns, ~5% at 70 microns, and ~4% at 160 microns; see Figure 9.1-Figure 9.3.

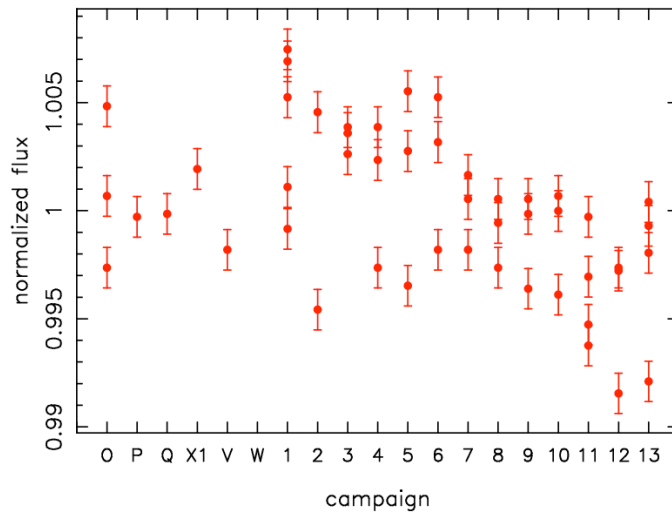


Figure 9.1: Repeatability of 24 micron observations as a function of MIPS campaign. Note the scale on the y-axis.

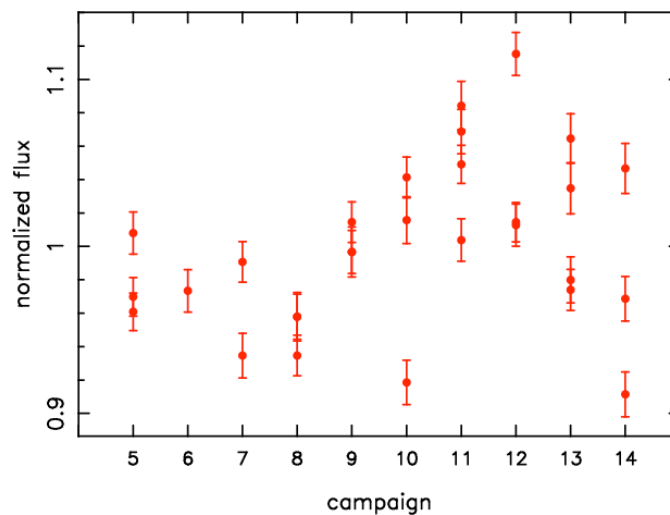


Figure 9.2: Repeatability of 70 micron observations as a function of MIPS campaign.

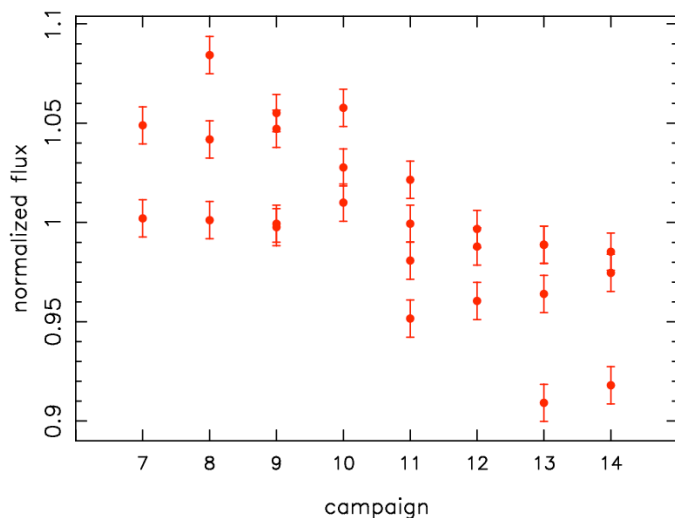


Figure 9.3: Repeatability of 160 micron observations as a function of MIPS campaign. Note that this is measured on a star and is thus dominated by the spectral leak.

9.2 Calibration observations

A summary of all of the calibration observations as of the 13th MIPS campaign appears in Table 9.1. Note that the 160 micron stars are affected by the spectral leak, and thus used for stability and templates, not flux calibration.

For an overview of MIPS calibration, please see the SOM; interested readers should consult sections 8.1.3.5 and 8.1.3.6 on calibration in general, 8.2.2.8 on accuracy and stability, and section 8.3.1 on specific calibration procedures (all sections refer to SOM v. 6.x).

Table 9.1: Calibrator summary as of the 23th MIPS campaign (August 2005).

Mode	Total	Unique	Flux range (Jy)	Types (A/G/K/M)
24 micron	280	105	0.01-6	33/16/42/1
70 micron default scale	277	86	0.05-19	9/6/51/15
70 micron fine scale	37	11	0.3-19	1/0/5/4
SED	93	26	0.3-19	1/0/16/8
160 micron stars	177	40	0.02-0.7	5/1/22/7
160 micron asteroids	126	50	0.07-3	N/A

To retrieve actual calibration observations, if you don't know specific names of targets, then you need a program id (pid) to retrieve the entire MIPS calibration program for a given campaign. MIPS calibrations are assigned a PID = 1700+MIPS campaign number. For example, MC 7 corresponds to 1710 and MC 18 to 1721, etc. These campaigns should include calibration for everything (all MIPS modes), so you have to investigate the specific AORs to find ones that match your needs. MIPS calibrations are done every campaign, so you should be able to start with downloading just one. If the data are not accessible from a

given observation, it is most likely because there is an approved science program that is also observing that target in that mode.

A complete list of the campaign numbers can be found on the SSC website: <http://ssc.spitzer.caltech.edu/approvdprog/sched/>. A complete list of MIPS calibrators can also be found on the SSC MIPS website.

9.3 Absolute Calibration

9.3.1 Methodology

MIPS is calibrated using primary (routine) stars and secondary calibrator stars; see the SOM for more discussion on overall calibration philosophy.

The routine stars are used to monitor stability of the array in the absolute calibration. Currently for routine stars, we use HD159330 (which is a K star) at 24 microns, and HD163588 and HD180711 star for 70 and 160 microns. These stars are observed at least once every 3 days.

The secondary stars have been chosen from our MIPS calibrator list of about 150 stars. Stars on this list are bright enough ($S/N > 100$) and well within the linear range of the detector, i.e., less than 1/4 of the saturation limit. Most of the calibrators are located in regions of low cirrus background, but there are a few stars with a high background in order to test photometry in high background conditions.

9.3.2 Uncertainties

We derived the flux conversion using both primary and secondary stars by fitting the relationship between predicted flux and DN. We have to rely on models to predict the fluxes at MIPS bands. Kurucz models are used for A stars, templates from Cohen et al. (2003 and references therein) are used for K stars, and direct transfer of solar spectrum (Tobiska et al. 2000) for G stars. We extrapolated the Cohen templates and Kurucz models to far infrared using the Engelke function (Engelke 1992) for A and K stars. The derived conversion factors are shown in Table 3.9.

The absolute calibration is accurate to better than 5% at 24 microns. The stellar photometry using the primary calibrator of HD159330 shows that the flux is repeatable at the <1.2% level. However, errors in the absolute calibration come additionally from uncertainty in model prediction (<5%) and aperture and color corrections (<1%). Efforts to improve the absolute calibration are underway and it is likely that this absolute calibration accuracy will improve as our understanding of the stars themselves improves and is propagated to the models.

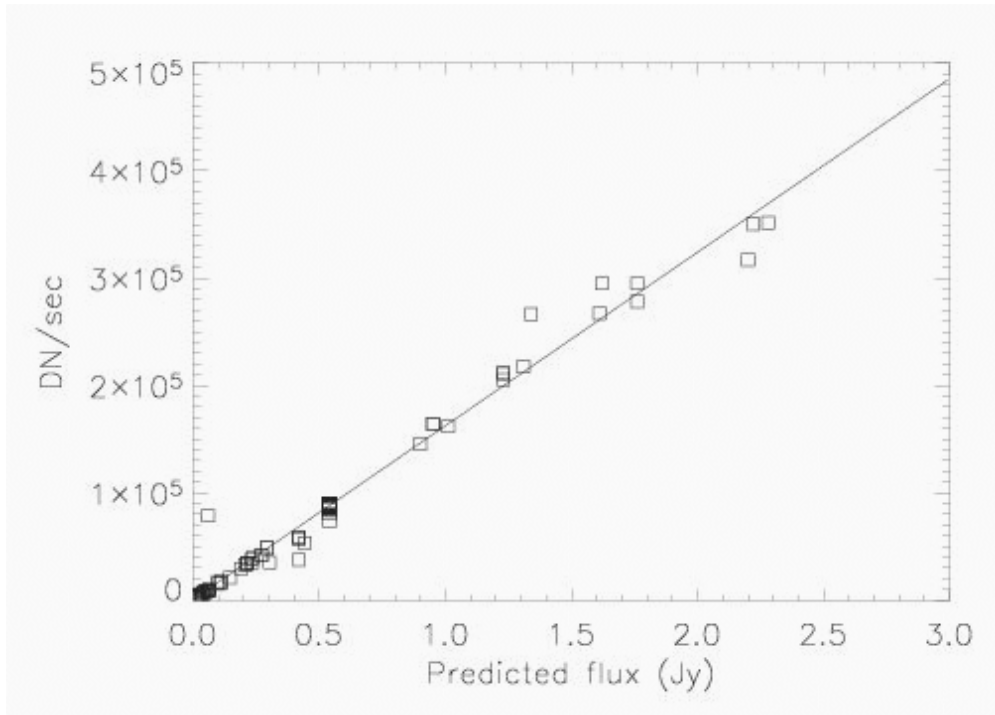


Figure 9.4: Calibration factor determination for 24 microns.

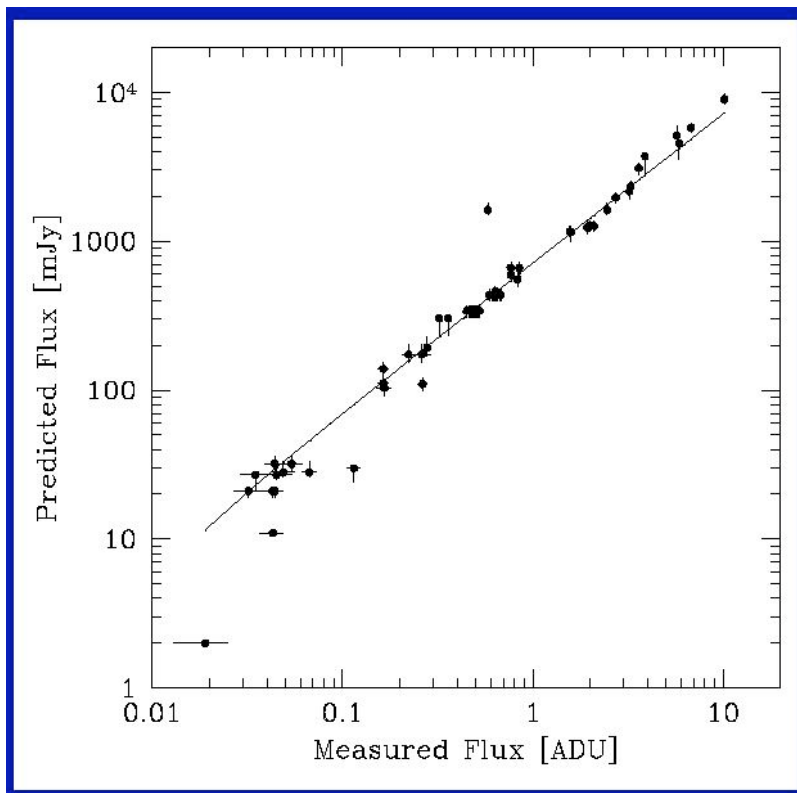


Figure 9.5: Calibration factor determination for 70 microns.

9.4 Flat fields

We select certain pointings to provide flat fields for all 3 cameras; see Figure 9.6. These fields are known to have bright, relatively unstructured Zodiacal light, no bright stars or galaxies, and limited (uncrowded) faint sources. The same positions are used for all three bands.

Since the saturation levels at 70 microns are higher than expected pre-launch, we are experimenting with using bright Galactic cirrus rather than Zodiacal light. Preliminary SED illumination corrections suggest that cirrus is a better choice, at least for this AOT.

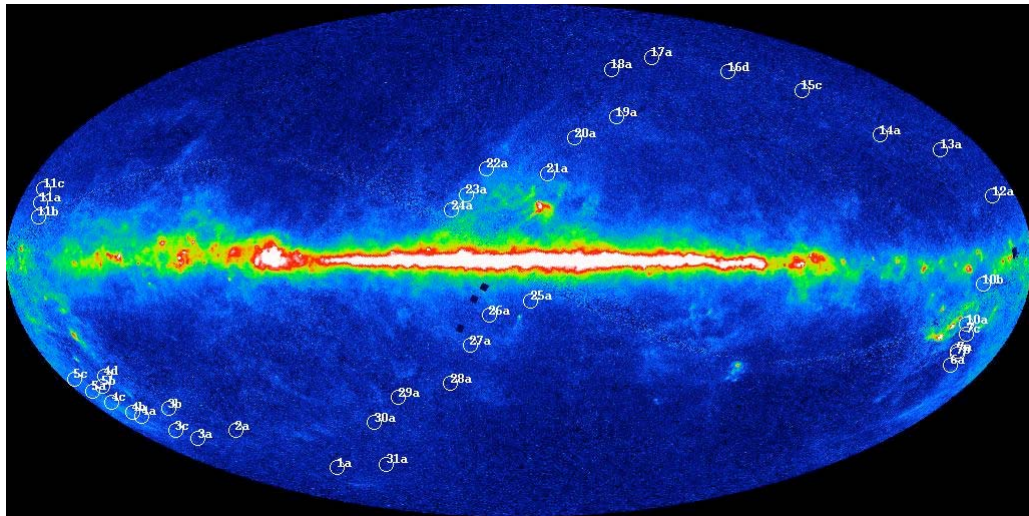


Figure 9.6: MIPS flat field positions indicated on a DIRBE 140 micron all-sky map.

9.5 Ge calibration overview

Initially, we start with uncalibrated data in units of DN/s. We define $U(t)$ to be the slopes of raw ramps after cosmic ray removal such that

$$U(t) = [I(t) * O + D] R(t),$$

where I =sky image, O =combined optical response of telescope and instrument, D =dark current, and $R(t)$ is the response of the detectors as a function of time which is tracked by stim flashes $[S]$.

The necessary calibration files are:

- Illumination correction (IC), which is the median of $I(\text{skyflats}) * O * R(t) / [S * R(t)] \sim O/S$ (the normalized median of observations of uniform sky).
- Dark, which is the median of $D * R(t) / [S * R(t)] \sim D/S$ (the median of observations of internal darks).

- Flux calibration (FC), which is the conversion between Jy and DN (derived from calibration sources).

Calibrated BCD data arrive in MJy/sr:

$$I(t) = FC * [U(t)/S * R(t) - \text{DARK}] / IC,$$

where IC is the illumination correction and FC is the flux calibration conversion.

Note that the pixel responsivity is measured as a function of time using the internal stimulator flash calibration (we measure the stim minus the background). The response can vary by 10% to more than a factor of 2 over a couple of minutes for the worst cases. Stim calibration works for the calibration of both point sources and extended sources.

10 Appendix: FITS header keywords

The keywords are sorted into five categories: keywords common to every wavelength, then keywords for MIPS-24, MIPS-70, MIPS-70 SED, and MIPS-160, in that order. They are listed in the order they appear in the header.

Still can't find your keyword? An alphabetical list is available on the SSC MIPS website.

10.1 Common header keywords

Note that for SED mode, CRVAL* and CTYPE* have slightly different definitions; see below.

Items flagged with "(S12)" are new for S12 and subsequent pipeline versions; similarly, items flagged with "(S13)" are new for S13 and subsequent versions.

Table 10.1: MIPS header keywords common to all wavelengths.

Type	Keyword	Notes or comments
<i>Basic FITS keywords</i>		
logical	SIMPLE	Fits standard
integer	BITPIX	-32 = 4-Byte float, 16 = 2-Byte integer
integer	NAXIS	Standard FITS format
integer	NAXIS1	FITS standard
integer	NAXIS2	FITS standard
integer	NAXIS3	FITS standard
string	FILETYPE	Image type
string	TELESCOP	Spitzer Space Telescope
string	INSTRUME	Spitzer Space Telescope instrument ID
integer	CHNLNUM	This image: 1=24um, 2=70um, 3=160um
string	AOT_TYPE	Observation Template Type (MipsScan, MipsPhot, etc)
string	AORLABEL	AOR Label (Observer-defined)
string	REQTYPE	Request type (AOR, IER, or SER)
string	EXPTYPE	Exposure Type
integer	FOVID	Field of View ID (see Table 4.4 in SOM v.4.0)
string	FOVNAME	Field of View Name
integer	PRIMEARR	Was this image taken with the prime array? 1=prime,2=not prime,3=not valid
string	RDOUTMOD	Readout mode
<i>Proposal information</i>		
string	OBSRVR	Observer Name (Last, First)
integer	OBSRVRID	Observer ID of Principal Investigator

integer	PROCYCL	Proposal Cycle
integer	PROGID	Program ID
string	PROTITLE	Program Title
integer	PROGCAT	Program Category
<i>Time and exposure information</i>		
string	DATE_OBS	Date & time at DCE start
double	MJD_OBS	[days] MJD at DCE start (JD-2400000.5)
double	UTCS_OBS	[sec] J2000 ephemeris time at DCE start
double	SCLK_OBS	[sec] SCLK (Spacecraft CLoCK) time (since 1/1/1980) at DCE start
float	SAMPTIME	[sec] Sample integration time
float	EXPTIME	[sec] Effective integration time per pixel
<i>Target and pointing information</i>		
string	OBJECT	Object Name
string	OBJTYPE	Object Type
double	CRVAL1	[deg] RA at CRPIX1,CRPIX2 averaged over DCE
double	CRVAL2	[deg] DEC at CRPIX1,CRPIX2 averaged over DCE
string	RA_HMS	[hh:mm:ss.s] CRVAL1 as sexagesimal
string	DEC_DMS	[dd:mm:ss] CRVAL2 as sexagesimal
double	CD1_1	[deg/pix] CD matrix element 1_1
double	CD1_2	[deg/pix] CD matrix element 1_2
double	CD2_1	[deg/pix] CD matrix element 2_1
double	CD2_2	[deg/pix] CD matrix element 2_2
string	RADESYS	International Celestial Reference System
float	EQUINOX	Equinox for ICRS celestial coordinate system
string	CTYPE1	RA---TAN with distortion in pixel space
string	CTYPE2	DEC--TAN with distortion in pixel space
float	CRPIX1	Reference pixel along axis 1
float	CRPIX2	Reference pixel along axis 2
double	CRDER1	[deg] Uncertainty in CRVAL1
double	CRDER2	[deg] Uncertainty in CRVAL2
double	UNCRTPA	[deg] Uncertainty in position angle
double	CSDRADEC	[deg] Costandard deviation in RA and Dec
double	SIGRA	[arcsec] RMS dispersion in RA over DCE
double	SIGDEC	[arcsec] RMS dispersion in DEC over DCE
double	SIGPA	[arcsec] RMS dispersion of PA over DCE
double	RA_REF	[deg] Commanded RA (J2000) of ref. position
double	DEC_REF	[deg] Commanded Dec (J2000) of ref. position
double	RA_RQST	[deg] Requested RA at CRPIX1
double	DEC_RQST	[deg] Requested Dec at CRPIX2
double	PA_RQST	[deg] Requested position angle of TPF Z axis (E of N)
double	PA	[deg] pos. angle of axis 2 (E of N,+=CCW)
double	PXSCAL1	[arcsec/pix] Scale for axis 1 at CRPIX1,CRPIX2
double	PXSCAL2	[arcsec/pix] Scale for axis 2 at CRPIX1,CRPIX2
float	PM_RA	[arcsec/yr] Proper Motion in RA (J2000)

float	PM_DEC	[arcsec/yr] Proper Motion in Dec (J2000)
float	CSM_PRED	Predicted mirror start pos (DAC)
float	CSM_SKY	Predicted mirror start pos on sky (arcsec)
float	CSM_RATE	Mirror scan rate (milli-arcsec/sec)
double	RMS_JIT	[arcsec] RMS jitter during DCE
double	RMS_JITY	[arcsec] RMS jitter during DCE along Y
double	RMS_JITZ	[arcsec] RMS jitter during DCE along Z
double	SIG_JTYZ	[arcsec] YZ costandard deviation of jitter
double	PTGDIFFF	[arcsec] offset between actual and requested pointing
double	PTGDIFFX	[arcsec] requested-actual pointing along axis 1 (S12)
double	PTGDIFFY	[arcsec] requested-actual pointing along axis 2 (S12)
logical	USEDDBPHF	True (T) if Boresight Pointing History File was used
double	ZODY_EST	Zodiacal Background Estimate (S13)
double	ISM_EST	Interstellar Medium Estimate (S13)
double	CIB_EST	Cosmic IR Background Estimate (S13)
integer	WARMFLAG	Whether or not the MIPS campaign from which these data come is an 8.5K or 5.5K campaign.
<i>Moving target information</i>		
integer	NAIFID	NAIF ID number for target
string	NAIFNAME	Solar System Object name
string	EPHMFIL	Ephemeris file used for moving target
string	MTEPOCH	[Julian date] Epoch
string	T_PERI	[Julian date] Perihelion date
double	LITOMEGA	[deg] Argument of perihelion with respect to ecliptic
double	BIGOMEGA	[deg] Long. of ascending node with respect to ecliptic
float	ECCENTR	Eccentricity
double	PERIHEL	[AU] Perihelion distance
float	INCLINAT	[deg] Inclination of orbit
<i>Distortion keywords</i>		
integer	A_ORDER	polynomial order, axis 1, detector to sky
double	A_0_2	distortion coefficient
double	A_0_3	distortion coefficient
double	A_1_1	distortion coefficient
double	A_1_2	distortion coefficient
double	A_2_0	distortion coefficient
double	A_2_1	distortion coefficient
double	A_3_0	distortion coefficient
double	A_DMAX	[pixel] maximum correction
integer	B_ORDER	polynomial order, axis 2, detector to sky
double	B_0_2	distortion coefficient
double	B_0_3	distortion coefficient
double	B_1_1	distortion coefficient
double	B_1_2	distortion coefficient
double	B_2_0	distortion coefficient
double	B_2_1	distortion coefficient

double	B_3_0	distortion coefficient
double	B_DMAX	[pixel] maximum correction
integer	AP_ORDER	polynomial order, axis 1, sky to detector
double	AP_0_1	distortion coefficient
double	AP_0_2	distortion coefficient
double	AP_0_3	distortion coefficient
double	AP_1_0	distortion coefficient
double	AP_1_1	distortion coefficient
double	AP_1_2	distortion coefficient
double	AP_2_0	distortion coefficient
double	AP_2_1	distortion coefficient
double	AP_3_0	distortion coefficient
integer	BP_ORDER	polynomial order, axis 2, sky to detector
double	BP_0_1	distortion coefficient
double	BP_0_2	distortion coefficient
double	BP_0_3	distortion coefficient
double	BP_1_0	distortion coefficient
double	BP_1_1	distortion coefficient
double	BP_1_2	distortion coefficient
double	BP_2_0	distortion coefficient
double	BP_2_1	distortion coefficient
double	BP_3_0	distortion coefficient
<i>Photometry</i>		
string	BUNIT	Units of image data
float	FLUXCONV	Flux conversion factor to BUNIT
<i>General mapping keywords</i>		
integer	CYCLENUM	Current cycle number
integer	COLUMN	Current column number
integer	ROW	Current row number
integer	MAPNUM	Current map cycle number
integer	CLPOSNUM	Current cluster position
integer	SCLEGNUM	Scan leg number
string	SCANDIR	Scan direction
<i>MIPS scan map</i>		
string	SCANRATE	Scan map rate (slow, med, fast)
logical	REQ160	160 micron data required (T/F)
logical	FASTRES	160 micron fast reset (T/F)
integer	XSCNOFF	[arcsec] Cross-scan offset
integer	INSCNOFF	[arcsec] In-scan offset
integer	NSCANLEG	Number of scan legs
float	SCANLEN	[deg] Scan leg length
integer	STEPFOR	[arcsec] Cross-scan step size for forward leg
integer	STEPREV	[arcsec] Cross-scan step size for reverse leg
integer	NMAPCYCL	Number of Scan Map Cycles
<i>MIPS photometry-super resolution</i>		

logical	SELEC24	MIPS-24 selected
logical	LARGE24	MIPS-24 Field Size; T=large, F=small
float	DELTA24	[arcsec] Distance to sky reference position
integer	NCYCL24	Number of MIPS-24 photometry cycles
logical	RMAP24	MIPS-24 Raster Map (T/F)
integer	NCOLS24	Number of MIPS-24 columns in raster map
integer	NROWS24	Number of MIPS-24 rows in raster map
string	CSTEP24	[arcsec] MIPS-24 raster map column step size
string	RSTEP24	[arcsec] MIPS-24 raster map row step size
integer	MCYCLE24	Number of MIPS-24 raster map cycles
logical	SELEC70	MIPS-70 selected
logical	LARGE70	MIPS-70 Field Size; T=large, F=small
float	DELTA70	[arcsec] Distance to sky ref. position
logical	FINESCAL	Image scale (T= fine, F=default)
integer	NCYCL70	Number of MIPS-70 photometry cycles
logical	RMAP70	MIPS-70 Raster Map (T/F)
integer	NCOLS70	Number of MIPS-70 columns in raster map
integer	NROWS70	Number of MIPS-70 rows in raster map
string	CSTEP70	[arcsec] MIPS-70 raster map col. step size
string	RSTEP70	[arcsec] MIPS-70 raster map row step size
integer	MCYCLE70	Number of MIPS-70 raster map cycles
logical	SELEC160	MIPS-160 selected
logical	LARGE160	MIPS-160 Field Size; T=large, F=small
float	DELTA160	[arcsec] Distance to sky reference position
integer	NCYCL160	Number of MIPS-160 photometry cycles
logical	RMAP160	MIPS-160 Raster Map (T/F)
integer	NCOLS160	Number of MIPS-160 columns in raster map
integer	NROWS160	Number of MIPS-160 rows in raster map
string	CSTEP160	[arcsec] MIPS-160 raster map col. step size
string	RSTEP160	[arcsec] MIPS-160 raster map row step size
integer	MCYCLE160	Number of MIPS-160 raster map cycles
<i>MIPS TPM</i>		
logical	SEL24TP	MIPS-24 selected
integer	NCY24TP	Number of 24 micron cycles
logical	SEL70TP	MIPS-70 selected
integer	NCY70TP	Number of 70 micron cycles
logical	SEL160TP	MIPS-160 selected
integer	NCY160TP	Number of 160 micron cycles
<i>Instrument telemetry data</i>		
integer	CE_SIDE	Common Electronics Side (1=A, 2=B)
float	GRPARVTC	[Sec] Coarse Spacecraft Group Time
float	GRPARVTF	[Sec] Fine Spacecraft Group Time
integer	CRSESYNC	[Sec] Mirror Sync Pulse Coarse Time
double	FINESYNC	[1/65535 Sec] Mirror Sync Pulse Fine Time
integer	CSM_MOD	CSMM Mode: 0=Chop,1=Ramp

integer	ANCSMDIR	CSMM Ramp Dir: 0=negative=forward, 1=positive=reverse
integer	DCE_FRMS	[Fr/DCE] Ge frames per DCE command
integer	FRMFLYBK	[Frames] CSMM Flyback duration in data frames
double	CSM_SLP	[DAC/s] CSMM Ramp Slope Command
integer	DCE_CALC	DCEs per Calibration Cycle Command
integer	ACREJCNT	Command Reject Counter
integer	AIRSPCNT	Invalid Response Count
integer	ALIMVCNT	Limit Violation Counter
integer	AFIFOBAD	Science Data FIFO Bad Half Full Interrupts
integer	ASDMGRFA	SDM Groups Not Accepted By CDH
integer	ALSTERLD	Last Error Id
integer	ALSTERPM	Last Error Parameter
integer	ATOTALER	Total Errors Posted Count
double	CSM_POS	[DAC] CSMM Position Output
double	CSM_POSF	[DAC] CSMM Fine Position DAC
double	CSM_POSC	[DAC] CSMM Coarse Position DAC
double	ANCSMCUR	[uAmps] CSMM Current
double	ANCSMGN	CSMM Gain Adjustment DAC
double	CSM_OFFS	[arcsec] CSMM Position Offset DAC Output
double	ANCSMPS1	[DAC] CSMM Scanpos1 Command
double	ANCSMPS2	[DAC] CSMM Scanpos2 Command
double	ANCSMRP1	[DAC] CSMM Relpos1 Command
double	ANCSMRP2	[DAC] CSMM Relpos2 Command
double	ANCSMSTP	[DAC] CSMM Scanoffset Command
integer	CSM_PIDX	Scan Position Index
integer	CMD_DCES	Number of DCEs in Exposure
integer	CSM_OOLC	CSMM Out Of Limits Count
integer	SC_SYNCC	Total HTG CSMM to SC Synch Pulse Count
integer	GROUPCNT	MIPS Group Count Per DCE
integer	GROUPIDX	MIPS Exp. Manager Index for Next SDM Group
integer	ANIMCYFC	Frames per Image Cycle Commanded
integer	ANHTGEFC	HTG Frames In Exposure Counter
integer	IMGCYCLC	Total Image Cycles Since HTG Ready
integer	EXPIMGCY	Image Cycles in Exposure Counter
integer	ANCALCYC	DCEs completed in Calibration Cycle
float	ACSMMTMP	[Deg_K] CSMM Base Temp
float	ACEBOXTM	[Deg_C] CE Box Temp
float	AVDSUBV	[Volts]VD Sub Voltage
integer	ABASTMCR	Coarse Component of CE Base Time
integer	ABASTMFN	Fine Component of CE Base Time
integer	AFSWMJRV	CE Flight Software Major Version Number
integer	AFSWMINV	CE Flight Software Minor Version Number
integer	HSPLSTMC	MIPS Scan Mirror Pulse Timestamp Coarse
integer	HSPLSTMF	MIPS Scan Mirror Pulse Timestamp Fine

float	SC_AT_Q1	ATDT_SC_QUATERNION_Q1
float	SC_AT_Q2	ATDT_SC_QUATERNION_Q2
float	SC_AT_Q3	ATDT_SC_QUATERNION_Q3
float	SC_AT_Q4	ATDT_SC_QUATERNION_Q4
float	SC_R8_X	[asec/s]
float	SC_R8_Y	[asec/s]
float	SC_R8_Z	[asec/s]
integer	SLEWING	ACG_MANEUVER_IN_PROGRESS
<i>Data flow keywords</i>		
string	DATE	[YYYY-MM-DDThh:mm:ss UTC] file creation date
string	ORIGIN0	Site where raw-FITS file was written
string	CREATOR0	SW system that created raw-FITS file
string	SIS_SVER	SIS SW VERSION of CREATOR0
long	AORKEY	AOR or IER key. Unique identifier for Astronomical Observation Request or Instrument Engineering Request in SSC databases
string	DS_IDENT	Data Set Identification for ADS/journals
integer	EXPID	Exposure ID (0-9999)
integer	DCENUM	DCE number (0-9999)
integer	TLMGRPS	Number of expected telemetry groups
integer	FILE_VER	Version of the raw file made by SIS
string	RAWDATE	SIS file creation date
string	RAWFILE	Raw data file name
string	CPT_VER	Channel Parameter Table FOS version
logical	EXPDFLAG	(T/F) expedited DCE
integer	MISS_LCT	Total Missed Line Count in this FITS
logical	MANCPKT	T if this FITS is Missing Ancillary Data
logical	MISSDATA	T if this FITS is Missing Image Data
integer	PAONUM	PAO Number
string	CAMPAIGN	Campaign
integer	DCEID	Data Collection Event ID
integer	DCEINSID	DCE Instance ID
integer	DPID	Data Product Instance ID
integer	PIPENUM	Pipeline Script Number
integer	PLSCRPID	Pipeline Script ID
integer	SOS_VER	Data-Product Version
integer	PLVID	Pipeline Version ID
integer	CALID	CalTrans Version ID
string	CTD_VER	Commanded telemetry data version
string	CALBUNIT	Units for which calibration data applies
integer	EXPECTN	Expected number inputs for ensemble
integer	ACTUALN	Actual number inputs in ensemble
integer	EPVERSN	Ensemble Product Version
integer	EPID	Ensemble Product ID

10.2 Header for 24 microns

Items flagged with “(S12)” are new for S12 and subsequent pipeline versions.

Table 10.2: Header keywords unique to MIPS-24.

Type	Keyword	Notes or comments
<i>Time and exposure information</i>		
integer	IGN_FRM1	Initial frames ignored for DCENUM = 0
integer	IGN_FRM2	Initial frames ignored for DCENUM > 0
integer	SATTHDIF	[DN/SAMPTIME] Saturation threshold in difference
logical	BOOSTFRM	True (T) if DCE with bias boost
<i>Target and pointing information</i>		
float	CSM_RATE	Mirror scan rate (milli-arcsec/sec)
float	CSM_AVG	[degree] Average mirror position during exposure
float	SPOT_X	[pix] X-position of characteristic spot (S12)
float	SPOT_Y	[pix] Y-position of characteristic spot (S12)
<i>Photometry</i>		
float	GAIN	e/DN conversion
<i>Refined pointing information (only for scan mode) (S12)</i>		
boolean	RFNDFLAG	T if pointing was actually refined
double	RARFND	[deg] Refined RA
double	DECRFND	[deg] Refined Dec
double	CT2RFND	[deg] Refined CROTA2
double	PA_RFND	[deg] Refined PA (=CROTA2_refined)
double	ERARFND	[deg] Error in refined RA
double	EDECRFND	[deg] Error in refined Dec
double	EPA_RFND	[deg] Error in refined PA or CROTA2
double	CSRDRFND	[deg] Co-standard deviation in refined RA, Dec
int	NASTROM	Number astrometric sources for absolute refinement
double	RARESID	[arcsec] Residual: observed-refined RA
double	DECRESID	[arcsec] Residual: observed-refined Dec
double	PA_RESID	[arcsec] Residual: observed-refined PA
double	XC_RESID	[pix] Refinement correction in CRPIX1
double	YC_RESID	[pix] Refinement correction in CRPIX2
double	EXCRESID	[pix] Uncertainty in correction for CRPIX1

double	EYCRESID	[pix] Uncertainty in correction for CRPIX2
double	CSDXCYC	[pix] Co-standard deviation in ref. CRPIX1, CRPIX2
double	CD11RFND	[deg/pix] Refined CD matrix element 1_1
double	CD12RFND	[deg/pix] Refined CD matrix element 1_2
double	CD21RFND	[deg/pix] Refined CD matrix element 2_1
double	CD22RFND	[deg/pix] Refined CD matrix element 2_2
<i>Instrument telemetry data</i>		
integer	D24FRAME	Total D24 Frame Count
integer	D24EXPDC	D24 DCEs in Exposure Counter
float	CMD_T_24	[Deg_K]
float	AD24TMPA	[Deg_K]
float	AD24TMPB	[Deg_K]
float	AD24STMI	[uAmps]
float	AD24HTRI	[uAmps]
float	APROFF1V	[Volts]
float	APROFF2V	[Volts]
float	APROFF3V	[Volts]
float	APROFF4V	[Volts]
float	AD24ANLI	[uAmps]
integer	AD24PWEN	Det 24u Power Enable Commanded State
integer	AD24SITM	Det 24u Temperature Sensor Status
integer	AD24PWRS	Det 24u Power Enable Status
integer	AD24TMSE	Det 24u Temperature Sensor Commanded State
integer	AD24STMC	Det 24u Stimulator Enable Commanded State
integer	A24HTDAC	D24 Heater DAC Load Value
integer	A24HTCMD	MIPS D24 Heater Enable Commanded State
integer	AD24ANLS	MIPS D24 Anneal Status
integer	A24HTMEN	D24 Heater Monitor Enable Status
<i>Data flow keywords</i>		
string	CALBUNIT	Units for which calibration data applies
integer	EXPECTN	Expected number inputs for ensemble
integer	ACTUALN	Actual number inputs in ensemble
integer	EPVERSN	Ensemble Product Version
integer	EPID	Ensemble Product ID
<i>Calibration history</i>		
string	EPIDDARK	Dark ensemble product ID
string	EPIDFLAT	Flat ensemble product ID
string	EPIDNONL	Non-linearity ensemble product ID
string	EPIDROWF	Row-flux correction ensemble product ID
string	FBIDDARK	Dark fallback product ID
string	FBIDFLAT	Flat fallback product ID
string	FBIDNONL	Non-linearity fallback product ID
string	FBIDROWF	Row-flux correction fallback product ID
string	FBIDPMSK	Pixel-mask fallback product ID

string	FBIDDNT	DN-to-Flux single file fallback ID
string	FBIDDNT1	DN-to-Flux interpolation file 1 fallback ID
string	FBIDDNT2	DN-to-Flux interpolation file 2 fallback ID
string	SCETDARK	Dark product acquisition time
string	SCETFLAT	Flat product acquisition time
string	SCETNONL	Non-linearity acquisition time
string	SCETROWF	Row-flux correction acquisition time
string	SCETPMSK	Pixel-mask acquisition time
string	SCETDNT	Time of DN-to-Flux single fallback file
string	SCETDNT1	Time of DN-to-Flux interpolation file 1
string	SCETDNT2	Time of DN-to-Flux interpolation file 2

10.3 Header for 70 microns

Table 10.3: Header keywords unique to MIPS-70.

Type	Keyword	Notes or comments
<i>Time and exposure information</i>		
integer	COADD	Ge coadd parameter
<i>MIPS SED</i>		
string	CHOPDIST	[arcmin] Chop distance
integer	NCYCLES	Number of SED cycles
integer	NCOLS	Number of columns
integer	NROWS	Number of rows
string	COLSTEP	Column step
string	ROWSTEP	Row step
<i>Instrument telemetry data</i>		
integer	STMID_70	Det 70u Stimulator Power Enables
integer	ANHTR_70	Det 70u Anneal Heater Enable
float	STMFL_70	Det 70u Stimulator Flashed
integer	STM_MODE	Stimulator Manual or Auto Mode
integer	STMP_70	[Frames] Det 70u Stimulator Period in Data
integer	RSTP_70	[Frames] Det 70u Normal Reset Period in Data
double	CSM_POS	[DAC] CSMM Position Output
double	CSM_POSF	[DAC] CSMM Fine Position DAC
double	CSM_POSC	[DAC] CSMM Coarse Position DAC
double	ANCSMCUR	[uAmps] CSMM Current
double	IDUCA_70	[uAmps] Det 70u Unit Cell Drain Current A-half
double	IDUCB_70	[uAmps] Det 70u Unit Cell Drain Current B-half
double	VOFFA_70	[Volts] Det 70u Offset Voltage A-half
double	VOFFB_70	[Volts] Det 70u Offset Voltage B-half
double	VMREF_70	[Volts] Det 70u minus 5.00 Reference Voltage
double	ISTIM_70	[uAmps] Det 70u Stimulator Current DAC
double	IANNL_70	[mAmps] Det 70u Anneal Heater Current DAC

double	VQRST_70	[Volts] Det 70u Q Reset High Level Voltage
double	BRD_T_70	[Deg_C] Det 70u Control Board Temp
double	VBIAS_70	[Volts] Det 70u Common Bias Voltage at Detector
double	VRST1_70	[Volts] Det 70u Reset Voltage 1 @ Detector
double	VRST2_70	[Volts] Det 70u Reset Voltage 2 @ Detector
double	VRST3_70	[Volts] Det 70u Reset Voltage 3 @ Detector
double	VRST4_70	[Volts] Det 70u Reset Voltage 4 @ Detector
double	VRST5_70	[Volts] Det 70u Reset Voltage 5 @ Detector
double	VRST6_70	[Volts] Det 70u Reset Voltage 6 @ Detector
double	VRST7_70	[Volts] Det 70u Reset Voltage 7 @ Detector
double	VRST8_70	[Volts] Det 70u Reset Voltage 8 @ Detector
integer	DCE_NUM	DCEs in Observation Counter
integer	ANCALCYC	DCEs completed in Calibration Cycle
double	AD70JNCT	[Deg_K] 70u FPA Junction Temp
double	ABASET70	[Deg_K] 70u FPA Cold Plate
double	AD70TMPA	[Deg_K] 70u Detector Temp A
double	AD70TMPB	[Deg_K] 70u Detector Temp B
float	AD70BRDT	[Deg_C] MIPS 70 Micron Board Temp
integer	ACREJCNT	Command Reject Counter
integer	AIRSPCNT	Invalid Response Count
integer	ALIMVCNT	Limit Violation Counter
integer	AFIFOBAD	Science Data FIFO Bad Half Full Interrupts
integer	ASDMGRFA	SDM Groups Not Accepted By CDH
integer	ALSTERLD	Last Error Id
integer	ALSTERPM	Last Error Parameter
integer	ATOTALER	Total Errors Posted Count
<i>Data flow keywords</i>		
string	CAMPAIGN	Campaign
integer	PIPE_ID1	Pipeline Script ID
integer	PIPE_ID2	Pipeline Script ID
integer	PIPE_ID3	Pipeline Script ID
integer	PIPE_ID4	Pipeline Script ID
integer	PIPE_ID5	Pipeline Script ID
<i>Calibration history</i>		
integer	EPIDDARK	Dark ensemble product ID
integer	EPIDILC	IC ensemble product ID
integer	EPIDRNO	Readnoise ensemble product ID
integer	FBIDPMSK	Pixel-mask fall-back product ID
integer	EPIDSTLT	Stimlatent cal file fall back product ID
integer	EPIDFLUX	Jansky conversion value fall back product ID
integer	FBIDDARK	Dark fall-back product ID
integer	FBIDILC	IC fall-back product ID
integer	FBIDENL	Electronic Non-linearity fall-back product ID
integer	FBIDENL	Saturation Cal file fall back id
integer	FBIDPMSK	Pixel-mask fall-back product ID

string	SCETDARK	Dark product acquisition time
string	SCETILC	Flat product acquisition time
string	SCETENL	Non-linearity acquisition time
string	SCETPMSK	Pixel-mask acquisition time
float	MEDFLT	Median Filter width in pixels
integer	INDEG	Degree for STIM Interpolation
float	ANNLTIME	Actual time since the last anneal

10.4 Header for 70 microns-SED mode

Note that for SED mode, CRVAL* and CTYPE* have slightly different definitions.

Table 10.4: Header keywords unique to MIPS-70 SED.

Type	Keyword	Notes or comments
<i>Target and pointing information</i>		
double	RA_SLT	[deg] RA at slit center averaged
double	DEC_SLT	[deg] DEC at slit center
double	PA_SLT	[deg] PA at slit center averaged
double	CRVAL1	[deg] Slit reference position
double	CRVAL2	[micron] Slit reference position
string	CTYPE1	Coordinate type along axis 1
string	CTYPE2	Coordinate type along axis 2
string	CUNIT1	Coordinate units for axis 1
string	CUNIT2	Coordinate units for axis 2
integer	DISPAXIS	Dispersion axis
double	CDELTA1	[deg/px] Scale for axis 1 at CRPIX1, CRPIX2
double	CDELTA2	[micron/px] Scale for axis 2 at CRPIX1, CRPIX2
double	CROTA2	[deg] Rotation of dispersion direction from axis 2
double	SPECTILT	[deg] Spectral tilt
<i>Time and exposure information</i>		
integer	COADD	Ge coadd parameter
<i>MIPS SED</i>		
string	CHOPDIST	[arcmin] Chop distance
integer	NCYCLES	Number of SED cycles
integer	NCOLS	Number of SED map columns
integer	NROWS	Number of SED map rows
string	COLSTEP	SED map column step
string	ROWSTEP	SED map row step
<i>Instrument telemetry data</i>		
integer	STMID_70	Det 70u Stimulator Power Enables
integer	ANHTR_70	Det 70u Anneal Heater Enable
float	STMFL_70	Det 70u Stimulator Flashed
integer	STM_MODE	Stimulator Manual or Auto Mode
integer	STMP_70	[Frames] Det 70u Stimulator Period in Data

integer	RSTP_70	[Frames] Det 70u Normal Reset Period in Data
double	CSM_POS	[DAC] CSMM Position Output
double	CSM_POSF	[DAC] CSMM Fine Position DAC
double	CSM_POSC	[DAC] CSMM Coarse Position DAC
double	ANCSMCUR	[uAmps] CSMM Current
double	IDUCA_70	[uAmps] Det 70u Unit Cell Drain Current A-half
double	IDUCB_70	[uAmps] Det 70u Unit Cell Drain Current B-half
double	VOFFA_70	[Volts] Det 70u Offset Voltage A-half
double	VOFFB_70	[Volts] Det 70u Offset Voltage B-half
double	VMREF_70	[Volts] Det 70u minus 5.00 Reference Voltage
double	ISTIM_70	[uAmps] Det 70u Stimulator Current DAC
double	IANNL_70	[mAmps] Det 70u Anneal Heater Current DAC
double	VQRST_70	[Volts] Det 70u Q Reset High Level Voltage
double	BRD_T_70	[Deg_C] Det 70u Control Board Temp
double	VBIAS_70	[Volts] Det 70u Common Bias Voltage at Detector
double	VRST1_70	[Volts] Det 70u Reset Voltage 1 @ Detector
double	VRST2_70	[Volts] Det 70u Reset Voltage 2 @ Detector
double	VRST3_70	[Volts] Det 70u Reset Voltage 3 @ Detector
double	VRST4_70	[Volts] Det 70u Reset Voltage 4 @ Detector
double	VRST5_70	[Volts] Det 70u Reset Voltage 5 @ Detector
double	VRST6_70	[Volts] Det 70u Reset Voltage 6 @ Detector
double	VRST7_70	[Volts] Det 70u Reset Voltage 7 @ Detector
double	VRST8_70	[Volts] Det 70u Reset Voltage 8 @ Detector
integer	DCE_NUM	DCEs in Observation Counter
integer	ANCALCYC	DCEs completed in Calibration Cycle
double	AD70JNCT	[Deg_K] 70u FPA Junction Temp
double	ABASET70	[Deg_K] 70u FPA Cold Plate
double	AD70TMPA	[Deg_K] 70u Detector Temp A
double	AD70TMPB	[Deg_K] 70u Detector Temp B
float	AD70BRDT	[Deg_C] MIPS 70 Micron Board Temp
integer	ACREJCNT	Command Reject Counter
integer	AIRSPCNT	Invalid Response Count
integer	ALIMVCNT	Limit Violation Counter
integer	AFIFOBAD	Science Data FIFO Bad Half Full Interrupts
integer	ASDMGRFA	SDM Groups Not Accepted By CDH
integer	ALSTERLD	Last Error Id
integer	ALSTERPM	Last Error Parameter
integer	ATOTALER	Total Errors Posted Count
<i>Calibration history</i>		
integer	EPIDDARK	Dark ensemble product ID
integer	EPIDILC	IC ensemble product ID
integer	EPIDRNO	Readnoise ensemble product ID
integer	FBIDPMSK	Pixel-mask fall-back product ID
integer	EPIDSTLT	Stimlatent cal file fall back product ID
integer	EPIDFLUX	Jansky conversion value fall back product ID

integer	FBIDDARK	Dark fall-back product ID
integer	FBIDILC	IC fall-back product ID
integer	FBIDENL	Electronic Non-linearity fall-back product ID
integer	FBIDENL	Saturation Cal file fall back id
integer	FBIDPMSK	Pixel-mask fall-back product ID
string	SCETDARK	Dark product acquisition time
string	SCETILC	Flat product acquisition time
string	SCETENL	Non-linearity acquisition time
string	SCETPMSK	Pixel-mask acquisition time
float	MEDFLT	Median Filter width in pixels
integer	INDEG	Degree for STIM Interpolation
float	ANNLTIME	Actual time since the last anneal

10.5 Header for 160 microns

Table 10.5: Header keywords unique to MIPS-160.

Type	Keyword	Notes or comments
<i>Time and exposure information</i>		
integer	COADD	Ge coadd parameter
<i>Instrument telemetry data</i>		
integer	STMID160	Det 160u Stimulator Power Enables
integer	ANHTR160	Det 160u Anneal Heater Enable
float	STMFL160	Det 160u Stimulator Flashed
integer	STM_MODE	Stimulator Manual or Auto Mode
integer	STMP160	[Frames] Det 160u Stimulator Period in Data
integer	RSTP160	[Frames] Det 160u Normal Reset Period in Data
double	IDUCD160	[uAmps] Det 160u Unit Cell Drain Current A-half
double	IDUCB160	[uAmps] Det 160u Unit Cell Drain Current B-half
double	VOFFA160	[Volts] Det 160u Offset Voltage A-half
double	VOFFB160	[Volts] Det 160u Offset Voltage B-half
double	VMREF160	[Volts] Det 160u minus 5.00 Reference Voltage
double	ISTIM160	[uAmps] Det 160u Stimulator Current DAC
double	IANNL160	[mAmps] Det 160u Anneal Heater Current DAC
double	VQRST160	[Volts] Det 160u Q Reset High Level Voltage
double	CSM_OFFS	[arcsec] CSMM Position Offset DAC Output
double	BRD_T160	[Deg_C] Det 160u Control Board Temp
double	VBIAS160	[Volts] Det 160u Common Bias Voltage at Detector
double	VRS1_160	[Volts] Det 160u Reset Voltage 1 @ Detector
double	VRS2_160	[Volts] Det 160u Reset Voltage 2 @ Detector
double	VRS3_160	[Volts] Det 160u Reset Voltage 3 @ Detector
double	VRS4_160	[Volts] Det 160u Reset Voltage 4 @ Detector
integer	DCE_NUM	DCEs in Observation Counter
integer	ANCALCYC	DCEs completed in Calibration Cycle

double	AJNCT160	[Deg_K] 160u FPA Junction Temp
double	AD160BSE	[Deg_K] 160u FPA Cold Plate
double	AD160TMA	[Deg_K] 160u Detector Temp A
double	AD160STM	[Deg_K] 160u Stimulator Temp
double	AD160TMB	[Deg_K] 160u Detector Temp B
integer	ACREJCNT	Command Reject Counter
integer	AIRSPCNT	Invalid Response Count
integer	ABASTMCR	Coarse Component of CE Base Time
integer	ABASTMFN	Fine Component of CE Base Time
integer	ALIMVCNT	Limit Violation Counter
integer	AFIFOBAD	Science Data FIFO Bad Half Full Interrupts
integer	ASDMGRFA	SDM Groups Not Accepted By CDH
integer	ALSTERLD	Last Error Id
integer	ALSTERPM	Last Error Parameter
integer	ATOTALER	Total Errors Posted Count
<i>Data flow keywords</i>		
integer	PIPE_ID1	Pipeline Script ID
integer	PIPE_ID2	Pipeline Script ID
integer	PIPE_ID3	Pipeline Script ID
integer	PIPE_ID4	Pipeline Script ID
integer	PIPE_ID5	Pipeline Script ID
<i>Calibration history</i>		
integer	EPIDDARK	Dark ensemble product ID
integer	EPIDILC	IC ensemble product ID
integer	EPIDRNO	Readnoise ensemble product ID
integer	FBIDPMSK	Pixel-mask fall-back product ID
integer	EPIDSTLT	Stimlatent cal file fall back product ID
integer	EPIDFLUX	Jansky conversion value fall back product ID
integer	FBIDDARK	Dark fall-back product ID
integer	FBIDILC	IC fall-back product ID
integer	FBIDENL	Electronic Non-linearity fall-back product ID
integer	FBIDENL	Saturation Cal file fall back id
integer	FBIDPMSK	Pixel-mask fall-back product ID
string	SCETDARK	Dark product acquisition time
string	SCETILC	Flat product acquisition time
string	SCETENL	Non-linearity acquisition time
string	SCETPMSK	Pixel-mask acquisition time
float	MEDFLTNT	Median Filter width in pixels
integer	INDEG	Degree for STIM Interpolation
float	ANNLTIME	Actual time since the last anneal

10.6 Header for Post-BCD products

The post-BCD header is substantially similar to the “standard” BCD header as found in Table 10.1, except the “Instrument telemetry” section is omitted, there is

a new “Processing History” section, and three sections are subtly different: “Time and exposure information,” “Target and pointing information,” and “Data Flow.”

Table 10.6: Header keywords found in post-BCD products.

Type	Keyword	Notes or comments
<i>Time and exposure information (from header of 1st BCD in mosaic)</i>		
double	MJD_OBS	[days] MJD at DCE start (JD-2400000.5)
double	UTCS_OBS	[sec] J2000 ephemeris time at DCE start
double	SCLK_OBS	[sec] SCLK time (since 1/1/1980)
float	SAMPTIME	[sec] Sample integration time
float	EXPTIME	[sec] Int. time per pixel
integer	IGN_FRM1	Initial frames ignored for dcnun = 0
integer	IGN_FRM2	Initial frames ignored for dcnun > 0
integer	SATTHDIF	[DN/SAMPTIME] Saturation Threshold in difference
<i>Target and pointing information</i>		
string	OBJECT	Object Name
string	OBJTYPE	Object Type
double	CRVAL1	[deg] RA at CRPIX1,CRPIX2
double	CRVAL2	[deg] DEC at CRPIX1,CRPIX2
string	RADESYS	International Celestial Reference System
float	EQUINOX	Equinox for ICRS celestial coord. system
string	CTYPE1	RA---TAN
string	CTYPE2	DEC--TAN
float	CRPIX1	Reference pixel along axis 1
float	CRPIX2	Reference pixel along axis 2
float	CDELTA1	[deg/pix] Plate scale for axis 1 at CRPIX1,CRPIX2
float	CDELTA2	[deg/pix] Plate scale for axis 2 at CRPIX1,CRPIX2
float	CROTA2	[deg] Position angle of axis 2 (W of N, +=CW)
double	RA_REF	[deg] Commanded RA (J2000) of ref. position
double	DEC_REF	[deg] Commanded Dec (J2000) of ref. position
float	PM_RA	[arcsec/yr] Proper Motion in RA (J2000)
float	PM_DEC	[arcsec/yr] Proper Motion in Dec (J2000)
float	CSM_RATE	[milli-arcsec/sec] Mirror scan rate
<i>Data flow keywords</i>		
string	DATE	[YYYY-MM-DDThh:mm:ss UTC] file creation date
string	ORIGIN0	Site where raw-FITS file was written
string	CREATOR0	SW system that created raw-FITS file
string	SIS_SVER	SIS SW VERsion of CREATOR0
long	AORKEY	AOR or IER key. Astronomical Observation Request/Instrument Engineering Request
string	DS_IDENT	Data Set Identification for ADS/journals

integer	PAONUM	PAO Number
string	CAMPAIGN	Campaign
integer	SOS_VER	Data-Product Version
integer	PLVID	Pipeline Version ID
integer	CALID	CalTrans Version ID
string	CTD_VER	Commanded telemetry data version
string	CALBUNIT	Units for which calibration data applies
<i>Processing history</i>		
integer	TOTALBCD	Total number of BCDs used in this mosaic

11 Appendix: Suggested namelists

Sample namelists for use with the MOPEX code can be found on the SSC website for several examples discussed in this document.

12 Appendix: Analysis code

A variety of contributed routines for several tasks such as column filtering of MIPS-70 data is available on the SSC website.